Effect of removal of the Oosterschelde storm surge barrier

TU Delft Delft University of Technology

Van Oord

Deltares
Enabling Delta Life

Report title	Effect of removal of the Oosterschelde storm surge barrier
Report type	MSc. thesis
Author	P.D. de Pater
Student number	4022289
Date	June, 2012
Institute	Delft University of Technology Faculty of Civil Engineering and Geosciences Hydraulic Engineering Section
MSc. Committee	Prof.Dr.Ir. M.J.F. Stive Prof.Dr.Ir. Z.B. Wang Dr.Ir. R.J. Labeur Dr.Ir. A. Hibma Ir. M. Eelkema

[1]Cover picture: https://beeldbank.rws.nl/

Preface

This M.Sc. thesis is written as final part of my master in Coastal Engineering at the Faculty of Civil Engineering and Geosciences of Delft University of Technology. The study concerns the effect of removal of the Oosterschelde storm surge barrier.
Several people have helped and advised me during my graduation. I would like to thank professor Stive for being chairman of my graduation committee. Ms. Hibma for introducing me in the topic, arranging the contacts with Deltares and guidance during my graduation. Mr. Wang for the discussions regarding tidal dynamics and Delft3D. Mr. Labeur for his help and remarks on the analytical model. Mr. Eelkema for his involvement in my research and his help by providing and evaluating the bathymetric data. Besides that I want to thank the graduation students at van Oord and Deltares for the exchange of ideas regarding Matlab and Latex.

I hope you will enjoy reading this report,

Pim de Pater,

June 2012

Summary

The south-western delta of the Netherlands has undergone big changes in the period 1960 till nowadays. Several dams have been constructed to guarantee the safety of Zeeland in the context of the Deltaworks. Especially the Oosterschelde storm surge barrier has influenced the hydrodynamics in the Oosterschelde. The basin area of the Oosterschelde, the tidal prism, the tidal range and the tidal currents changed as a consequence of the Deltaworks. Due to the flow and sediment exchange reduction by the storm surge barrier, the Oosterschelde basin is not in morphological equilibrium nowadays and in need of sediment. The consequence of the lack of sediment is a redistribution of the sediment inside the basin. The lack of sediment in the channels is filled in by a supply from the shoals, causing loss of intertidal area. Which in turn has detrimental effects on the ecology, shipping, recreation, fishery and dike maintenance.

The research objective of this thesis is to determine the new hydrodynamic and morphodynamic situation in case the Oosterschelde storm surge barrier is removed, with emphasis on the development of the intertidal area. To reach the objectives of this study a literature study is performed which describes the impact of the Deltaworks. An analytical model is developed to evaluate the effect of the Philipsdam and Oesterdam on the hydrodynamics in the Oosterschelde when the barrier is removed. Besides that a Delft3D model, the Kustzuid model, is used to determine the effect of bathymetric changes, removal of the barrier and realignment of the basin. Several adaptations have been made to the Kustzuid model to improve the performance.

A theory by [Friedrichs and Aubrey, 1988] is used to analyse the distortion of the water level and discharge signal. The applied theory uses the relative phase of the M_2 and M_4 component to indicate the asymmetry.

Removal of the barrier causes an increase of the tidal range by 10 to 20%. This is indicated both by the analytical model as by the Delft3D model. The tidal range will not get as large as it was before the Deltaworks. Removal of the barrier will cause an increase of the tidal prism and strengthen the ebb dominance of the basin. Besides that shoal build up will be enforced by the higher current velocities.

Simulations with different bathymetries dating from 1983, 2008 and 2100 indicate that the loss of sediment from the shoals to the channels leads to a less ebb dominant system. A sligthly less ebb-dominant system is found in 2008 compared to the 1983 scenario. Ongoing loss of sediment from the intertidal area leads to a scenario without intertidal flats in 2100. In the 2100 scenario without barrier the system gets flood dominant in the eastern parts of the basin. Flood dominance throughout the entire basin is found when the barrier is still in place in 2100.

Large scale realignment of the Oosterschelde is simulated by adding intertidal area to the Oosterschelde without increasing the channel volume. These simulations show increased ebb-dominance, leading to export of sediment. The set back of part of the dikes will increase the flow velocities inside the basin, however not enough to cause shoal build up. When the barrier is removed in combination with realignment, shoal build up will occur. Based on empirical relations, realignment of the Oosterschelde is not expected to have a large effect on the relative flat area.

Contents

List of symbols

Δx	Cell size in x-direction	$[m]$
Δy	Cell size in y-direction	$[m]$
η	Water level	$[m]$
κ	Linear friction factor	$[1/s]$
ω	Angular frequency	$[rad/s]$
ϕ	Phase of the tidal velocity	$[rad]$
σ	Relation between friction and inertia	[-]
θ	Phase of the water level	$[rad]$
$\tilde{\zeta}$	Complex water level amplitude	$[m]$
$\tilde{Q}$	Complex discharge amplitude	$[m^3/s]$
A	Expression for the distorted sea surface height	$[m]$
a	Water level amplitude of the tidal wave	$[m]$
A_s	Flow carrying cross section	$[m^2]$
A_{basin}	The horizontal area of the entire basin	$[m^2]$
A_{eff}	Effective wet cross sectional area of one grid cell	$[m^2]$
A_{eq}	Minimum equilibrium cross section of the entrance channel below mean sea level	$[m^2]$
A_{flats}	The horizontal area of the intertidal flats	$[m^2]$
A_{tot}	Total cross sectional area of one grid cell	$[m^2]$
B	Basin width	$[m]$
B_s	Flow carrying width	$[m]$
C	Empirical coefficient	[-]
c_f	Friction factor	[-]
C_V	Empirical coefficient	$[m^3]$
C_+	Complex constant	[-]

C_-	Complex constant	[-]
C_{drag}	Drag coefficient	[-]
c_{loss-U}	Energy loss coefficient	[-]
D	Channel depth	$[m]$
D_c	The characteristic channel depth	$[m]$
d_{pile}	Diameter of the pile	$[m]$
g	Gravitational acceleration	$[m/s^2]$
h	Water level	$[m]$
H_m	Mean tidal range	$[m]$
L	Length of the branch	$[m]$
M_2	Principal lunar tide	[-]
M_4	First even harmonic of M_2	[-]
M_6	First uneven harmonic of M_2	[-]
M_ξ	Momentum source/sink	$[m/s^2]$
N	Number of piles per grid cell	[-]
P	Tidal prism	$[m^3]$
p	Complex propagation constant	$[1/m]$
Q	Discharge	$[m^3/s]$
q	Empirical coefficient	[-]
R	Hydraulic radius	$[m]$
r	Amplification factor	[-]
t	Time	$[s]$
$U_{m,n}$	Velocity in m or n direction	$[m/s]$
V	Expression for the distorted tidal velocity	$[m/s]$
v	Amplitude of the tidal velocity	$[m]$
V_c	Equilibrium total channel volume below mean sea level	$[m^3]$
x	X coordinate along channel axis	$[m]$
NAP	Dutch ordnance datum	[-]

List of Figures

List of Tables

Chapter 1

Introduction

1.1 Research background

The south-western delta of the Netherlands has undergone big changes in the period 1960 till nowadays. Several dams have been constructed to guarantee the safety of Zeeland. The Oosterschelde has experienced the effects of the Veere inlet dam (1961), the Grevelingen dam (1965), the Volkerak dam (1969), the Oosterschelde storm surge barrier (1986), the Oesterdam (1986) and the Philipsdam (1986). The basin area of the Oosterschelde, the tidal prism, the tidal range and the tidal currents changed as a consequence of these measures. Due to the flow reduction by the storm surge barrier, the Oosterschelde basin is not in morphological equilibrium nowadays and in need of sediment. To attain an equilibrium a decrease of the channel cross-sectional area leading to higher flow velocities is required. There used to be two external sources of sediment: The rivers Rijn and Maas, but they do not supply sediment anymore since the basin is cut off from these rivers. The other possible source of sediment, the ebb-tidal delta, is blocked by the Oosterschelde storm surge barrier. To attain an equilibrium in the Oosterschelde an amount of 400-600 million m^3 is necessary [Mulder and van Heteren, 2009]. The consequence of the lack of sediment sources is a redistribution of the sediment inside the basin. The lack of sediment in the channels is filled in by a supply from the shoals. Wave action leads to erosion of the shoals according to [Mulder and van Heteren, 2009]. Before the closure of the Oosterschelde by the storm surge barrier, the flow in the channels was high enough to cause shoal build up. At present there is no balance between the building and eroding forces, causing erosion of the shoals. [van Zanten and Adriaanse, 2008] report that the inter-tidal area reduced from 12.000 hectares to 10.430 hectares in the period 1986-2001. 700 hectares of this reduction is an instant loss because the tidal range reduced.

The intertidal areas are important from an ecological point of view. Several bird species and seals are dependent on the shoals. The biggest issue is the decrease of the period that the shoals fall dry, because this reduces the time for birds to feed. The importance of the inter-tidal flats in the Oosterschelde basin is stressed by protection by several European laws. [Geurts van Kessel, 2004] Besides the detrimental effects on nature; also shipping, recreation, shellfish fisheries and dike maintenance are influenced by the sand demand. Because of the sand demand, the forelands in front of the dikes get lower, resulting in higher wave loads on the dikes. For shipping extra maintenance dredging in the main navigation channel is needed. [van Zanten and Adriaanse, 2008]

In addition to the stated problem of the reduced tidal flow, sea level rise also has to be taken into account. The current sea level rise of 2mm per year causes a rise of the sediment demand in the basin of 0,75Mm^3 per year. Besides the effect of sea level rise on the sand demand, it also has an effect on the lifetime of the Oosterschelde storm surge barrier. The expected (extended)

lifetime of the Oosterschelde barrier ends between 2075 and 2125. After that, measures have to be taken to guarantee the safety of the hinterland. [Deltacommittee, 2008] They also report that the largest part of the inter-tidal flats will be lost by 2050.

In principle there are two solutions to counteract the erosion in the Oosterschelde, nourishments and increasing the tidal prism. If sediment is imported from outside the Oosterschelde basin with a quantity of 1,5Mm^3 per year, the shoal erosion will be compensated and the sand demand will decrease by 0,75Mm^3 per year. Another possibility to counteract the erosion of the shoals in the basin is to recover the tidal prism, for instance by removing the Oosterschelde storm surge barrier. This gives an opportunity to recover the morphological dynamic balance by a natural way [Mulder and van Heteren, 2009]. The [Deltacommittee, 2008] also prefers a solution for the Oosterschelde that recovers the tidal dynamics of the area as much as possible on the long term. However, it is unknown what the morphological equilibrium of the Oosterschelde basin will be if the Oosterschelde storm surge barrier is removed.

In this thesis a Delft3D model will be used to calculate the hydrodynamic and morphological effects of the removal of the Oosterschelde storm surge barrier. The impact of this interference will be reviewed on two scales. The effect on the basin as a whole will be investigated. Besides this the consequences for the inter-tidal flats will be studied.

1.2 Research objectives and research questions

The Oosterschelde basin has not been in morphological equilibrium during the past centuries, because of both natural and human induced changes to the basin. At present sedimentation takes place inside the basin because of the reduced tidal prism. As stated above a significant change in inter-tidal area is reported. Because the geometry of the basin affects the propagation of the tidal wave in the basin, the situation after removal of the barrier is not expected to be the same as the situation before the construction of the barrier. The research objective of this thesis is to determine the new hydrodynamic and morphodynamic situation in case the Oosterschelde storm surge barrier is removed, with emphasis on the development of the intertidal area. In order to reach this objective several research questions have been formulated:

- What is the effect of the Philipsdam and Oesterdam on the hydrodynamics in the Oosterschelde basin?
- What is the development of the hydrodynamic response under changing bathymetry in the period 1983 to 2008?
- Will removal of the barrier stop shoal erosion?
- Will the Oosterschelde start exporting sediment like before the closure when the barrier is removed? And what will the equilibrium situation look like?
- What is to be expected for the hydrodynamic and morphological situation in 2100?
- Are there other measures possible to enhance growth of the intertidal area, besides removal of the barrier?

1.3 Research approach

The impact of most of the mentioned closure dams is known and described in literature. Therefore the first step will be to give an overview of these impacts by means of a literature study. The hydrodynamic effect of the Philipsdam and Oesterdam apart from the effect of the Oosterschelde storm surge barrier is not clear, because these dams were finished after the closure of the Oosterschelde inlet. Because this impact is not clear, the next step will be to use an analytical model to gain insight in the effect of the Philipsdam and the Oesterdam. To answer the other research questions a Delft 3D model will be used. The Kustzuid model will be adapted by implementing different bathymetries and by removing the Oosterschelde storm surge barrier. With this adapted Kustzuid model hydrodynamic calculations will be performed. The obtained results will be evaluated with a theory developed by [Friedrichs and Aubrey, 1988]. The used theory approximates the asymmetry by looking at two components, M_2 and M_4. Next to the analysis of the asymmetry of the signal, estimates of the equilibrium situation of each considered alternative are made with the help of empirical relations.

Chapter 2

Literature study

2.1 Historical development of the Oosterschelde

In 1953 a big storm hit the south-western delta causing a lot of casualties and damage. This was the reason to appoint the 'delta committee' which gave a number of advices between 1953 and 1955 amongst which the closure of several tidal channels. This chapter will describe the situation before the closures and effects of the interferences. First the situation before the execution of the Deltaplan will be described. After that a summary of all the closures and their global effect on the system will be given. Finally the effects for the basin and the ebb-tidal delta will be treated separately and more in detail.

2.1.1 Situation before closures

Before the closures, the Oosterschelde was connected to the Grevelingen and the Haringvliet by a deep channel, halfway the basin, called the Zijpe. Because of this the rivers Rijn and Maas influenced the water motion to a small extent. However the water motion in the Oosterschelde is dominated by the tidal flow, predominantly by the semi-diurnal component (M_2). Some characteristic information about the Oosterschelde before and after the closures is present in table 2.1. The Oosterschelde ebb-tidal delta was morphologically highly active in the period

	Before Deltaworks	After Deltaworks
Total area (km^2)	452	351
Water area (km^2)	362	304
Intertidal area (km^2)	183	118
Mean tidal range (m)	3.70	3.25
Maximum flow velocity (m/s)	1.5	1
Average tidal prism(10^6) m^3	1230	880
Freshwater discharge by rivers (m^3/s)	50-100	10

Table 2.1: Characteristics of the Oosterschelde before and after the Deltaworks [Geurts van Kessel, 2004]

before 1953. The tidal volume increased slowly but steadily, causing the main channels to scour. The result of this, is transport of a large amount of sediment from the basin towards the ebb-tidal delta. The most probable cause for the steady increase in tidal volume is the inundation of a large area in the back of the basin in 1530 because of a large storm, the St Felix flood. As a result the ebb-tidal delta grew steadily outward in the decades before 1953. An important event at the inlet is the emergence of a new channel, called the Schaar van de Roggenplaat, between

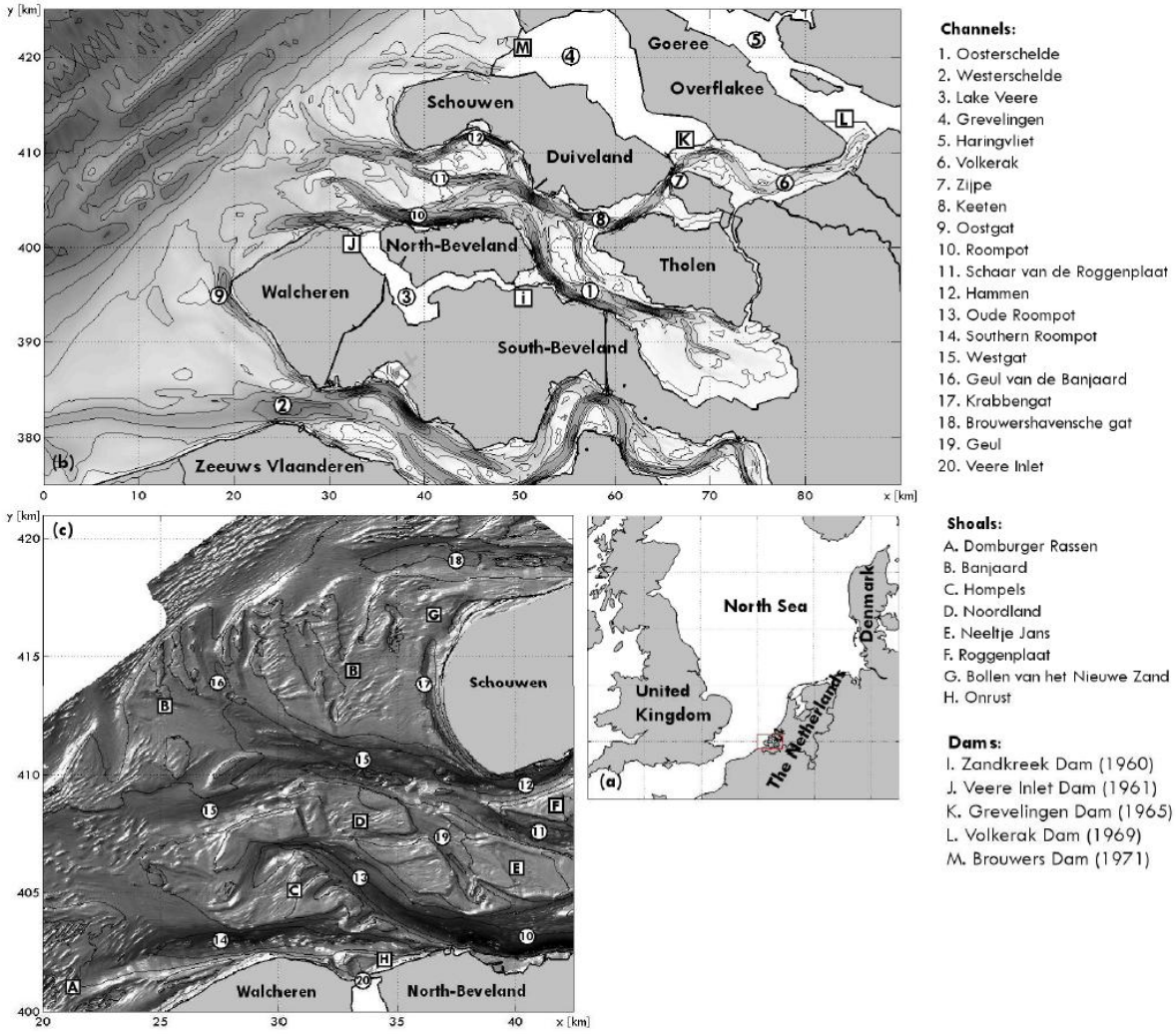

Figure 2.1: Overview of (a) the North Sea, (b) the Southwestern Delta, and (c) the Eastern Scheldt ebb-tidal delta around 1971.[Eelkema et al., 2011]

1933 and 1953. Before this period there were two channels, the Hammen channel in the north and the Roompot in the south. These channels were separated by a large shoal system called Neeltje Jans. When the new channel, Schaar van de Roggenplaat, emerged the Neeltje Jans shoal was separated from the Roggenplaat. [Eelkema et al., 2011]

2.1.2 Effect of the closures

The Delta project began with the closure of the Veerse Gat by constructing the Zandkreek dam (1960) and the Veerse gat dam (1961). This created Lake Veere which is a fresh water lake now. The next step was the construction of the Grevelingen dam (1965). This dam was built on the tidal divide between the Oosterschelde and the Grevelingen in the Grevelingen estuary. In 1969 the Volkerak dam was built, which cuts off the Haringvliet from the Oosterschelde. Two other closures did not affect the Oosterschelde basin. The Haringvliet and the Grevelingen turned into fresh water lakes by the construction of the Haringvliet dam (1970) and the Brouwersdam (1971). The last scheduled closure was the Oosterschelde. Because of growing environmental awareness it was decided to build a storm surge barrier in stead of a dam. It was recognised that this barrier would severely restrict the tidal flow in the basin and thereby damage important

ecological environments. Therefore compartmentalisation dams had to be built to maintain the tidal amplitude. In the eastern part of the basin the Oesterdam (1986) was built and the Volkerak was cut off by the Philipsdam (1986). [de Bok, 2001] The effect of the Zandkreek dam and the Veerse gat dam are only local and did not affect the large scale hydrodynamics. Also the Grevelingen dam did not change the hydrodynamics in the Oosterschelde basin radically, because this dam is built on the tidal divide between the Grevelingen and the Oosterschelde. The completion of the Volkerak dam however did; the closure caused an increase of the tidal prism of 7% within a year according to [de Bok, 2001]. The reason for this increase in tidal prism is that the construction of the Volkerak dam enlarged the area of the Oosterschelde. This caused scour of the channels. Besides the instantaneous increase in tidal prism, an additional increase is measured. The cause of this additional increase is not clear, it could have been scouring of the main channels which made them more hydraulically efficient. [Eelkema et al., 2011] The Oesterdam, the Philipsdam and the Oosterschelde storm surge barrier caused a large decrease of tidal prism. The decrease can be allocated to the construction of the Oesterdam and Philipsdam which reduced the area of the basin and to the reduction of the cross sectional area of the inlet by the Oosterschelde storm surge barrier which constricts the flow.

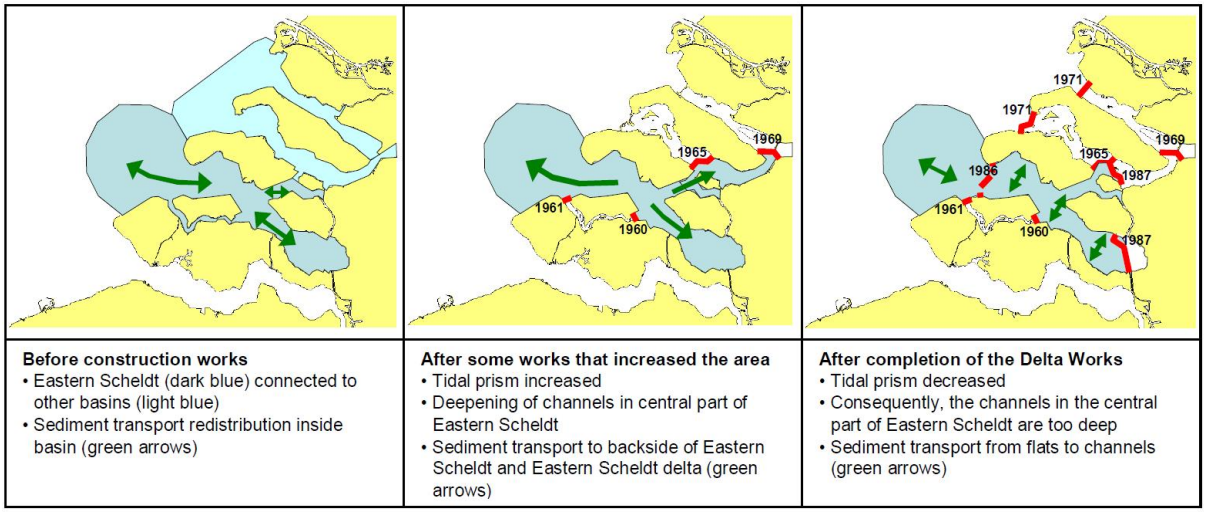

Figure 2.2: Development of the Oosterschelde basin [Huisman and Luijendijk, 2009]

The morphological effect of the closures is as follows. The finalization of the Volkerak dam amplified the erosive trend throughout the entire Oosterschelde, although some parts experienced accretion. It is estimated that the basin lost about 120Mm^3 between 1960 and 1989. A large part, 80Mm^3, was due to sand mining activities. The remaining 40Mm^3 were lost due to natural export. [Eelkema et al., 2011] The channels at the inlet experienced scour because the increase of the tidal prism. This scour was amplified even more by the construction of two artificial islands in the inlet during the 1970's, constricting the flow in the remaining channels. The changes inside the basin also started to become apparent on the ebb-tidal delta. Because of the larger tidal prism the channels on the ebb-tidal delta also started deepening and lengthening. In particular the Oude Roompot channel expanded rapidly in seaward direction. Another important event is the connection of the Oude Roompot to the Westgat channel around 1972. It is not certain whether the connection is a direct result of the increase in tidal prism or not. In the past similar breakthroughs occurred at this location. As pointed out before the channels experienced increased flow and they started to expand seawards. The distinctive terminal lobe also expanded mostly in north-western direction, where the Banjaard channel deposited large quantities of sand on its ebb shield. At this location the Brouwersdam does

have effect, because it decreased the flow in the Brouwershavensche gat. This channel marks the edge of the Banjaard. The Krabbengat and the Banjaard channel both started to deposit sand in the Brouwershavensche gat. In its entirety, the ebb-tidal delta seemed to become wider by means of shoals accreting on their seaward sides and channels pushing their ebb-shields seaward. In 1986 the basin area was reduced by two dams namely the Oesterdam in the eastern part of the basin and the Philipsdam at southwest end of the Volkerak. Furthermore the Oosterschelde storm barrier was finalized which led to a decrease of the cross sectional area of the inlet from 80000m^2 to 14000m^2 according to [de Bok, 2001]. [Huisman and Luijendijk, 2009] state that the cross sectional area below NAP reduced to 17900m^2. The stated interferences caused a reduction of the tidal prism and consequently of the tidal range and the flow velocities. The consequence of a reduction of the area of the inlet is an increase in the flow velocity, which will erode the inlet until a new equilibrium situation is reached with flow velocities approximately the same as in the original situation. In case of the Oosterschelde barrier erosion of the inlet is impossible because of the bed protection. However the areas near the barrier without bed protection did erode, resulting in deep erosion holes. [de Bok, 2001] Inside the basin, as a consequence of the reduction in tidal prism, the maximum flow velocity decreased. The result of this decrease is that the channels inside the basin are not in morphological equilibrium. It is expected that the channels will fill up over time. On the basis of empirical relations between the tidal prism and cross-sectional area in the tidal channels it is estimated that the cross-sectional area of the channels will reduce by 25%. This corresponds with a sand volume of 400-600Mm^3. The sand that is necessary to fill the channels can not be imported from the ebb-tidal delta because the Oosterschelde storm surge barrier severely restricts the import. Therefore the channels are filled with sand that is eroded from the inter-tidal areas. [Huisman and Luijendijk, 2009] According to [van Zanten and Adriaanse, 2008] there is a storage of 140 Mm^3 of sand within the inter-tidal areas. [Quyen, 2010] states that the tidal volume in the period 1976-1980 decreased but that it was still bigger than the tidal volume that was present before the closures. Therefore the erosion of the channels and the sedimentation of the shoals continued but at a smaller rate than before. After completion of the barrier, the tidal prism is 30% smaller compared to the situation before implementation of the barrier. The consequence is that sand volume of the ebb-tidal delta is too large, therefore the ebb-tidal delta has eroded since the completion of the barrier. This argumentation is based on the empirical relation between the tidal prism and the sand volume of the ebb-tidal delta stated by [Walton and Adams, 1976].

2.1.3 Present situation

First it must be stated that the Oosterschelde has been out of equilibrium for a long time. The basin was adapting to a new equilibrium already before the execution of the Delta plan. The discussed interferences changed the hydrodynamics radically, forcing the system to adapt. At present, as a consequence of the reduction in the maximum flow velocities inside the basin, the tidal channels of the Oosterschelde basin are not in equilibrium. According to [van Zanten and Adriaanse, 2008] the tidal flats are eroding. They report that the area of the inter-tidal flats has decreased by 8% in the period 1986-2001. The shoals also became lower in the mentioned period; the average elevation of the shoals has decreased by 14cm. On the ebb-tidal delta the morphology is also changing because of the reduced tidal prism. At present the morphology changes only slowly on the ebb-tidal delta. In general the shoals are eroding and migrating landward. There is a reorientation of the channels towards the north, while they are silting up.

2.2 Physical processes

To understand the development in the past and to predict the future situation, a good understanding of the physical processes is indispensable. In this paragraph the physical processes and parameters that relate to the hydrodynamic and morphological development are explained. With respect to the morphological development there are two ways of reasoning. One can reason from the distortion of the tidal wave, paragraph 2.2.1, or from empirical relations between the tidal prism and several other parameters, paragraph 2.2.2. Both methods will be explained. Next to this some conclusions from a master's thesis by [Das, 2010] will be stated, with respect to the processes that govern the shoal build up/degradation.

2.2.1 Distortion of the tidal wave

The astronomical tide is a very important forcing factor for the water motion in the Oosterschelde. This implies that it is also important for the sediment transport in tidal basins. The tidal wave can be described by a series of harmonic components, with frequencies that are astronomically determined. A part of the components is directly related to the motion of the celestial bodies. Others originate from non-linear interactions of tidal components. These non-linear interactions can distort the tidal wave and thereby cause a residual sediment transport. To explain the asymmetry of the tidal wave first some definitions are given:

- **Vertical tide:** relates to the water levels, high tide means high water levels.
- **Horizontal tide:** relates to the tidal currents, flood currents are currents that have the same direction as the wave propagation. Ebb currents are directed against the propagation direction.
- **Slack water:** is the tidal flow reversal. Low water slack is the flow reversal from ebb to flood. The opposite holds for high water slack.

Both the horizontal and the vertical tide can be asymmetric. The asymmetries of the horizontal tide are of importance to the net sediment transport. The different types of asymmetry will be explained next. Tidal asymmetry means that the flood part of the velocity-time or water level-time curve does not have the same shape as the ebb part. The shape of the tidal wave can differ in two ways, in vertical direction and in horizontal direction.

In vertical direction the amplitude of the maxima and minima differ. In case of the horizontal tide, when the average peak flood velocity is higher than the average peak ebb velocity. This type of asymmetry influences the bed load transport, the transport of coarse grains.

In the horizontal direction, along the time axis, the falling period can differ from the rising period. This means for the horizontal tide that the duration of HW slack is different than that of LW slack. This affects the residual transport for fine sediment, because fines need time to settle. Fine sediments are allowed to deposit if the slack duration is long enough [Bosboom and Stive, 2011]. The skewness of the horizontal tide is of importance for the residual (net) sediment transport in tide dominated areas, such as the Oosterschelde. For instance, if the maximum flood velocity exceeds the ebb velocity, a residual sediment transport in flood direction is likely to happen, since sediment transport responds non-linearly to the velocity. Systems in which the maximum flood velocities are higher than the maximum ebb velocities are called flood-dominant. Flood dominance can be expected for large ratio of tidal amplitude over the water depth. In that case propagation of high tide is faster than that of the low water. Ebb-dominance holds for the opposite situation, large inter-tidal storage volume and deep channels enhance ebb-dominance. [Friedrichs and Aubrey, 1988] state that tidal distortion is a compromise between

the effects of frictional distortion in channels and inter-tidal storage in tidal flats and marshes. Shallow channels slow down the propagation of low water through the inner estuary, shortening the flood, whereas extensive inter-tidal storage slows the propagation of high water, shortening the ebb.

Theory by Friedrichs

[Friedrichs and Aubrey, 1988] described a theory to analyse the tidal asymmetry. As mentioned before the tidal wave can be modelled by a superposition of the components. The expression for the distorted sea-surface height, A, and the tidal velocity, V, are given below for the most important components M_2 and M_4.

$$A = a_{M_2} cos(\omega t - \theta_{M_2}) + a_{M_4} cos(\omega t - \theta_{M_4}) \tag{2.1}$$

$$V = v_{M_2} cos(\omega t - \phi_{M_2}) + v_{M_4} cos(\omega t - \phi_{M_4}) \tag{2.2}$$

Where t is time, ω is the angular tidal frequency, a is the amplitude of the water level, v is the amplitude of the tidal velocity, θ is the phase of the water level and ϕ is the phase of the tidal velocity. The M_4 to M_2 amplitude ratio is a direct measure for the non linear distortion of the tidal wave. When this ratio is larger than zero, the tide is distorted. The relative sea-surface phase can be used to determine the direction of the tidal asymmetry.

$$\text{Relative sea surface phase} = 2M_2 - M_4 = 2\theta_{M_2} - \theta_{M_4} \tag{2.3}$$

$$\text{Relative velocity phase} = 2M_2 - M_4 = 2\phi_{M_2} - \phi_{M_4} \tag{2.4}$$

When the relative sea surface phase is between 0 and 180 degrees, the system is flood dominant. Between 180 and 360 degrees the system is ebb dominant. For the relative velocity phase a similar relation holds, if a linear relationship between velocities and surface elevation is assumed. This assumption holds for small basins with a standing wave. This is not the case because the Oosterschelde is a basin with a partly progressive wave. However [Wang et al., 2002] shows that the presented relation also applies to long basins by considering the Westerschelde. He also found that the existing theory does not apply quantitatively.

The system is flood-dominant when the relative velocity phase is between -90 and 90 degrees and ebb-dominant between 90 and 270 degrees. The flow velocity however is not a single value but a vector; therefore the tidal constituents are represented by ellipses. Due to this it is in general not possible to characterise the asymmetry by an amplitude ratio and relative phase difference according to [Wang, 1999]. The relation can therefore not be applied to the velocity signal, it can be applied though to the instantaneous discharge signal because this signal is not a vector. [Friedrichs and Aubrey, 1988] processed the amplitude ratio and relative phase into diagrams that show the dependence on the intertidal storage and tidal range using 84 model systems. The diagrams for the water level signal are included in figure 2.3.

The same relations as stated by [Friedrichs and Aubrey, 1988] are found by [van de Kreeke and Robaczewska, 1993] but they used a more general approach and investigated extra tidal components. Besides the interaction between M_2 and M_4, they investigated the interaction of M_2 and M_6. They found that the interaction of M_2 and M_6 will always result in a tidally averaged bed load transport that is zero. There is however a contribution to the net sediment flux by the triple interaction of M_2, M_4 and M_6. [van de Kreeke and Robaczewska, 1993] state that although this contribution is of second order, it can be relatively important depending on the values of the phase angles. [Wang et al., 2002] state that the sixth-diurnal tide M_6 affects the asymmetry of the tide in the Westerschelde. In addition they mention that theories relating tidal asymmetry caused by M_6 to the estuarine morphology are still lacking.

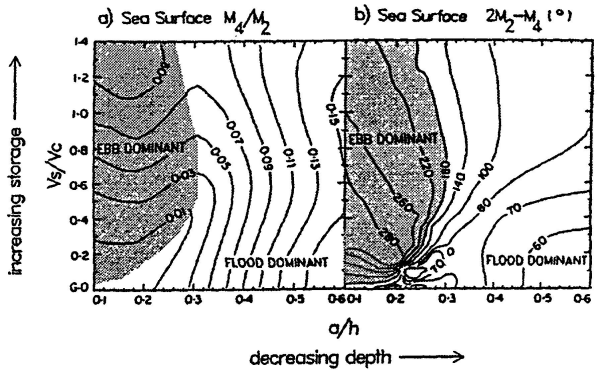

Figure 2.3: Contour plots of the parameters that indicate nonlinear distortion as a function of a/h and V_s/V_c. [Speer et al., 1991] after [Friedrichs and Aubrey, 1988]

2.2.2 Empirical relations

As explained, predictions about the sediment transport can be done by considering the distortion of the tidal wave. Besides this, several empirical relations exist to describe the equilibrium situation of several parts of a basin system (Inlet and the basin itself). Those relations can be used to explain the morphological development of a basin. Some of the available relations are stated below.

Stability of the inlet

The general form of the empirical relationship for the equilibrium cross-section based on the tidal prism is as follows:

$$A_{eq} = CP^q \tag{2.5}$$

in which:

A_{eq} = Minimum equilibrium cross section of the entrance channel below mean sea level
P = Tidal prism, often the spring tidal prism
C, q = Coefficients

According to [Bosboom and Stive, 2011] this equation seems equally valid for both large estuary mouths and for bays and tidal lagoons. But a combination of values for the coefficients C and q is valid only for a set of inlets with the same sediment characteristics and that are subject to the same wave conditions and tidal conditions. [van de Kreeke and Haring, 1979] derived the values of C and q for the Oosterschelde, being respectively $8.2{\cdot}10^{-5}$ and 1. They used average tide conditions to derive the empirical coefficients. This relation is not only applicable to the cross section of the entrance channel but also to cross sections in the basin according to [Bosboom and Stive, 2011]. This makes it possible to evaluate the behaviour of seperate areas of the Oosterschelde.

Equilibrium relation for total channel volume

$$V_c = C_V P^{3/2} \tag{2.6}$$

in which:

V_c = Equilibrium total channel volume below mean sea level
C_V = Empirical coefficient
P = Tidal prism

The empirical coefficient for this relation is stated by [Eysink, 1991]. For the Westerschelde, Oosterschelde and Grevelingen a range from 73-80·10^{-6} is given. [Bosboom and Stive, 2011] suggest that relation 2.6 can be adapted to determine the area of the flats. The following relation (2.7) is given by [Bosboom and Stive, 2011]:

$$A_{flats} = A_{basin} - \beta \frac{H_m}{D_c} A_{basin}^{3/2} \tag{2.7}$$

in which:

A_{flats} = Horizontal area of the intertidal flats
A_{basin} = Horizontal area of the entire basin (channels and flats)
β = Constant of proportionality
H_m = Mean tidal range
D_c = The characteristic channel depth

The constant of proportionality β is not given by [Bosboom and Stive, 2011]. A similar relation for 22 tidal basins along the German Bight based on [Renger and Partenscky, 1974] is available, see equation 2.8. That relation does only relate the area of the flats to the total basin area. So it cannot be used to evaluate the effect of measures that increase the tidal prism without affecting the basin area. [Eysink, 1991] states that a similar relation as the one found by [Renger and Partenscky, 1974] is available for the South-west of the Netherlands. The result however is only available in a figure, see figure 2.4.

$$A_{flats} = A_{basin} - 0.025 {A_{basin}}^{3/2} \tag{2.8}$$

in which:

A_{flats} = Horizontal area of the intertidal flats
A_{basin} = Horizontal area of the entire basin (channels and flats)

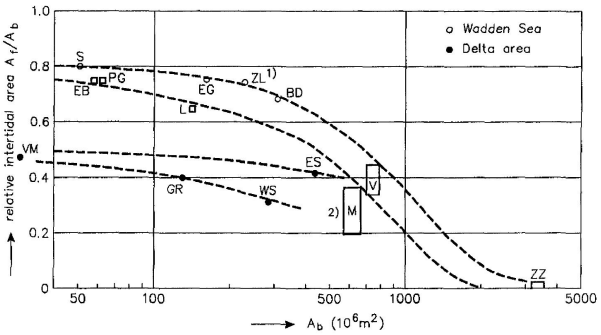

Figure 2.4: Relative area of intertidal flats, the Oosterschelde is indicated by ES. [Eysink, 1991]

Figure 2.4 gives a relation between the total basin area and the relative flat area, defined as A_{flats}/A_{basin}.

2.2.3 Shoal accretion/erosion

A study by [Das, 2010] focuses on the development of the Galgeplaat, which is a large intertidal flat in the central part of the Oosterschelde. The interaction between the channel and the shoal is investigated. In this study a more detailed model of the Galgeplaat is nested into the Kustzuid model. The boundary conditions for this detailed model consists of three open boundaries, two current boundaries and one water level boundary. These conditions are

generated by the Kustzuid model. Several parameters (wind, waves and tidal velocities) were varied to determine their importance. To evaluate the effect of higher tidal velocities [Das, 2010] manually multiplied the current boundaries by a factor 2, which is thought to represent the tidal flow before the closure of the Oosterschelde. [Das, 2010] concludes that higher flow velocities will enforce shoal build up. Besides this [Das, 2010] concludes that waves are the governing process for degradation of the Galgeplaat. Both during calm and storm conditions erosion of the inter-tidal area takes place. The degradation is not only due to wave breaking but also due to wave-induced currents that transport the suspended sediment from the shoal to the channel. In the present situation the shoals are degrading because the wave forcing did not change significantly with the construction of the Oosterschelde storm surge barrier while the building force, the tidal current, decreased.

Chapter 3

Analytical model

The objective of the analytical model is to gain insight in the hydrodynamic development of the Oosterschelde when the storm surge barrier is removed from the system. The emphasis in this chapter will be on the physical processes that play a role and not so much on the quantitative response of the system. When the Oosterschelde storm surge barrier is removed a new situation arises. The system of the Oosterschelde after the removal of the barrier is not as it was before because of the Philipsdam and the Oesterdam. Those dams were constructed after the finalization of the Oosterschelde storm surge barrier in order to retain the tidal amplitude in the basin. The analytical model will be used to calculate the hydrodynamic situation in this possible future situation. To model the Oosterschelde basin, the basin is split up in a network of branches. The branch network is explained more elaborately in paragraph 3.3.

3.1 Model description

The model is based on the shallow water equations:

$$B\frac{\partial h}{\partial t} + \frac{\partial Q}{\partial x} = 0 \tag{3.1}$$

$$B\frac{\partial Q}{\partial t} + \frac{\partial}{\partial x}\frac{Q^2}{A_s} + gA_s\frac{\partial h}{\partial x} + c_f\frac{|Q|\,Q}{A_s R} = 0 \tag{3.2}$$

Linear approximations of the continuity equation 3.1 and momentum equation 3.2 are used to get insight in the development of amplitude and phase of the wave along the basin. Non linear effects, like variation of the flow profile with the water level, are not included in the calculation. This implies that deformation of the wave is not calculated by the model, which is a drawback. The advantage of this method is that it generates the amplitude of the water level and the discharge of the system quickly. This makes it possible to calculate the effect of the interventions of the Deltaplan in a short time span. The assumptions made to linearize the equations are stated below:

- Low waves: the advective inertia term is small
- Low waves: the profile dimensions are constant in time
- Prismatic elements: the profile dimensions are constant in x-direction in every branch.
- Linear friction: the friction term is linearized under the condition of similar energy dissipation compared to the quadratic friction term.

Processing of these assumptions in the system of equations yields the linearized shallow water equations:

$$B\frac{\partial h}{\partial t} + \frac{\partial Q}{\partial x} = 0 \tag{3.3}$$

$$B\frac{\partial Q}{\partial t} + gA_s\frac{\partial h}{\partial x} + \kappa Q = 0 \tag{3.4}$$

The κ factor is a linear friction factor, which depends on the amplitude of the velocity or the discharge. Because the velocity amplitude is not known in advance iteration is necessary to solve the system of equations. [Battjes, 2002]

3.1.1 Input

The input of the model consists of two parts: Boundary conditions and five input parameters, that are stated in table 3.1.

Parameter	**Symbol**	**Unit**
Length of the branch	L	[m]
Storage channel width	B	[m]
Flow carrying channel width	B_s	[m]
Flow carrying depth	D	[m]
Friction factor	c_f	[-]

Table 3.1: Input parameters

The boundary conditions that are imposed at the sea boundary are based on tidal predictions of a spring and neap tide in January 2012. For the spring tide a water level amplitude of 1,66m is applied. The water level amplitude for neap tide is 1.21m. This information is obtained from [Actuele waterdata, 2012]. The angular frequency of the tidal wave ω=1.41e-4.

3.1.2 Calculation process

A summary of the calculation process is given here, for a more extensive explanation see appendix A. The calculation is based on the propagation of two sine shaped waves that are travelling through prismatic channels in opposite direction. The propagation is described by two general equations for the water level amplitude(eq 3.5) and the discharge amplitude(eq 3.6).

$$\tilde{\zeta}(x) = C_+e^{-px} + C_-e^{px} \tag{3.5}$$

$$\tilde{Q}(x) = \frac{i\omega B}{p}\left[C_+e^{-px} - C_-e^{px}\right] \tag{3.6}$$

The variable in these equations is p, this variable contains the wave number without the effect of friction k_0 and a complex factor that holds information about the variation of the amplitude and phase of the wave under the influence of friction σ.

$$p = ik_0\sqrt{1 - i\sigma} \tag{3.7}$$

For each branch a matrix containing the two general equations is stated. These matrices are added together in one matrix, which is solved for a given set of boundary conditions. This yields the water level amplitudes and subsequently the amplitudes of the discharge.

3.2 Characteristics of the system

In order to get insight in the characteristics of the system first a coarse model is used. The situation in 1971 is modelled, which means that the storm surge barrier, Philipsdam and Oesterdam are not present in the model. The Oosterschelde basin is modelled as a basin that is closed at one end. Practically this means that the basin is represented by one branch reaching from the ebb-tidal delta to the most south-eastern part, the present Markiezaatsmeer. The ratio of the water level amplitude at the closed end to the water level amplitude at the open end (amplification factor) can be determined by using two dimensionless parameters k_0L and σ. The relative basin length is represented by the parameter k_0L, the parameter σ represents the friction. The length of the branch is 60km, the representative width and flow carrying width are respectively 7500 and 2500m. The applied depth is 15m, which is the depth of the channels. The friction factor, c_f, is used to calibrate the result and has a value of 0.0015. Using a water level amplitude of 1.66m as boundary condition, a water level amplitude of 2.24m is found at the end of the basin. Measurements at Razernijpolder, which lies in the south-eastern part of the basin, indicate that the tidal amplitude is 2,34m. Therefore it can be concluded that this rough model approximates the measurements reasonably. As mentioned before the amplification of the tide can be described by two dimensionless parameters. When the relative basin length k_0L is close to a quarter of the wave length, then resonance occurs. The friction is represented by the factor σ. In order to understand the hydrodynamics of the Oosterschelde, the amplification factor is plotted against the relative basin length for several values of σ, see figure 3.1. The formula that is used to plot the amplification factor is given below (eq 3.8).

$$r = \frac{1}{|cosh(pL)|} \tag{3.8}$$

In figure 3.1 a red star is plotted to mark the situation in the Oosterschelde. It appears that the basin is shorter than a quarter of the wave length and that the damping is not very high. The wave amplitude is amplified to 1.35 times the value at the mouth. Figure 3.1 can also be used to make some predictions with respect to interferences in the basin. For example, shortening of the basin by construction of the Oesterdam will reduce the tidal prism. This implies that the representative discharge reduces and thereby directly the friction parameter σ. See appendix A for an explanation of the effect of the representative discharge in the friction parameter σ. Looking at figure 3.1 this means that the star shifts to the left, away from the resonance zone, and upwards, because of the reduced friction. In the parts of the basin with larger friction the amplification of the tide will be smaller i.e. the areas with large shoals, than in areas with large channels and relatively small flats. For clarity amplification throughout the entire basin is expected, however in areas with large shoals, i.e. the southeastern part, smaller amplification is foreseen.

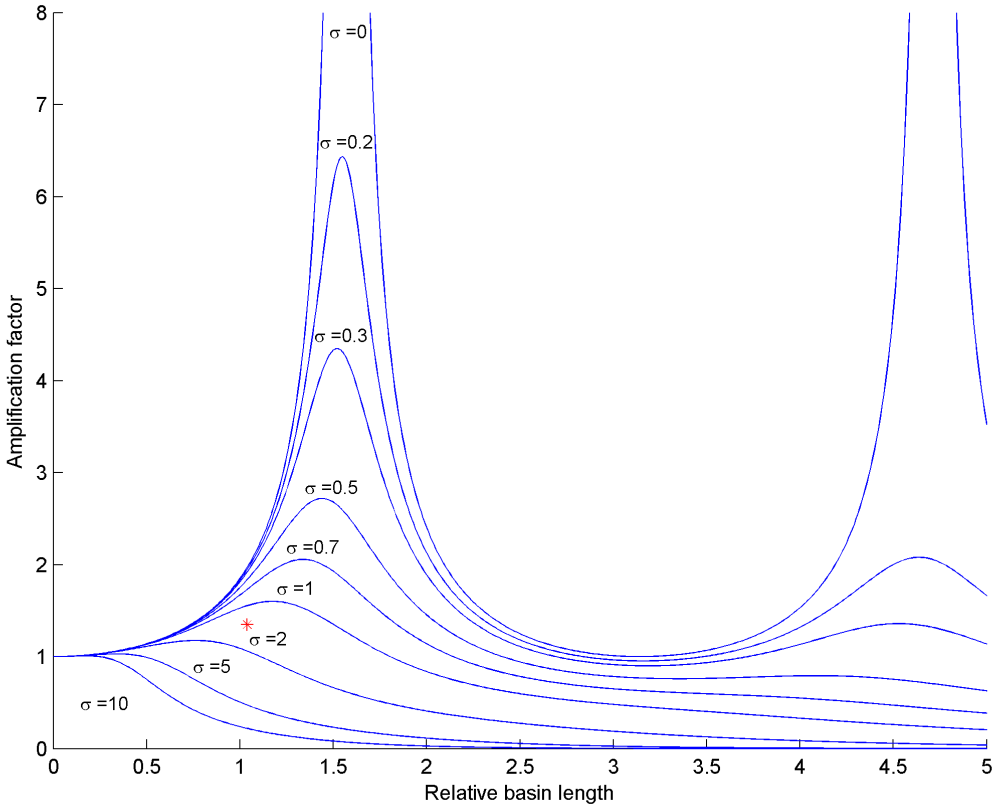

Figure 3.1: Amplification of the tide

3.3 Calculations

In this paragraph a more detailed calculation is made using a model with 55 branches, see figure 3.2. The total system is used to model the situation in 1971. The red parts can be excluded to model the Philipsdam and the Oesterdam.

In order to model the situation without Oosterschelde storm surge barrier but with the Oesterdam and Philipsdam, two situations must be calibrated. The situation in 1971 is calibrated to obtain the right friction factors for the area of the Oosterschelde storm surge barrier. At the same time the obtained set of friction factors must represent the present situation well. The Oosterschelde is divided in several sections of branches. For each of these sections a friction factor is determined. When the optimal set of friction factors is found, the new situation without the Oosterschelde storm surge barrier can be calculated. Both the sections and the input values are included in appendix B.

The boundary condition that is imposed on the points 1-7 is based on tidal predictions for January 2012. For the spring tide situation an tidal amplitude of 1.66m is used, for the neap tide situation an amplitude of 1.21m is applied. This boundary condition is applied for all the calculations.

3.3.1 Situation in 1971

The depth values for the calculation of 1971 situation are derived from the bathymetry of 1968. By this time the working islands Roggeplaat, Neeltje Jans and Noordland were constructed or

Figure 3.2: System of branches and observation points

under construction according to [de Bok, 2001]. The construction of the bed protection for the new dam was not started yet according to [Eelkema et al., 2011]. In this calculation the entire system of branches as shown in figure 3.2 is used because the Oesterdam and Philipsdam did not exist in 1971. The model is calibrated by varying the friction factor. The applied values for the friction factor are included in appendix B.1. The results of the calculation are compared to tidal measurements of a spring and neap tide in July 1971 [Historische waterdata, 2012]. The measurement data is available at several locations along the basin. The used locations are;

- Burghsluis, which is the measurement location closest to the inlet of the basin.
- Stavenisse, which is a measurement location in the central part of the basin.
- Rak Zuid, is located at the end of the northern branch near the Volkerakdam.
- Razernijpolder, is located in the southern branch.

These stations approximately correspond with the model points 28, 37, 51, 44 respectively, see figure 3.2. The model results in the mentioned points are presented in table 3.2.

3.3.2 Situation in 2008

The present situation is modelled by excluding the branches 51-55 from the model, which represents the Volkerak and the Markiezaatsmeer. Furthermore the barrier is implemented in the model by restricting the flow carrying width and depth at the location of the barrier. The barrier consists of 62 gates which are 42m wide. This makes the total flow carrying width 2600m. Given this information, the depth at the barrier can be calculated by dividing the total cross sectional area of the barrier by the width. This results in a water depth of 7m at the barrier. The depth values of the other branches are derived using the 2007 bathymetry. As

Station	Burghsluis	Stavenisse	Razernijpolder	Rak Zuid
Measured range [cm]	232	269	316	338
Calculated range [cm]	261	298	312	333
Difference (%)	12.5	10.8	-1.3	-1.5
Measured range [cm]	346	368	467	465
Calculated range [cm]	340	385	404	431
Difference (%)	-1.7	4.6	-13.5	-7.3

Table 3.2: Results for 1971: The upper values represent the neap tidal range, the lower the spring tidal range

mentioned the same set of friction factors is used, except for the branches at the barrier. The input values are included in appendix B.2.

The results of this calculation are compared to tidal predictions by [Actuele waterdata, 2012] from a spring and neap tide in January 2012. Several measurement locations that are used in the previous calculation were removed after the finalization of the storm surge barrier. Therefore other locations are used which are situated at approximately the same place. The used locations are: Roompot buiten, Roompot binnen, Stavenisse, Krammersluizen and Bergse Diepsluis West. These locations are visible in figure 3.2 The results are presented in table 3.3.

Station	Roompot buiten	Roompot binnen	Stavenisse	Krammer-sluizen	Bergse diepsluis west
Predicted range [cm]	245	217	256	267	293
Calculated range [cm]	253	245	270	273	287
Difference (%)	3.3	12.9	5.5	2.2	-2.0
Predicted range [cm]	325	282	324	330	372
Calculated range [cm]	338	317	349	353	371
Difference (%)	4.0	12.4	7.7	7.0	-0.3

Table 3.3: Results for 2012: The upper values represent the neap tidal range, the lower the spring tidal range

3.3.3 Calibration results

As mentioned before one set of friction factors is used for the calibration of the 1971 and present situation. The calculation of both situations did not result in an accurate representation of the measured tidal range. The difference between the model results and the measurements goes up to 13.5% for the 1971 situation. The maximal deviation in the simulation of the present situation is 13%. However when the friction factors are altered, one of the tides gets represented better at the cost of another tide (e.g. neap tide 1971 is represented better and spring tide 2008 worse). The set of friction factors that resulted from the calibration of the models might not be the optimal set. With respect to the friction factors some additional remarks can be made. The friction factors that are necessary to approximate the measurements lie between 0.001 and 0.006. That is what one would in general expect the friction factor to be. Next to this the friction factor is expected to vary from large at the mouth of the estuary to smaller at the back. The reason for this is that the flow velocities are higher near the inlet, which implies larger grains and more influence of bed forms (like ripples and dunes) at that region. When going

further inside the basin the flow velocities get lower, so finer sediment will be present there and less influence of bed forms is expected. The distribution that is expected is visible in the used set of friction factors, except for the region around the barrier in the calculations without barrier. The friction factors are lower in that case to calibrate the results. The reason for this may be the constriction by the working islands.

The tidal prism is computed by calculating the average water level range in each branch. The found range is multiplied by the length and width of the branch. Summing all the volumes yields the tidal prism. For the situation in 1971 a value of $1254 \cdot 10^6 m^3$ for the mean tidal prism is found and for 2008 a value of $901 \cdot 10^6 m^3$. This agrees with the values of $1230 \cdot 10^6 m^3$ and $880 \cdot 10^6 m^3$ stated by [Geurts van Kessel, 2004]. Considering the results, both water levels and tidal prisms, it is concluded that the model is useful for generating the qualitative response of the system.

3.3.4 Removal of the Oosterschelde barrier

The model of the present situation is adapted to model the situation without the Oosterschelde storm surge barrier, but with the Philipsdam and the Oesterdam. The applied depth values are the same as the ones used in the calculation of the present situation, except for the region near the barrier. At the location of the barrier a water depth of 25m is applied, see appendix B.3. The top of the bed protection, averaged over the protected area, is located at this depth. [Rijkswaterstaat, 1991b]. It is assumed that in case of removal of the barrier, the sill at the location of the barrier is removed. The bed protection on both sides of the barrier consists of block mats or asphalt with a layer thickness of approximately 30cm. For this hydrodynamic calculation it is assumed that a 30cm smaller water depth will not influence the results, meaning that for the hydrodynamic response it will not make a big difference whether the bed protection is removed or not. The applied water depth of 25m is found in the surrounding channels, both on the sea- and landward side of the barrier, when the scour holes are not taken in consideration. The results of this calculation can only be used to predict the tidal range just after removal of the barrier. In case the bed protection is removed the cross sectional area will grow larger and will thereby change the hydrodynamic regime in the Oosterschelde. The stated results clearly

Station	Roompot buiten	Roompot binnen	Stavenisse	Krammer-sluizen	Bergse diepsluis west
Predicted range [cm]	245	217	256	267	293
Calculated range [cm]	262	263	289	292	307
Difference (%)	6.9	21.2	12.9	9.4	4.8
Predicted range [cm]	325	282	324	330	372
Calculated range [cm]	354	355	390	394	414
Difference (%)	8.9	25.9	20.4	19.4	11.3

Table 3.4: Comparison of the present situation and the situation without barrier: The upper values represent the neap tidal range, the lower the spring tidal range

show an increased amplification of the tide as a consequence of the removal of the barrier. The decreased tidal prism due to the Oesterdam and Philipsdam causes smaller damping. The precise amount of amplification cannot be derived from those results because the model is not accurate enough for that purpose. But a safe conclusion is an increase in tidal range between 10% and 20% with respect to the present situation, see table 3.4. The predicted values are tidal predictions obtained from [Actuele waterdata, 2012], the calculated range is the range

that yields from the calculations. Looking at these results it appears that the tidal amplitude will get higher throughout the entire basin. The tidal range will not be as large as it was before the Delta project. The tidal prism calculated for this scenario is 982 million m^3. So the tidal prism will increase when the barrier is removed, but it won't be as large as it was before the closure of the Oosterschelde.

Chapter 4

Delft3D model setup

4.1 Model description

In this thesis a Delft3D model is used to investigate the effect of natural and human induced developments. Therefore a general description of Delft3D is given, followed by a description of the Kustzuid model. Special attention will be paid to the way the barrier is schematised in the model.

4.1.1 General description Delft3D

Delft3D is the integrated flow and transport modelling system of Deltares for the aquatic environment. This process based model consists of several modules that can be executed independently or in combination with one or more other modules. The hydrodynamic module Delft3D-FLOW forms the basis for the other modules: waves, water quality, morphological developments and ecology. The flow module can be used in two dimensional mode, (2DH, depth averaged) or three dimensional mode (3D). In both modes the non-linear shallow water equations are solved respectively in two or three dimensions. These equations are derived from the three dimensional Navier-Stokes equations for incompressible free surface flow. Delft3D-FLOW is able to calculate non-steady flow and transport phenomena that result from tidal and meteorological forcing on a rectilinear or a curvilinear, boundary fitted grid. It aims to model flow phenomena of which the horizontal length and time scales are significantly larger than the vertical scales. The flow is forced by tide at the open boundaries, with wind stress at the surface, pressure gradients due to free surface gradients (barotropic) or density gradients (baroclinic). Source and sink terms are included in the equations to model the discharge or withdrawal of water. [Deltares, 2011]

4.1.2 Kustzuid model

The Kustzuid originally is a WAQUA model that is operationally used to predict the water levels in the south-western delta. The WAQUA model version 3 is converted to a Delft3D model. This Delft3D model is used to perform the calculations for this thesis. The Kustzuid model is a part of the kuststrook fijn model. The Kustzuid model includes a part of the Dutch coast, limited in the south by the Belgian-French border and in the north by the head of Goeree Overflakkee. The model extends 65km in seaward direction. The following basins are included: Oosterschelde, Keeten, Mastgat, Zijpe, Krammer, (Volkerak, Schelde-Rijnkanaal, Zoommeer) and the Westerschelde+Zeeschelde. The basins between brackets are not active in the model, they are excluded by thin dams.

The resolution varies within the model, see figure 4.1, at the sea boundary the grid cell size varies from 300x900m to 1500x2500m. In the Ooster- and Westerschelde the resolution is higher with about 200x300m. On the inter-tidal flats in the back of the Ooster- and Westerschelde the resolution is 500m. Locally the grid cell size is 100m.

The model is forced by astronomic boundary conditions at the sea boundary and a discharge boundary condition in the Schelde river. [RWS Waterdienst and Deltares, 2009] The bathymetry is based on survey data from 2004, for the missing parts older data was used.

All the closure dams and groynes except the Oosterschelde storm surge barrier are modelled as thin dams. Thin dams are infinitely thin objects which prohibit flow exchange between two adjacent computational cells without reducing the total wet surface area and volume of the model. Because the Oosterschelde storm surge barrier is very important in this research it will be treated in a separate paragraph. In the operational SIMONA/WAQUA model a time step of one minute is applied. When that timestep is applied in the Delft3D model, locally maximum courant numbers of 14 occur in the channels of the Oosterschelde.

Figure 4.1: Total Kustzuid grid (left) and the Kustzuid grid of the Oosterschelde (right)

4.1.3 Bathymetry

The applied bathymetries are based on survey data by Rijkswaterstaat and is available on a 20x20m grid. As mentioned in paragraph 4.1.2 the Kustzuid grid is coarser. Transferring the survey data to the KustZuid model means that information is lost. Therefore several parameters are compared to literature in order to check the reliability of the model. Two new bathymetries are used in this thesis. One with sample data from 1983(basin) and 1984(delta), and the other with sample data from 2007(basin) and 2008(delta). The samples don't cover the entire KustZuid grid, therefore the missing parts are filled in with the original KustZuid bathymetry. The used bathymetry files are provided by [Eelkema, 2012]

First the total volume of the Oosterschelde is considered. Following the literature, i.e. [Louters et al., 1998], a hypothesis can be stated that no sediment is transported in or out of the basin. Using the two new bathymetries and the bathymetry from the KustZuid model the volumes are determined.

Year	Volume [m^3]	Difference [m^3]	Difference [m sedimentlayer]
1983	$1.051832x10^{10}$		
2004	$1.059961x10^{10}$	$81.29x10^6$	0.21
2008	$1.050284x10^{10}$	$-15.48x10^6$	-0.04

Table 4.1: Total water volume of the Oosterschelde obtained from the model data below a reference level of +20m NAP, differences are given with respect to 1983

The results stated in table 4.1 indicate that in the period 1983-2004 sediment has been exported. In the subsequent period 2004-2008 almost 97 million cubic metres have been imported. This suggests that sediment is transported through the barrier. When this is not the case there must be an error in one or more of the bathymetry files. The fact that the sediment balance is not closed is also noticed by [Haskoning, 2008], however a much smaller loss is found. Because the sand volume in the intertidal area is of importance for the calculation of the tidal prism, it is necessary to determine where the inconsistencies in the bathymetry are located.

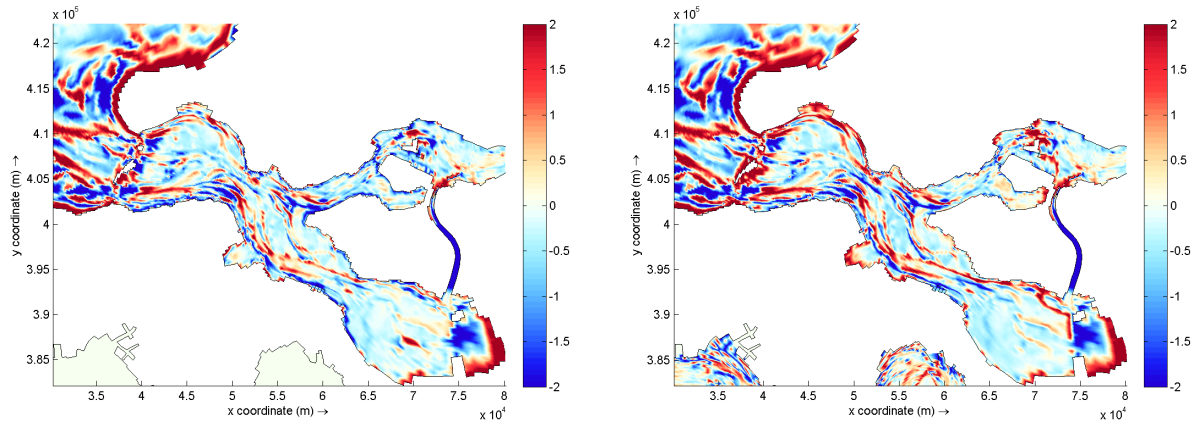

(a) Difference between 1983 and the original Kustzuid bathymetry

(b) Difference between 1983 and 2008

Figure 4.2: Changes in bathymetry, blue indicates erosion in metres, and red indicates deposition in metres

Year	Volume [de Bok, 2001]	Volume Delft3D model	Water surface area [de Bok, 2001]	Water surface area Delft3D model
1983	1.18	1.247	30.17	31.94
1994	1.19	-	31.00	-
2004	-	1.298	-	33.58
2008	-	1.237	-	31.52

Table 4.2: Comparison intertidal volume and area of the model with information by [de Bok, 2001]. Volumes are defined between NAP -2m and NAP +2m in 10^9 m^3, Areas are defined at NAP in 10^7 m^2

Table 4.2 shows that the volume of the model between NAP -2m and NAP +2m is bigger in Delft3D than what is found by [de Bok, 2001], the same holds for the water surface area at NAP. It is noteworthy that the water volume between NAP -2m and NAP +2m increases between

1983 and 1994 according to the [de Bok, 2001] while the water volume decreases between 1983 and 2008 using the Delft3D bathymetry. This means that the volume of the intertidal flats decreased according to [de Bok, 2001], while it increased according to the model.

When the loss of sand from the intertidal area is calculated, a loss of 10 million cubic metres is found by [de Bok, 2001] while the 2008 model bathymetry shows an increase of 10.1 million cubic metres. [van Zanten and Adriaanse, 2008] report that the sand volume of the intertidal area above low water reduced by 25,2 million cubic metres in the period 1985-2001. It is not clear what low water level is used by [van Zanten and Adriaanse, 2008]. When the original bathymetry of the KustZuid model is used, which dates from 2004 [RWS Waterdienst and Deltares, 2009], a sediment loss of 51.3 million cubic metres is found in the period 1983-2004. A low water level of NAP -2m is used to determine this value.

The same Delft3D bathymetry, from which the above stated values are derived, is used to plot figure 4.2a and 4.2b. In figure 4.2b sedimentation is visible at several locations: along the northern boundary of the grid in the basin, at the Philipsdam and Oesterdam and in the vicinity of the barrier. It is noted that the one of the used bathymetries contains data in the Markiezaatsmeer and Volkerak, this is visible in figure 4.2, these regions are excluded from the model. A closer look at the model bathymetries learns that sedimentation along the entire boundary of the Oosterschelde is found in the 2008 model with respect to the KustZuid bathymetry. The difference plot between 2004 and 2008 (figure 4.3) shows this clearly. The expected pattern of erosion on the flats and sedimentation in the channels is observed in the model bathymetries for all periods when looking at the center of the Oosterschelde. The transition from the basin to the dikes seems to be the problem.

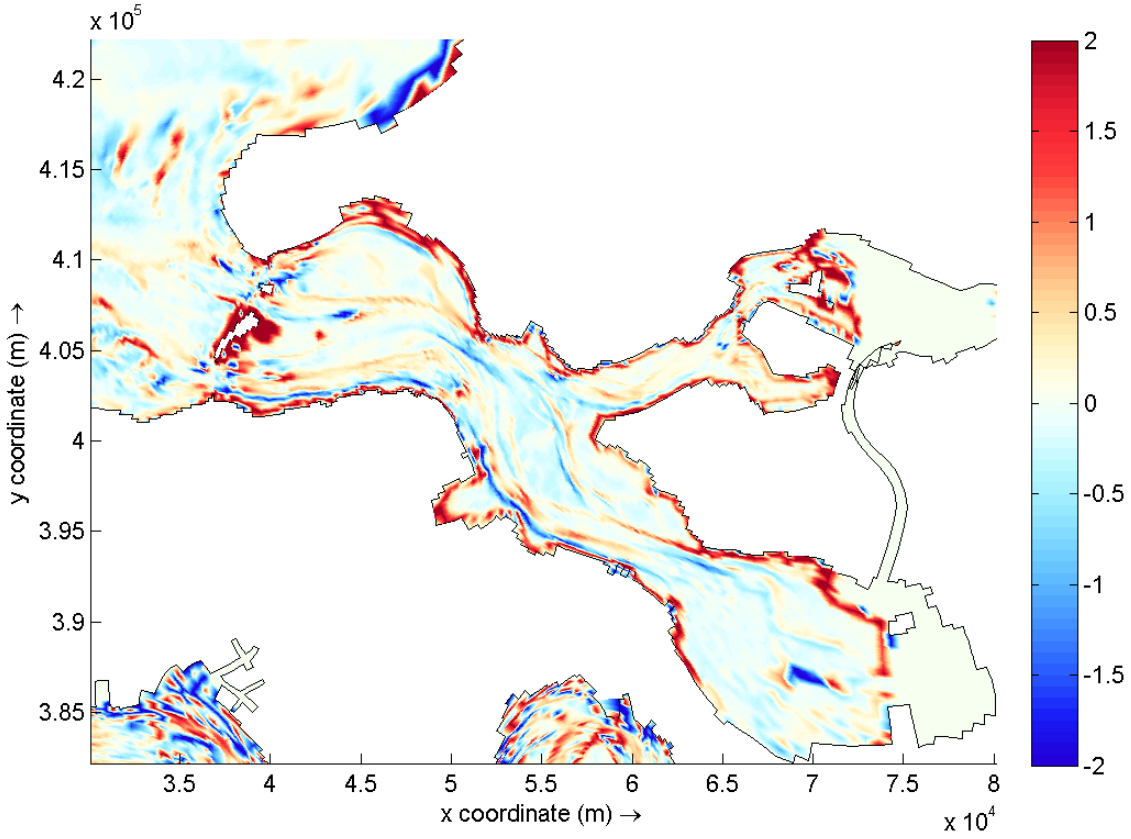

Figure 4.3: Difference between the KustZuid and 2008 bathymetry, blue indicates erosion in metres, and red indicates deposition in metres

To get a better overview of the bathymetric changes hypsometric curves are plotted, based on the model bathymetries and measurements, the curves are included in figure 4.4. These curves make it possible to allocate the changes to a certain depth. Figure 4.4a shows the watervolume in layers of one metre thick, i.e. the volume at label -30m NAP is the volume between -30m NAP and -29m NAP. From this figure it appears that the transfer from the measurements to the Kustzuid grid introduces an error. The model bathymetries have smaller volumes than the measurement curves in the deeper parts of the basin. In the region above -7m NAP larger water volumes are found in the model bathymetry. With regard to the model bathymetries, the Kustzuid bathymetry shows an increase of water volume in the intertidal zone with respect to the 1983 model bathymetry. The 2008 model bathymetry however shows a decrease of the water level in this zone, which indicates accretion in this zone. The cumulative water volume, included in figure 4.4b, shows that the measurements contain a larger water volume than the model bathymetries. It is noted again that the sediment balance based on the Delft3D bathymetries is not closed.

Based on the above stated findings it can be concluded that the 2007/2008 bathymetry does not represent the situation well. With respect to the bathymetry files several remarks have to be made. Because certain parts of the Oosterschelde are surveyed scarcely and in different periods, the bathymetry files are composed of several surveys. Next to this different survey methods were applied in 1983 than in 2007 and 2008 for example. This introduces errors in

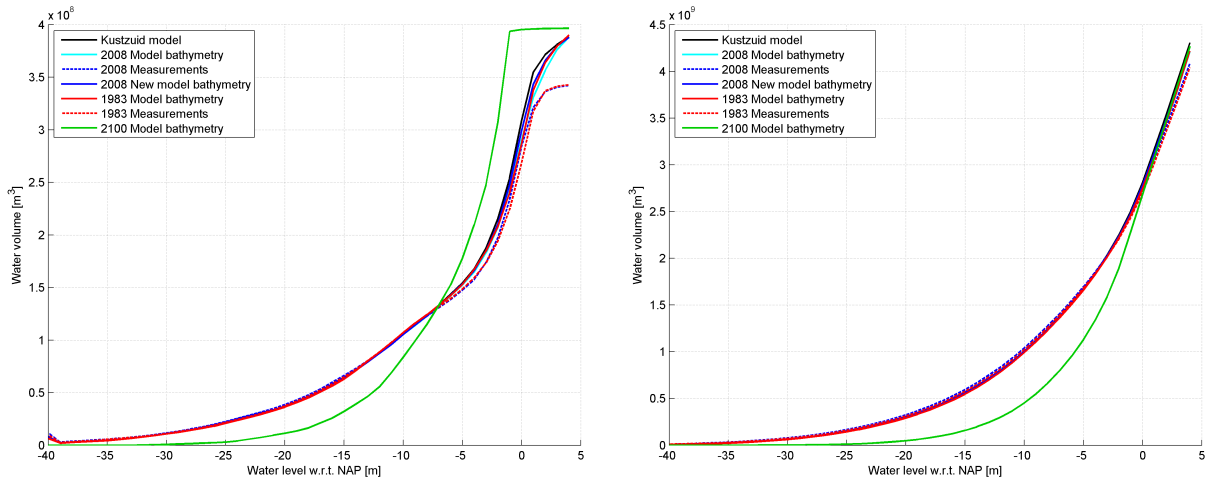

(a) Water volume per layer

(b) Cumulative water volume

Figure 4.4: Hypsometric curves of the Oosterschelde basin

the bathymetry files. Subsequently the samples obtained during the surveys are transferred to the KustZuid grid. As mentioned before this results in a loss of information which introduces an additional error. This is probably the cause of the surplus of sediment on the edges at the domain. Because the amount of sediment in the inter-tidal area is of importance for the calculation of the tidal prism an attempt is made to improve the 2007/2008 bathymetry. The depth in the outer two cells along the entire grid is replaced by the values from the KustZuid bathymetry. The hypsometric curve of this new bathymetry is also plotted in figure 4.4, with the label 2008 New model bathymetry. It shows that the sand volume in the intertidal area has decreased. When the sediment loss is calculated a volume of 24.96 million cubic metres is found. This value corresponds better to the value of 25,2 million cubic metres stated by [van Zanten and Adriaanse, 2008]. Looking at the sediment balance of the entire Oosterschelde a 'sediment import' of approximately 40 million cubic metres is found with respect to the 1983 bathymetry. The new bathymetry is representing the situation better and is used in the calculations instead of the original 2008 bathymetry.

4.1.4 Oosterschelde storm surge barrier in the Kustzuid model

Because the aim of this research is to gain insight in the situation without barrier it is important to remove the barrier from the model completely. To be able to do this it must be clear how the barrier is implemented in the model. The Oosterschelde barrier consists of two parts in general, the piers and gates and a bed protection. The bed protection horizontally extends to 550-650m from the centreline of the barrier on both sides. The Oosterschelde storm surge barrier restricts the flow because the cross-sectional area decreased drastically. The piers cause a loss of energy at the barrier.

A hydraulic structure generates an energy loss in Delft3D. Hydraulic structures, like the piers and gates of the Oosterschelde storm surge barrier, can be defined in several ways in the model. At the hydraulic structure an extra friction term is added to the momentum equation, to parameterise the extra loss of energy. The Oosterschelde storm surge barrier is modelled with porous plates and a barrier in the Kustzuid model. For the porous plates a quadratic friction term is implemented in Delft3D-FLOW. For a porous plate an energy loss coefficient c_{loss-U} should be specified. This leads to a source or sink of momentum in a certain direction.

[Deltares, 2011]

$$M_\xi = c_{loss-U} \frac{U_{m,n} |U_{m,n}|}{\Delta x} \tag{4.1}$$

In the original model (SIMONA/WAQUA) the barrier is modelled in a different way. The grid in this model is defined in such a way that three gates fit in one grid cell. Within the SIMONA model it is possible to define a barrier file. In the barrier file three properties are defined for each grid cell: The sill depth, the gate height and the barrier width. The part of the water column that is blocked (from the bed to the defined level) is defined by the sill depth. The gate height gives the height of the gates that can be closed. The width on top of the sill is restricted by the barrier width, a percentage is set to model the width restriction. Besides this, contraction coefficients are used to improve the water level predictions. The contraction coefficients are specified for sub- and supercritical flow at flood and ebb currents. An extra coefficient is added for the contraction by the piers. When the model was converted to Delft3D the decision was made to use porous plates and a barrier file to model the barrier. However there is no documentation describing this conversion. The Delft3D model makes use of the same grid as the WAQUA/SIMONA model.

The Oosterschelde barrier restricts the cross sectional area in the horizontal and the vertical direction. In the Delft3D model the width is reduced to 3059m by adding some dry points and thin dams. This width is approximately the same as in reality. The depth, at the gridline with the thin dams, is restricted in the model by a barrier file; A barrier is represented by a vertical gate from the water level down to a certain level. This barrier file only blocks a part of the vertical. There is no facility to add an energy loss in a barrier file, that is probably the reason the porous plates were implemented. The additional loss that is necessary to model the barrier is added by using porous plates on both sides of the barrier. Both the barrier and the porous plates are subgrid structures that are defined on a grid line. [Deltares, 2011] states a formulation that can be used to obtain the right loss factor for the porous plates:

$$c_{loss-U} = \frac{N C_{drag} d_{pile}}{2\Delta y} \left(\frac{A_{tot}}{A_{eff}} \right)^2 \tag{4.2}$$

In which N is the number of piles per grid cell, C_{drag} is a drag coefficient, d_{pile} is the diameter of the pile, Δy is the grid size, A_{tot} is the total cross sectional area of one grid cell and A_{eff} is the effective wet cross sectional area of one grid cell. Porous plates are in general used to model bridges or current deflection walls for example. Physically this means that there are several piles that reduce the cross sectional area of the cross section in a horizontal way. This is the case with the Oosterschelde barrier in the part above the sill beam. In the area below the sill beam the cross section is completely blocked by sand and rock. When equation 4.2 is applied to the cross section of the Oosterschelde barrier above the sill beam a loss factor of 0,084 results. In this calculation the used width is at the place where the flow is restricted by dry points and thin dams. When formula 4.2 is applied to the total cross section of the barrier including the sill, a loss factor of 0.47 is found. The underside of the barrier for this calculation is estimated at 20m, 10m of this height is blocked by the sill, the other 10m of height is constricted by the barrier piers. The porous plates are defined on both sides of the smallest cross section and over the entire depth. In the Kustzuid model a loss coefficient of 2,3 is applied. This does not agree with the calculated value at all and raises the question if the loss coefficient of 2,3 has a physical basis. It can be concluded that the porous plates are not used in the way [Deltares, 2011] suggests. The porous plates are probably used to calibrate the model, but once again no literature is available to confirm this.

Summarizing: in reality the channels are restricted in a horizontal direction. That restriction is modelled well in Delft3D. The vertical restriction in reality is a sill from the channel floor up

to a certain level, in the model however the depth is restricted by gates that close the channel from the waterlevel down. In reality energy is dissipated by the piers on top of the sill. In the model the porous plates are defined over the entire water column and not at the location of the piers.

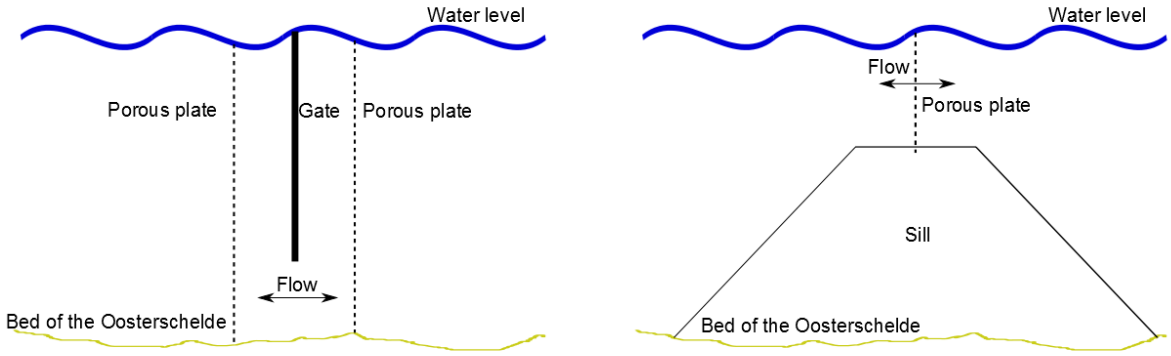

(a) Kustzuid model **(b)** New schematization

Figure 4.5: Barrier schematization

Because the accuracy of the barrier schematisation is moderate, an attempt is made to improve the barrier schematisation. The accuracy is described in paragraph 5.2.1 in detail. In the new schematization, the barrier file is removed from the calculation because simulations with closed gates are not performed in this thesis. The bathymetry at the location of the barrier is adapted to the sill depths as they are defined in the SIMONA model. On top of this 'sill' a porous plate is defined to model the energy loss by the piers and the contraction of the flow. Several loss factors of the porous plates are tested to get an optimal result. The optimalisation is discussed in chapter 5.

The bed protection is not included in the model, the effect of the bed protection however is visible in the bathymetry, because this part of the bed did not erode in the preceding decades. The bathymetry in the model includes the layer of bed protection, but not the sill at the location at the barrier. The water depths in the region of the barrier are assumed to be representative for the situation without the barrier in the hydrodynamic calculations. In case a morphodynamic calculation is to be performed extra attention has to be paid to this subject.

4.1.5 Observation points

Two new observation points are defined in the model to obtain better results. Station Roompot buiten (RPBU) is replaced by a observation point in the middle of the roompot channel at the seaside of the barrier. Roompot binnen (RPBI) is replaced by a observation on the Oosterschelde side in the middle of the roompot channel. A discontinuity in both the amplitude and phase of the components, that was probably caused by the location and thin dams that surrounded the official observation points, is eliminated by relocating these observation points.

4.2 Simulations

This paragraph describes the scenarios that are used to investigate the effect of removal of the Oosterschelde barrier. The adaptations that are made to the Kustzuid model are stated for each scenario. Besides that explanations of the intended goals for each simulation are set out.

4.2.1 General settings

The general settings that are used in every calculation are stated in table 4.3. A timestep of 0.5 minutes is chosen after [Das, 2010] to reduce the courant numbers. With the applied timestep the courant number is limited to a maximum of 7. Two spring neap cycles are simulated in order to improve the accuracy of the tidal analysis.

Parameter	Value	Unit
Delft3D version	3.42.00.17790	-
Timeframe		
Reference date	01-01-2000	-
Simulation start time	01-04-2008 00:00:00	-
Simulation stop time	30-04-2008 00:00:00	-
Time step	0.5	Minutes
Boundaries		
Type of open boundary	Astronomic water level condition	-
Physical parameters		
Gravity	9.813	m/s^2
Water density	1023	kg/m^3
Bed roughness (Manning)	0.025	$s/m^{1/3}$

Table 4.3: General model settings

4.2.2 Scenario 1: Reference

This scenario is simulated to be able to compare the results of the following scenarios to the present situation. For this calculation several adaptations were made to the Kustzuid model. The original 2004 bed is replaced by the 2008 bathymetry as explained in paragraph 4.1.3. The reason for the new depth values is the interest in the effect of the changes in bathymetry since the closure of the Oosterschelde. The effects of these changes are expected to become more distinct when the time interval between the simulated bathymetries gets bigger. Therefore the most recent data is used to model the present situation. Furthermore the new schematization of the barrier with the adapted bathymetry is used (see paragraph 4.1.4). Finally the friction factor of the porous plates is set to 1.7 because, after several calibration calculations, this appeared to represent the present situation in the best way. This will be elaborated further in chapter 5.

4.2.3 Scenario 2: Present situation without barrier

By removing the barrier, both the sill in the bathymetry and the porous plate, from the model and using the same bathymetry as in the reference scenario the present situation without the barrier is modeled. The removal of thin dams, dry points and the porous plates are the only adaptations made compared to the reference scenario. This scenario provides information to check the calculations made in chapter 3 and moreover flow velocities that are necessary to

evaluate if shoal build up will occur again. In figure 4.6 the adaptations near the barrier are depicted. In red the porous plate, in yellow thin dams and the green cells are dry points.

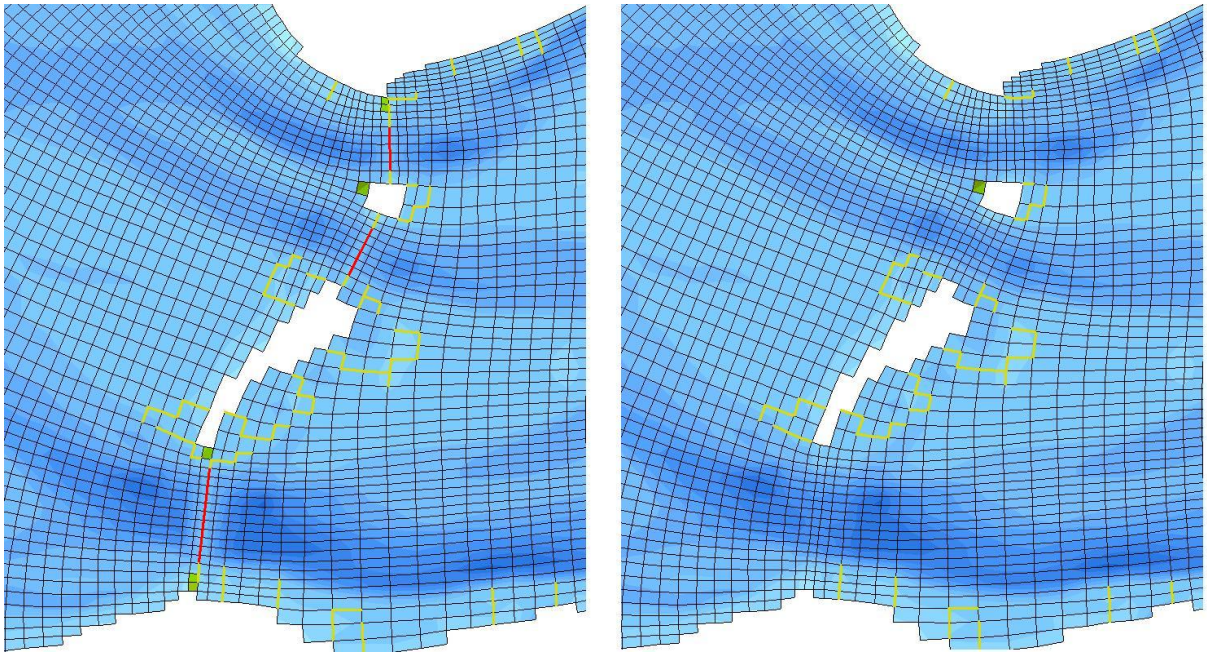

Figure 4.6: Model adaptations to represent the situation without barrier

4.2.4 Scenario 3: Old bathymetry

By duplicating scenario 2 and replacing the bathymetry by a bathymetry dating from before the closures, scenario 3 is obtained. Depth values from 1983 inside the basin and from 1984 on the ebb tidal delta are used. The survey data inside the basin from 1983 is more complete than the data from 1986, therefore the 1983 bathymetry is used. The bed level change between the depth files that are used as input for the model is shown in figure 4.2b. The erosion of the inter-tidal flats and shallowing of the channels is visible.

The aim of this scenario is to evaluate the effect of the changed bathymetry on the distortion of the tidal wave. By leaving the Philipsdam and Oesterdam in the model the change in the distortion of the tidal wave is solely attributable to the replaced bathymetry. It must be noted that this is a situation that never existed.

4.2.5 Scenario 4 & 5: Future situation

In these scenarios the bathymetry is adapted to model the situation in the year 2100. The crude assumption is made that all the intertidal area is lost by then. All the sediment above -2m NAP (in the bathymetry used in scenario 1 and 2) is removed and evenly spread in the channels. The underlying assumption for this is that no sediment transport through the barrier occurs. The hypsometric curve of this simulation is included in figure 4.4. The decrease of the water volume in the deeper parts and the increase in the intertidal zone is visible. The plot of the cumulative water volume, figure 4.4b, shows that the total volume of the Oosterschelde is equal to the 2008 bathymetry. This scenario gives insight in the changes in tidal asymmetry due to the loss of intertidal area. A simulation (4) with the barrier will be executed which provides an approximation of the situation in 2100. Subsequently a run without barrier will be executed

(5), which gives information on the development of the basin when the barrier is removed in 2100.

4.2.6 Scenario 6 & 7: Realignment of the Oosterschelde

In scenario 6 & 7 the dikes are set back, see figure 4.7, to model large scale realignment of the Oosterschelde. The bed dates from 2008 in both simulations, the added grid cells are set at a depth of 0m NAP. Scenario 6 includes the barrier, in scenario 7 the barrier is removed. These scenario's are used to investigate whether it is possible to enhance the growth of intertidal area by large scale realignment of the basin.

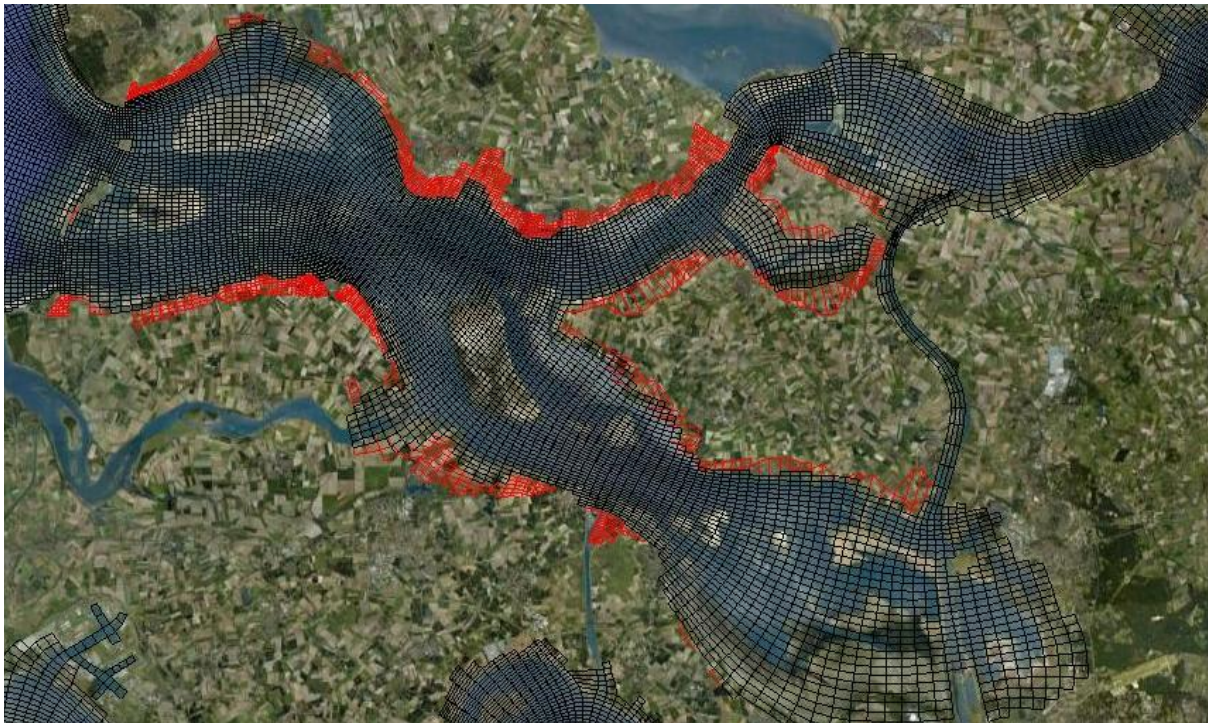

Figure 4.7: Realignment of the Oosterschelde

Chapter 5

Delft3D model results

In this chapter the Delft3D model will be used to predict the hydrodynamic conditions for the simulations described in paragraph 4.2. The indicative parameters for tidal asymmetry as explained in paragraph 2.2.2 are used in this chapter to analyse the results of the simulations. The output of Delft3D is analysed with the t_tide tool, a short description of t_tide is given in paragraph 5.1. The obtained amplitude and phase information is used to evaluate the distortion of the tidal wave. In paragraph 5.2 the asymmetry of the water level signal is given. The asymmetry of the discharge signal is elaborated in paragraph 5.3. The observation points and monitoring cross sections at which the output is generated are depicted in figure 5.1.

Figure 5.1: Overview of the applied observation points and monitoring cross sections

5.1 Approach of the analysis

T_tide is a matlab script that performs a classical tidal harmonical analysis including error estimates. The phase and amplitude estimates are made with algorithms by using complex algebra. T_tide uses an automated selection algorithm to select the constituents. In this automated selection, a basis of all astronomic and 24 of the most important shallow-water constituents are gathered together. The input timeseries is modelled as a sum of N of the selected constituents by t_tide [Pawlowicz et al., 2002]. The output is an estimate of the amplitude, the amplitude error, the phase and the phase error. For the error estimates a confidence interval of 95% is used. The input for t_tide consists of the output time series of the Delft3D calculations, a time interval of 0.5 minutes is used in the analysis. In the following indention the errors made by t_tide are stated. For clarity, those errors are not based on comparison with measurements but have to do with the confidence interval of t_tide. For the M_2, M_4 and M_6 component discharge amplitude errors smaller than one percent are found. The discharge phase error amounts less than 1 degree for the M_2 and M_4 components. For the M_6 values between 1 and 2 degrees are found. The water level amplitude errors are smaller than one percent for the M_2 component, for the M_4 component values around two percent are found. The M_6 component shows values between 2 and 7 percent. The phase error is smaller than one degree for M_2, around one degree for M_4 and between 2 and 7 degrees for M_6.

5.2 Water level

5.2.1 Calibration

A simulation was run with the original Kustzuid model with the 2007/2008 bed levels. This resulted in too large deviations of the water level from measurements, obtained from [Historische waterdata, 2012]. Therefore the decision was made to adapt and calibrate the model for the water level as described in paragraph 4.1.4. In order to calibrate the water level, several simulations with different Manning friction coefficients and with a range of loss factors for the porous plates were tested. The loss factors that were calculated in paragraph 4.1.4 are too low to accurately represent the barrier. Contrary to the WAQUA model the Delft3D model does not use extra coefficients to model the flow contraction that is caused by the barrier. The results obtained by varying the loss factor of the porous plates indicate that porous plates are not the right method to model the barrier. The flow contraction is not modelled well by the porous plates, which is probably the reason that the loss factor is higher than the calculated values. Finally the same Manning coefficient (0.025) as in the original Kustzuid model is chosen. For the loss factor of the porous plate a value of 1.7 is used.

The amplitude and phase of the M_2 component are both represented better by the adapted model. The maximum error in the amplitude is 2.4 percent and the maximum phase difference is 9.7 minutes or 4.7 degrees. The development of the amplitude and phase are shown in figure 5.2. The labels on the x-axis indicate the stations with on the left a station at sea and on the right stations at the end of the southern and northern branch close to the Oesterdam and Philipsdam, Bergse diepsluis west and Krammersluizen respectively, see figure 5.1. The label barrier consists of two measuring stations, Roompot buiten and Roompot binnen, that are located on both sides of the barrier. From this figure it appears that both the amplitude and phase of the M_2 component are modelled better by the adapted model than by the original Kustzuid model. The leap at the barrier is reduced significantly. Figure 5.3 shows the properties of the M_4 tidal component. The amplitude is slightly underestimated by the model outside the Oosterschelde and at the barrier. The new schematization of the barrier amplifies the error at station Roompot binnen considering the amplitude, but the other stations in the basin show

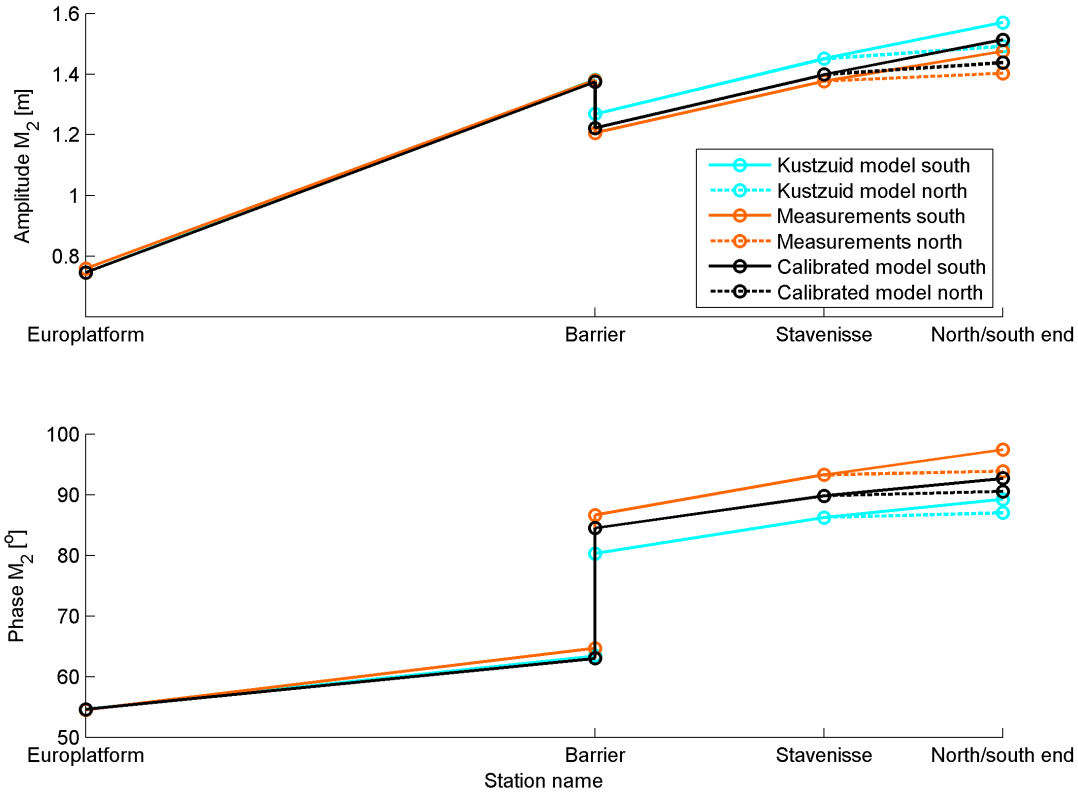

Figure 5.2: M_2 component: Water level amplitude and phase of the calibrated model, the Kustzuid model and measurements

better results. The phase is represented well out at sea and just outside the Oosterschelde, but at the barrier a large jump occurs. Variation of the friction coefficient and the loss factor of the porous plates improved the results but did not solve this problem completely. The phase difference that is caused by the barrier stays more or less constant in the basin.

An important remark is that the trend of both the amplitude and the phase is modelled well. It appears that the schematization of the barrier in the Kustzuid model and the improved model is not able to reproduce the development of the phase of the M_4 component well. Because the M_4 component is used as a measure of the tidal asymmetry, it is important to keep this in mind. The jump at the barrier will influence the parameters used to indicate the tidal asymmetry.

The phase of the M_4 component is decaying on the ebb tidal delta in contrast to the situation without barrier. It must be noted that the M_4 component of the tidal wave is not a propagating wave like the M_2 component, but a component that originates from non-linear interaction with the M_2 component.

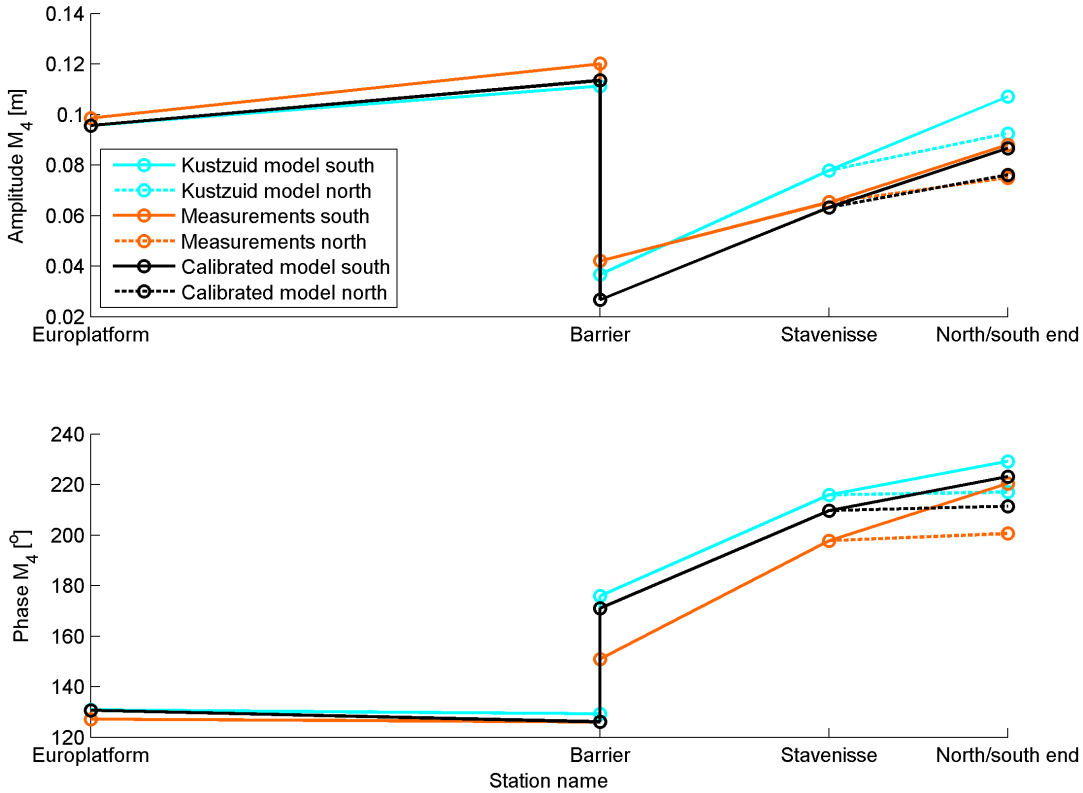

Figure 5.3: M_4 component: Water level amplitude and phase of the calibrated model, the Kustzuid model and measurements

The results are substituted in the parameters described by [Friedrichs and Aubrey, 1988] as explained in paragraph 2.2.1. From figure 5.4 it appears that the magnitude of the tidal asymmetry does not match the measurements precisely, however the deviations are not that large. The error that was made in the phase of the M_4 component is reflected in the relative sea surface phase. The trend of the relative phase is right, but the magnitude is not. The ratio of the amplitudes is larger than zero, so the tide is distorted. The implication of this is sediment transport in the direction that is indicated by the relative phase. At the barrier the relative phase based on the measurements is larger than zero which means that the system is flood dominant. Inside the basin however the relative phase gets negative, making the system an ebb dominant system. The same behaviour is observed for the branch that splits of to the Philipsdam in the north. The model results, indicated by the black line, show ebb dominance for the entire Oosterschelde because of the error in the M_4 component. Therefore it is important to keep this error in mind when comparing any of the following scenario's with the reference scenario (2008 bed with barrier in the figures).

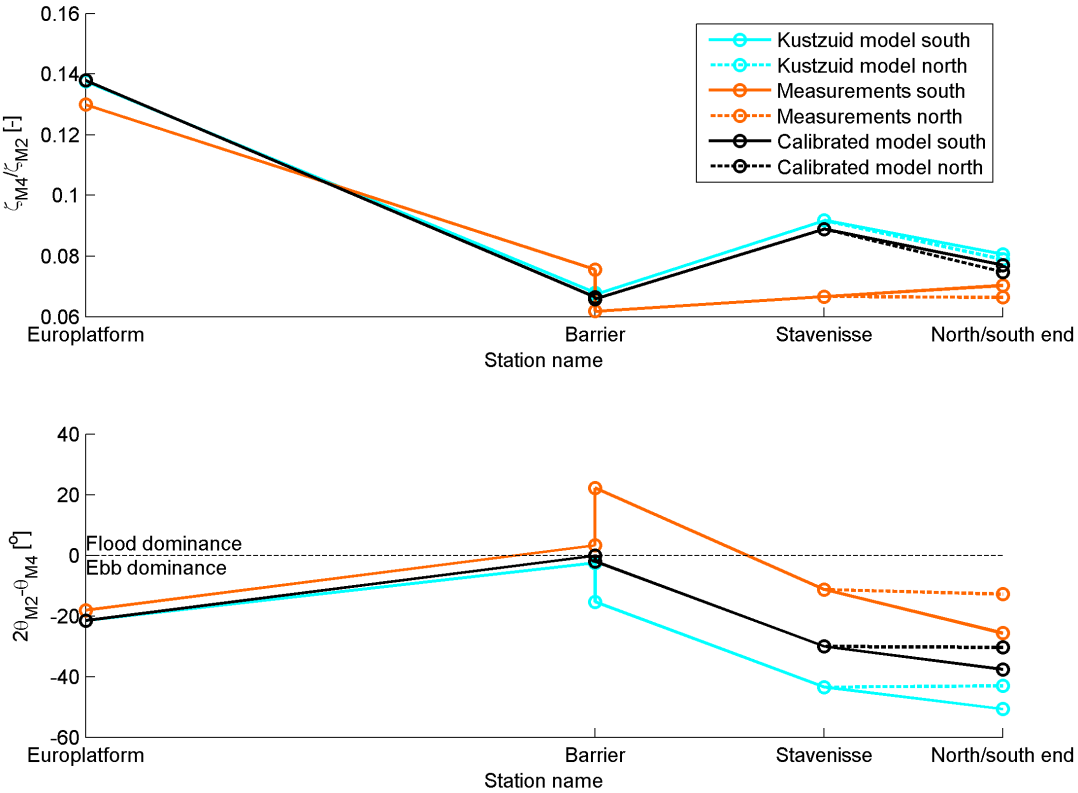

Figure 5.4: Water level parameters indicating tidal distortion of the calibrated model, the Kustzuid model and measurements. Upper panel: amplitude ratio, Lower panel: relative phase

5.2.2 Scenario 2 & 3: Situation without barrier

When the barrier is removed a larger tidal range is expected in the basin. Figure 5.5 indeed shows a larger tidal range. The results are compared to the outcomes of the analytical model. The average of the spring and neap values are used for the comparison. They turn out to be approximately the same. The deviations are in the order of 5-10 centimetre. In general the Delft3D model gives slightly lower values than the analytical model.

Looking at figure 5.5 the jump at the barrier should no longer be present in the results when the barrier is removed, this holds both for the phase and the amplitude of the M_2 component. However there still is a small delay of approximately two degrees visible in the M_2 phase for the 2008 calculation, this delay is constant in the entire basin. A closer look at the bathymetry learns that the bed in 2008 constricts the flow in a horizontal direction more than in the 1983 bathymetry. The channel width is smaller in the 2008 bathymetry compared to the 1983 bathymetry. This explains the phase leap in figure 5.5. Moreover the phase of the M_2 component shows that the tidal wave is propagating slower when the barrier is removed. This holds for both the ebb-tidal delta and the basin. Apparently the changes also influence the wave propagation on the ebb-tidal delta.

Figure 5.6 shows the amplitude and phase of the M_4 component. The amplitude of the M_4 component is higher in the basin when the barrier is removed. This can be explained with the theory of [Friedrichs and Aubrey, 1988]. They state that the distortion of the wave is a relation between two ratios, the ratio between the volume of intertidal storage and the volume of the channels and the ratio between the amplitude and waterdepth, see figure 2.3. Removal of the barrier means an increase of the amplitude of the wave over the waterdepth. This causes an increased distortion of the wave, which explains the larger M_4 component. Just like the M_2

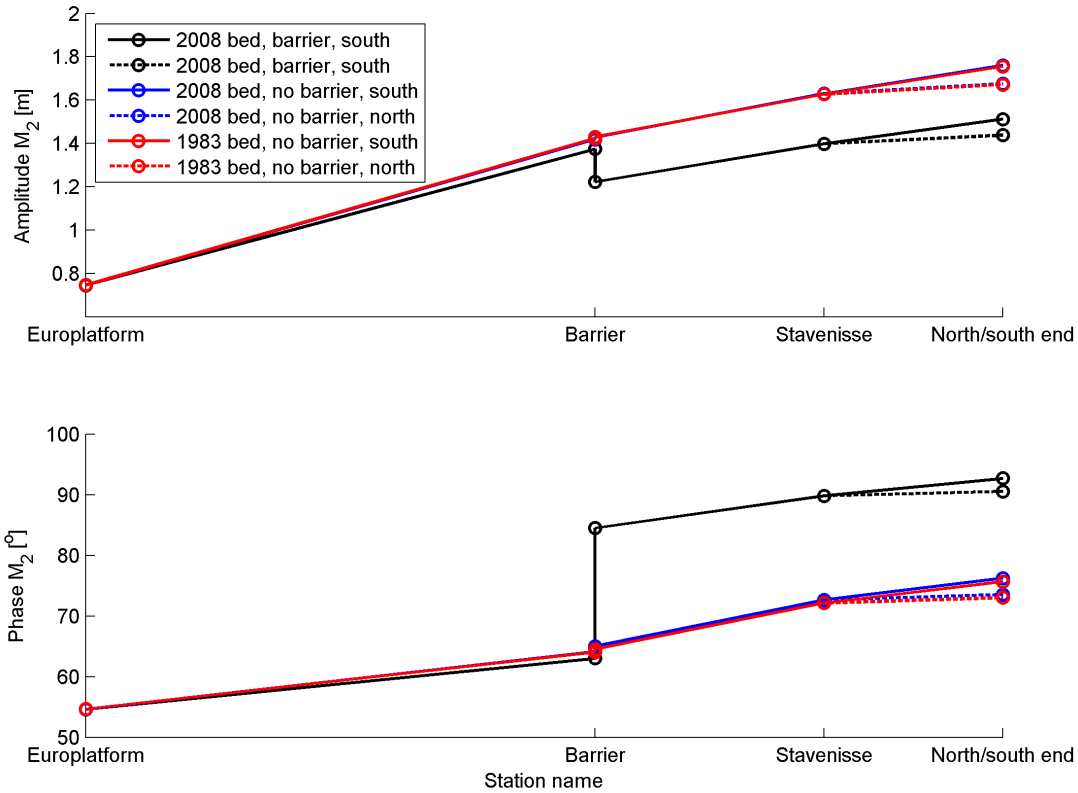

Figure 5.5: M_2 component: Water level amplitude and phase of scenario 1,2 & 3

component the jump at the barrier is no longer present. The M_4 phase shows a small delay at the barrier just like the M_2 component. This can partially be explained by the fact that the two values are plotted at one point in the figures, while there is a distance between the points in reality. Besides this it is possible that the M_4 component is influenced by the islands that restrict the flow in a horizontal direction. Because of the uncertainties in the M_4 component around the barrier in the model, it is not possible to explain the phase delay in the M_4 component as plotted in figure 5.6 completely.

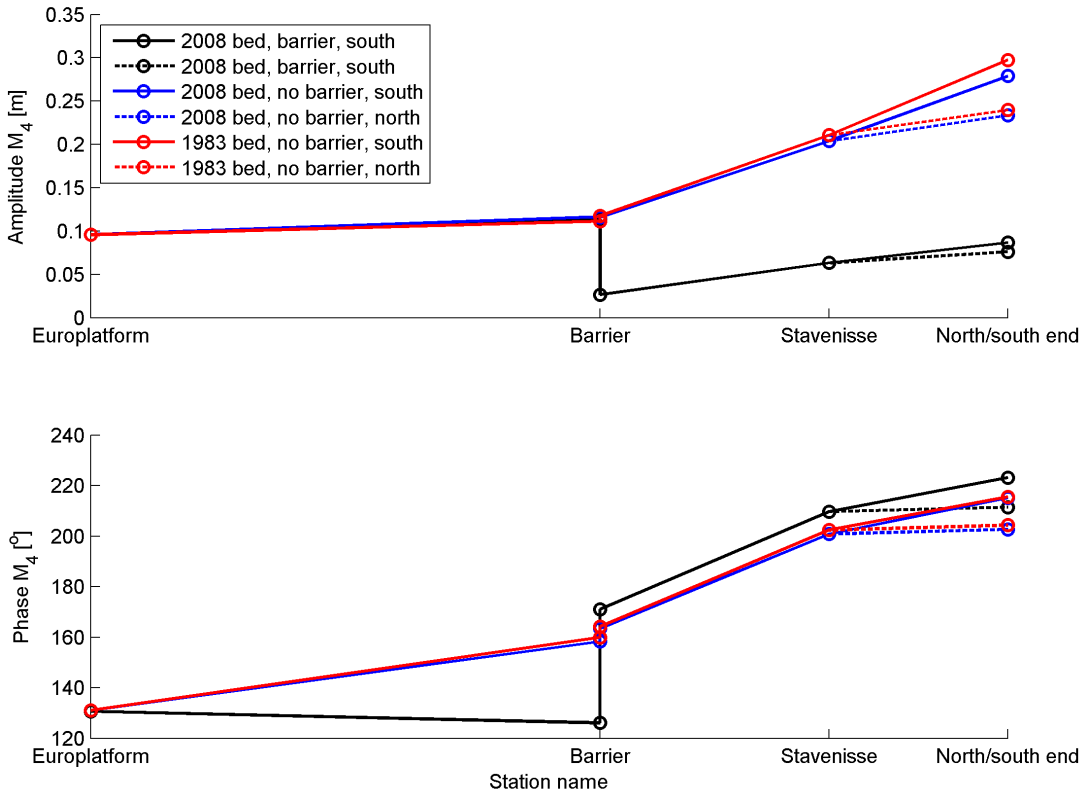

Figure 5.6: M_4 component: Water level amplitude and phase of scenario 1,2 & 3

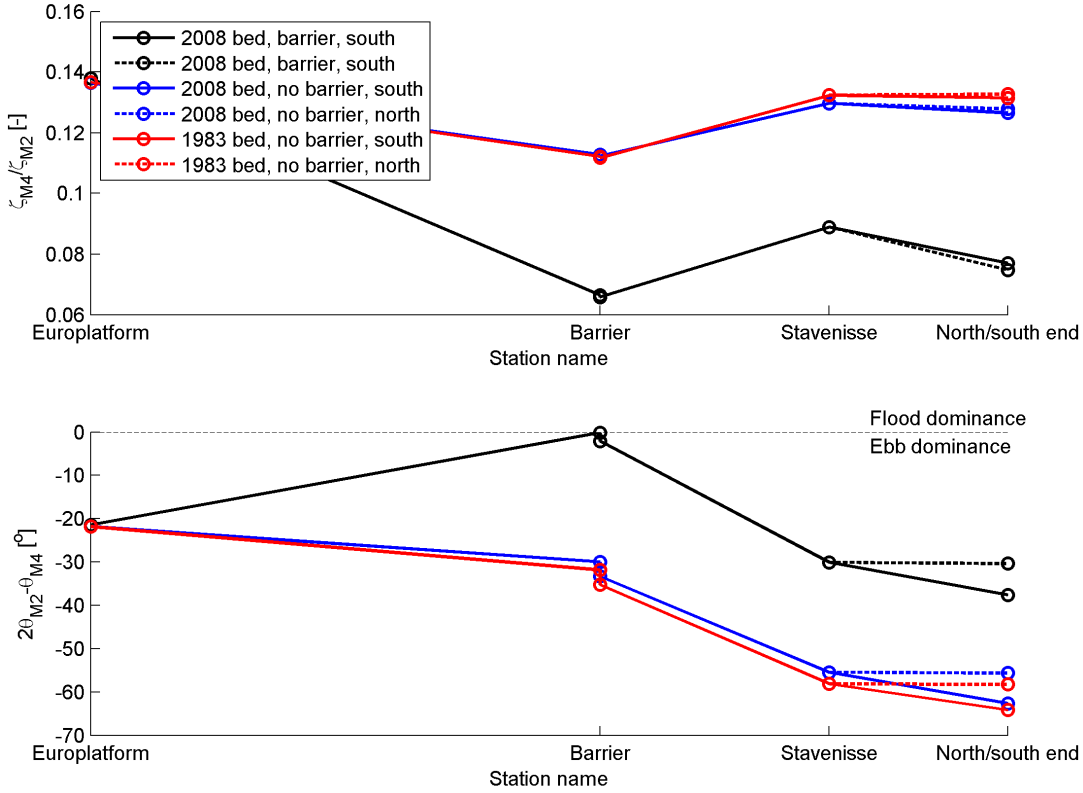

Figure 5.7: Water level parameters indicating tidal distortion of scenario 1,2 & 3. Upper panel: amplitude ratio, Lower panel: relative phase

Figure 5.7 clearly shows that the tidal distortion will become stronger when the barrier is removed. The relative sea surface phase is indicating that the system shifts towards a more ebb dominant system after removal of the barrier.

Comparison of the 1983 and 2008 bathymetry (both without barrier) is instructive because it shows the effect of the changed bathymetry on the distortion of the tidal wave. Looking at the waterlevel amplitude of the M_2 component, in figure 5.5, almost no difference is observed, the same holds for the phase of the water level. The M_4 component however shows a difference, the amplitude with the 1983 bathymetry is higher than with the 2008 bathymetry. This has to do with the differences in propagation speed at high and low water. [Friedrichs and Aubrey, 1988] state that in estuaries where the ratio between the volume of intertidal storage and the volume of the channels is large relative to the ratio between the amplitude and waterdepth, which is the case in the Oosterschelde, high water is slowed down by flats and marshes causing high tide to propagate slower than low tide. When sediment is lost from the intertidal area, the intertidal storage increases, causing high tide to propagate slower leading to decreased flood velocities. The transfer of sediment from the flats to the channels causes shallower channels which slows down the propagation of low water. This in turn leads to lower ebb velocities. These statements seem to contradict. Figure 5.7 shows that the system is ebb dominant and moreover that the 2008 scenario is closer to a flood dominant system. Therefore apparently the shallower channels influence the system more than the increased intertidal storage.

It must be emphasized that the theory suggested by [Friedrichs and Aubrey, 1988] is only an indicator of the tidal distortion. Therefore the results are checked by analyzing the time series of the water level. In figure 5.8 the timeseries of the waterlevel for scenario 1 & 2 is shown for three stations. The time delay caused by the barrier found in figure 5.5, is also visible in the timeseries, see figure 5.8a. The curve representing the present situation shows a distinct time delay between the stations Roompot buiten and binnen. Besides that figure 5.8a shows hardly any delay when the barrier is removed. Figure 5.8b, representing station Stavenisse, indicates that the system will get more ebb dominant when the barrier is removed, as the falling period gets shorter and the rising period longer. The comparison of scenario 2 and 3 (both without barrier) shows hardly any difference, scenario 2 is slightly less ebb dominant. The figures of the timeseries for scenario 1 & 2 and 2 & 3 are included in appendix C for all stations. The characteristics of the timeseries globally confirm the results found by analyzing the M_2 and M_4 components. Inside the basin the distortion is increasing ebb-dominant. Outside the basin however the falling period is getting bigger in contrast to the results found by using the relative phase difference between the M_2 and M_4 components.

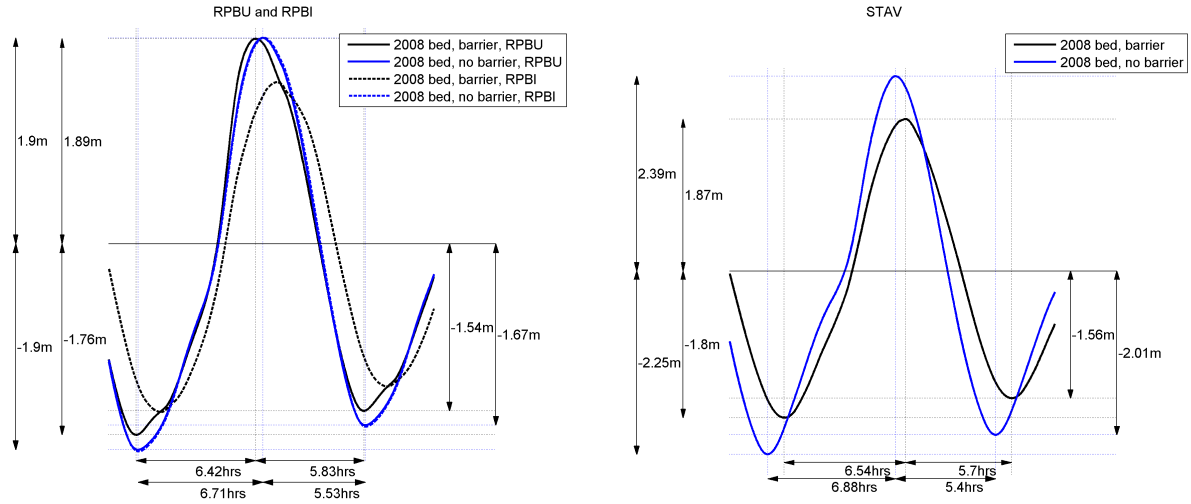

(a) Roompot buiten and binnen **(b)** Stavenisse

Figure 5.8: Timeseries of the water level, scenario 1 & 2

5.2.3 Scenario 4 & 5: Situation in 2100

Scenario 4 & 5 represent the situation in 2100. In these scenarios all the sediment above NAP -2m is removed and evenly spread in the channels. Figure 5.9 shows the characteristics of the M_2 component. It appears that the amplification of the tide will be smaller in 2100 than in 2008. This can be assigned to two effects, the increased storage and the decrease of the channel cross-sectional area. The effect of the increased storage is a larger tidal prism, see paragraph 5.3. This reduces the tidal range because only a limited volume of water can enter the Oosterschelde during one tidal cycle. The shallower channels cause less efficient transport of water through the channels and thereby also reduce the tidal range. The explanation stated above holds for the basin, looking at figure 5.9 however it appears that a major part of the change in the amplitude of the M_2 component is generated on the ebb-tidal delta and due to the barrier. The changes in the basin, in this particular case removal of intertidal area, affect the wave propagation on the ebb-tidal delta. Removal of the barrier results in higher amplitudes of the M_2 component, but the amplitude in 2100 is lower than in 2008. The explanation is the same as for the scenario with barrier, the increased intertidal storage causes a reduction of the tidal range. Besides that the influence of the friction gets higher because of the shallower channels. The effect of the loss of intertidal area is visible in the phase of the M_2 component, there is a larger phase difference between the inlet and the end of the basin. The increased effect of friction is attributable to the decrease of channel depth by approximately 3.2m. According to [van Zanten and Adriaanse, 2008] a storage of 140 million cubic metres of sediment is available in the intertidal area. In the simplified model of 2100 applied in this study a volume of about 300 million cubic metres is removed from the intertidal area and evenly spread in the channels. The channels are therefore too shallow and the intertidal storage is too large in this model. This implies that the effect of additional intertidal storage and friction is probably exaggerated by this simulation. Looking at the M_4 component, see figure 5.10, it appears that the amplitude of the M_4 in scenario 4 will be higher than in the reference scenario (2008). Scenario 5, without barrier, shows a smaller amplitude of the M_4 component than simulation 2. Another remarkable observation is the change in the jump at the barrier for the phase and amplitude of the M_4 component in simulation 4. The schematization of the barrier is the same for scenario 1 and 4, so apparently the bed inside the basin has influence on the processes at the barrier.

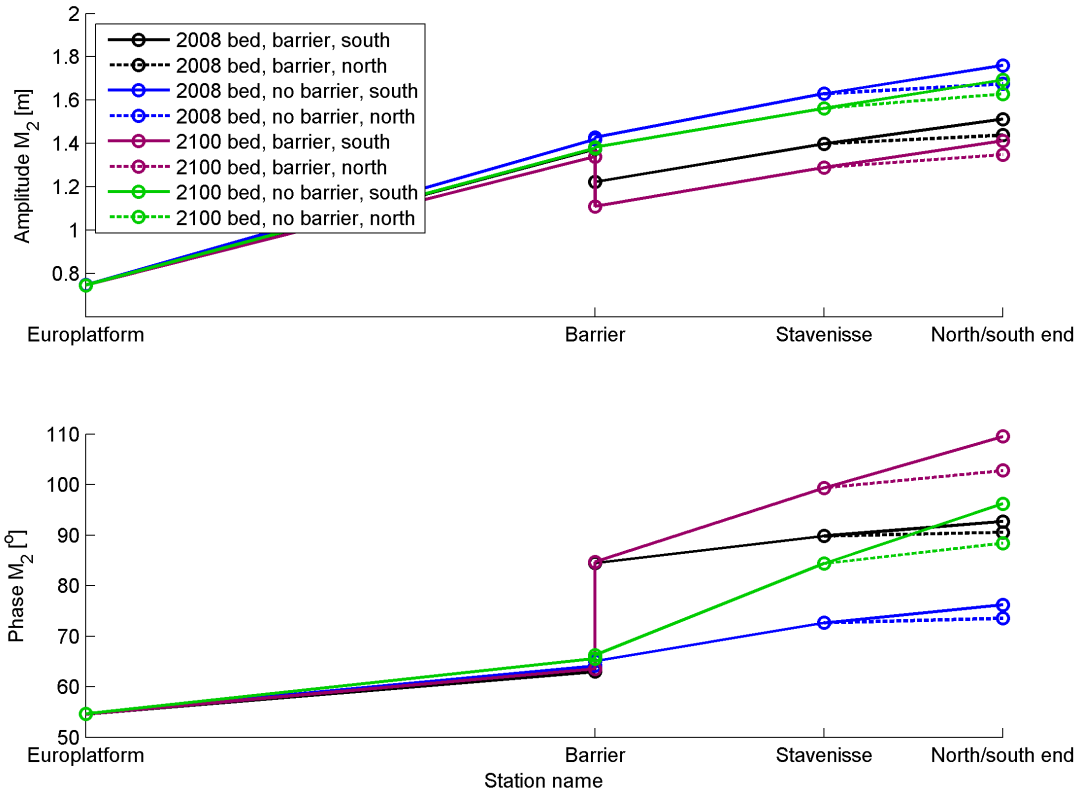

Figure 5.9: M_2 component: Water level amplitude and phase of scenario 1,2,4 & 5

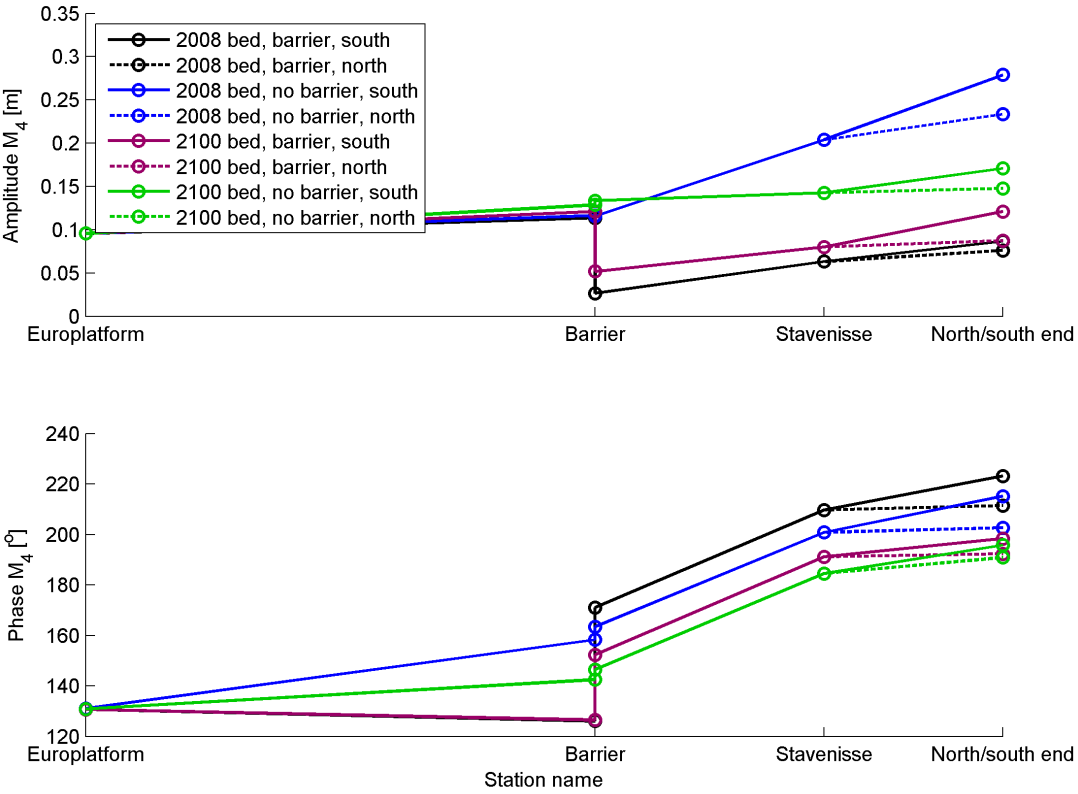

Figure 5.10: M_4 component: Water level amplitude and phase of scenario 1,2,4 & 5

Figure 5.11 shows that the distortion of the tidal wave will be stronger in 2100 comparing scenario 4 with the reference scenario. The tide will be distorted less when the barrier is removed in 2100 compared to 2008. In the previous simulations removal of the barrier caused an increase in the distortion. The decrease in the strength of the distortion can be allocated to the M_4 component. No adequate explanation for the different amplitude can be found. The M_4 phase however does not show a deviation. Therefore the relative phase is not influenced. Based on this it is expected that the direction of the tidal asymmetry is predicted right. The relative phase indicates that the basin will get flood dominant when all the intertidal area is lost. Scenario 5 shows that the systems shifts back to an ebb dominant system when the barrier is removed from simulation 4.

Analysis of the scenario 4 timeseries shows that the tidal wave becomes more symmetric, the duration of the rising and falling period differ less than in 2008, see figure 5.12a. The trend of the tidal asymmetry of run 4, with barrier, is indicated right by the relative phase. The relative phase of simulation 5, without barrier, shows that the system gets slightly more ebb dominant at station Stavenisse compared to the distortion at the barrier. The timeseries of the stations show that the falling period gets longer from the barrier landwards. Scenario 5 is therefore not represented perfect, the differences however are small. The timeseries of scenario 4 and 5 are included in appendix C. Comparison of scenario 4 and 5 clearly shows that the system will get ebb dominant when the barrier is removed.

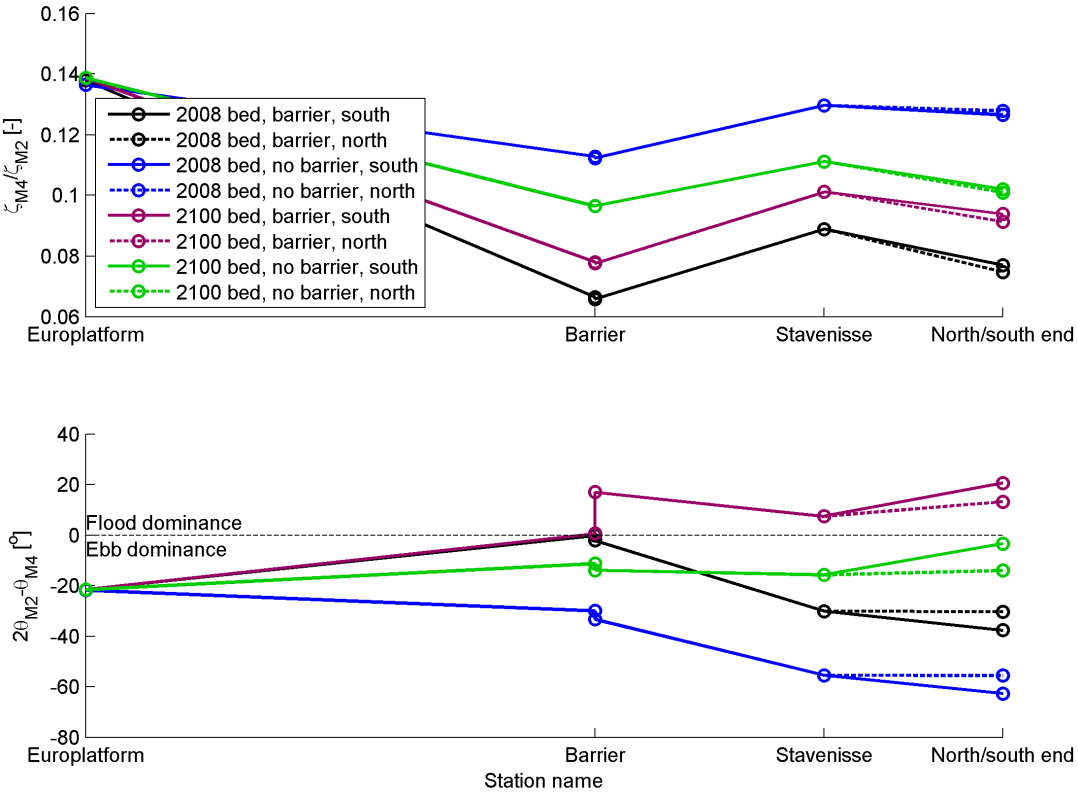

Figure 5.11: Water level parameters indicating tidal distortion of scenario 1,2,4 & 5. Upper panel: amplitude ratio, Lower panel: relative phase

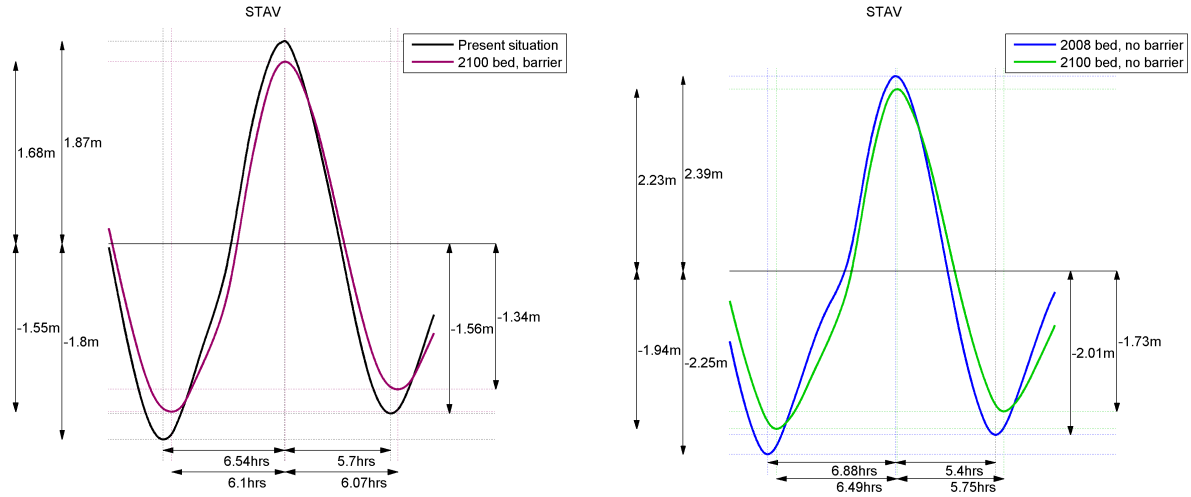

(a) Scenario 1 & 4 **(b)** Scenario 2 & 5

Figure 5.12: Timeseries of the water level, station Stavenisse

5.2.4 Scenario 6 & 7: Large scale realignment

The effect of large scale realignment of the Oosterschelde is investigated using simulation 6 & 7. In these scenarios part of the dikes around the Oosterschelde are set back, see paragraph 4.2.6. This means that intertidal area is added to the model, while the channel volume remains constant. The amplitude and phase characteristics of the M_2 component are included in figure 5.13. Considering the simulations with barrier it appears that the wave is amplified stronger on the ebb-tidal delta compared to the present situation. Besides that the amplitude reduction caused by the barrier is smaller than in the present situation. The amplitude amplification inside the Oosterschelde basin is approximately the same as in the reference situation. The phase of the M_2 component shows that the tidal wave propagates slightly slower on the ebb-tidal delta. Next to that the delay at the barrier is smaller than in the present situation, see figure 5.13. The propagation of the wave inside the realigned Oosterschelde basin is similar to the present situation.

When the barrier is removed higher M_2 amplitudes are found for the realigned basin compared to the simulation without realignment, see figure 5.13. It appears that the amplification inside the basin is almost the same, the difference is generated on the ebb-tidal delta. Considering the M_2 phase it appears that the wave is propagating slower between the inlet and station Stavenisse. The propagation speed in the northern and southern branch does not change significantly.

Figure 5.14 shows the amplitude and phase of the M_4 component. Similar to the M_2 component, a difference on the ebb-tidal delta is found. The jump in the amplitude at the barrier is comparable for the realigned and present basin. Besides that there are changes inside the basin. Comparing the two scenarios with barrier it appears that the amplitude of the M_4 component is larger in the realigned basin, see figure 5.14. The amplitude of the M_4 component will be stronger in the northern branch when the dikes are set back, analysing the situation without barrier. The amplitude ratios for the present basin and realigned basin do not show large differences. Comparing the amplitude ratio of the simulations without barrier in figure 5.15 it appears that the distortion of the tidal wave will be less strong when the barrier is removed. This is the case especially at the inlet and in the central part of the basin and to a smaller extent in the northern and southern branch. Looking at the relative phase of both scenarios with

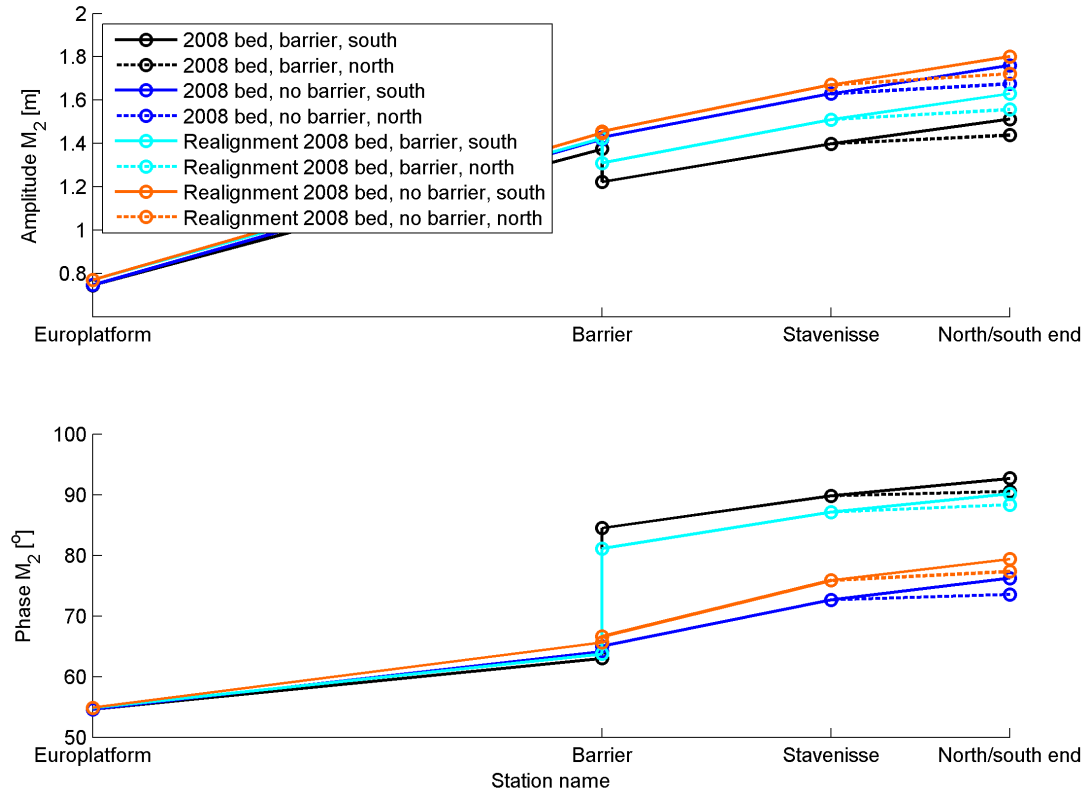

Figure 5.13: M_2 component: Water level amplitude and phase of scenario 1,2,6 & 7

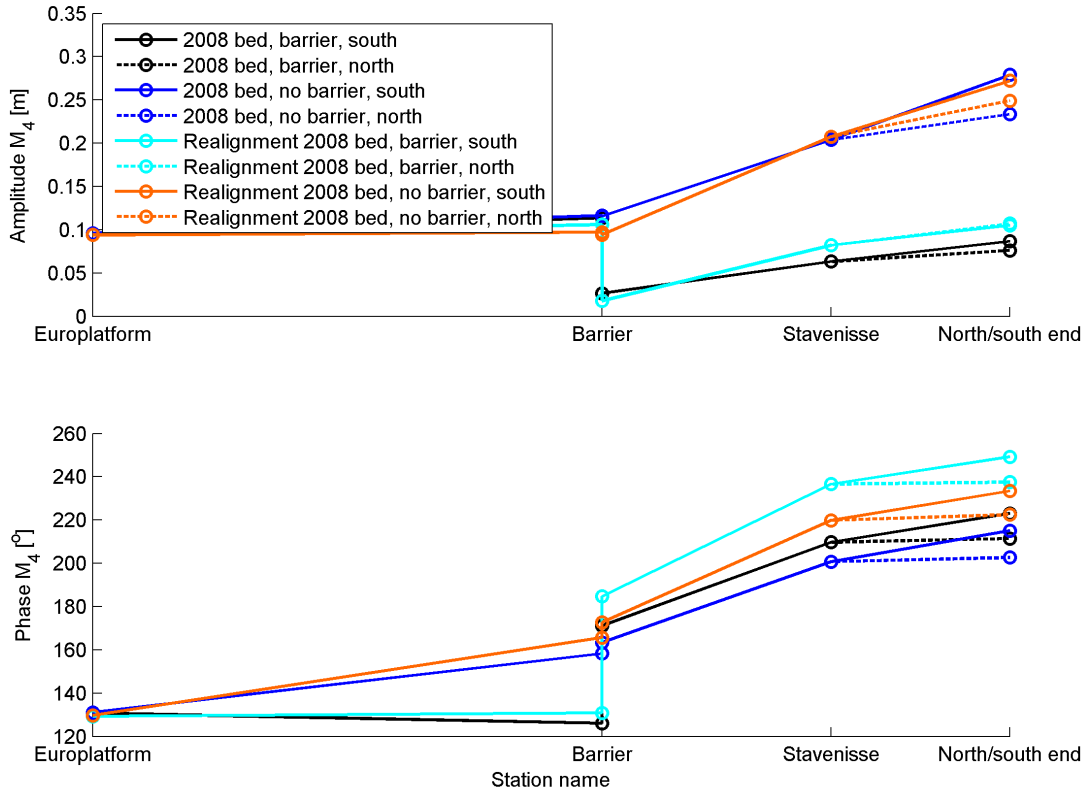

Figure 5.14: M_4 component: Water level amplitude and phase of scenario 1,2,6 & 7

barrier learns that the system will get more ebb dominant when the Oosterschelde is realigned. This result must be interpreted with care because a large contribution of the strengthened ebb dominance is due to the barrier. However inside the basin increased ebb dominance is found apart from the increase due to the barrier. The curves for the simulations excluding the barrier show increased ebb dominance for the situation in which the dikes are set back. This can also be explained by using the diagram of [Speer et al., 1991], see paragraph 2.2.1. In this scenario the a/h ratio stays approximately constant while the V_s/V_c ratio increases. This explains why the system becomes more ebb dominant. Looking at the timeseries shows that realignment causes

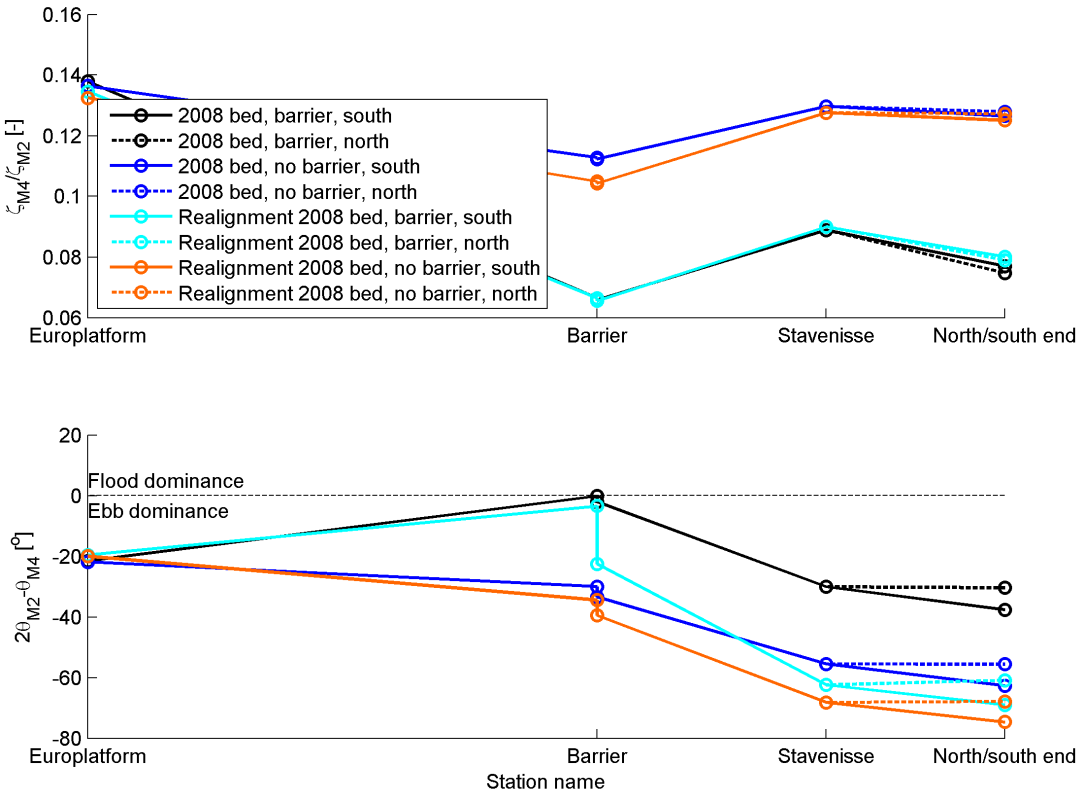

Figure 5.15: Water level parameters indicating tidal distortion of scenario 1,2,6 & 7. Upper panel: amplitude ratio, Lower panel: relative phase

a longer rising period and a shorter falling period for both simulations, see figure 5.16. This indicates that the system becomes more ebb dominant, which was also found by evaluating the relative phase. The water level amplitude in the realigned basin is larger than in the present situation which was also found M_2 amplitude figure. The timeseries for all stations are included in appendix C.

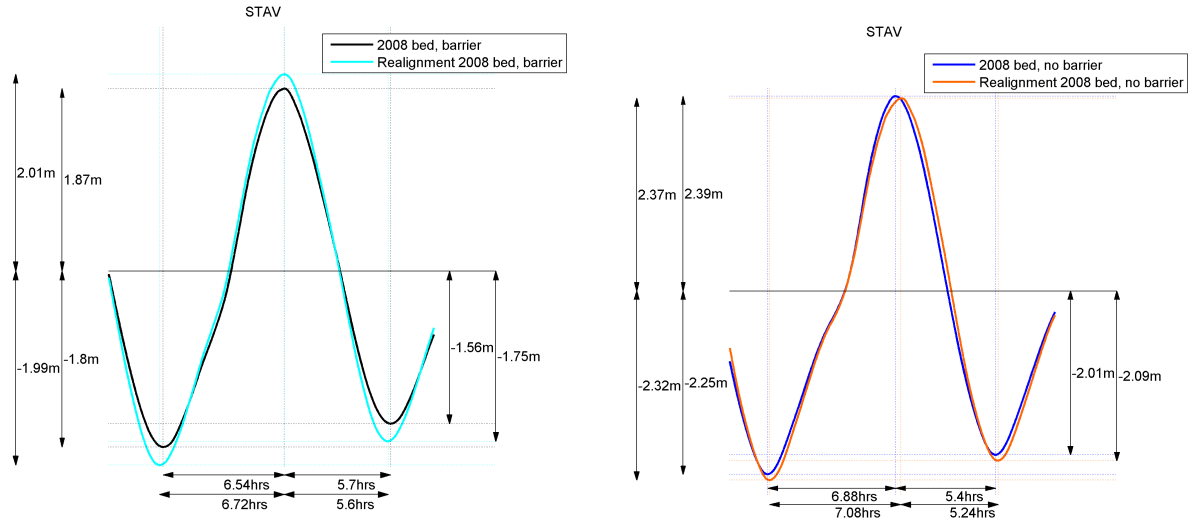

(a) Scenario 1 & 6 **(b)** Scenario 2 & 7

Figure 5.16: Timeseries of the water level, station Stavenisse

5.2.5 Implications

Analysis of the amplitude ratio, relative phase and timeseries of the water level has resulted in predictions for the sediment transport. In this paragraph a short description of the implications will be given. Removal of the barrier from the present situation results in a larger tidal range and increased ebb dominance. Comparison of the 1983, 2008 and 2100 bathymetry shows that erosion of the flats leads to decreased ebb dominance. Realigning the Oosterschelde basin leads to increased ebb dominance.

5.3 Discharge

5.3.1 Scenario 2 & 3: Situation without barrier

The cumulative discharge is obtained from Delft3D by defining several cross sections, see figure 5.1. Looking at the amplitude of the M_2 component of the discharge in figure 5.17 it appears that the discharge will increase significantly by removal of the barrier. Comparing the 1983 and 2008 curve learns that erosion of the intertidal flats increases the discharge through the cross sections further. In paragraph 5.2 the development of the water level was described. The M_2 component of the vertical tide showed no difference for the two applied bathymetries. Sand is lost from the intertidal zone according to paragraph 4.1.3, which explains the larger discharge in 2008 compared to 1983. A larger volume of water is necessary to fill the volume between the high and low water level.

Opposite to the M_2 amplitude that is higher in 2008, the M_4 amplitude is lower in 2008. A remarkable observation in the M_2 and M_4 phase of the discharge is the lower phase angle in the northern branch compared to the phase in the centre. The water level phase does not show this behaviour and is increasing along the northern branch. The explanation for this observation can be found in the continuity equation integrated over the basin length:

$$Q = \frac{\partial \eta}{\partial t} A \tag{5.1}$$

The variable η is the water level, this variable has an increasing phase as mentioned before. So apparently the changes in the phase angle of Q must be in the variable A, which is the

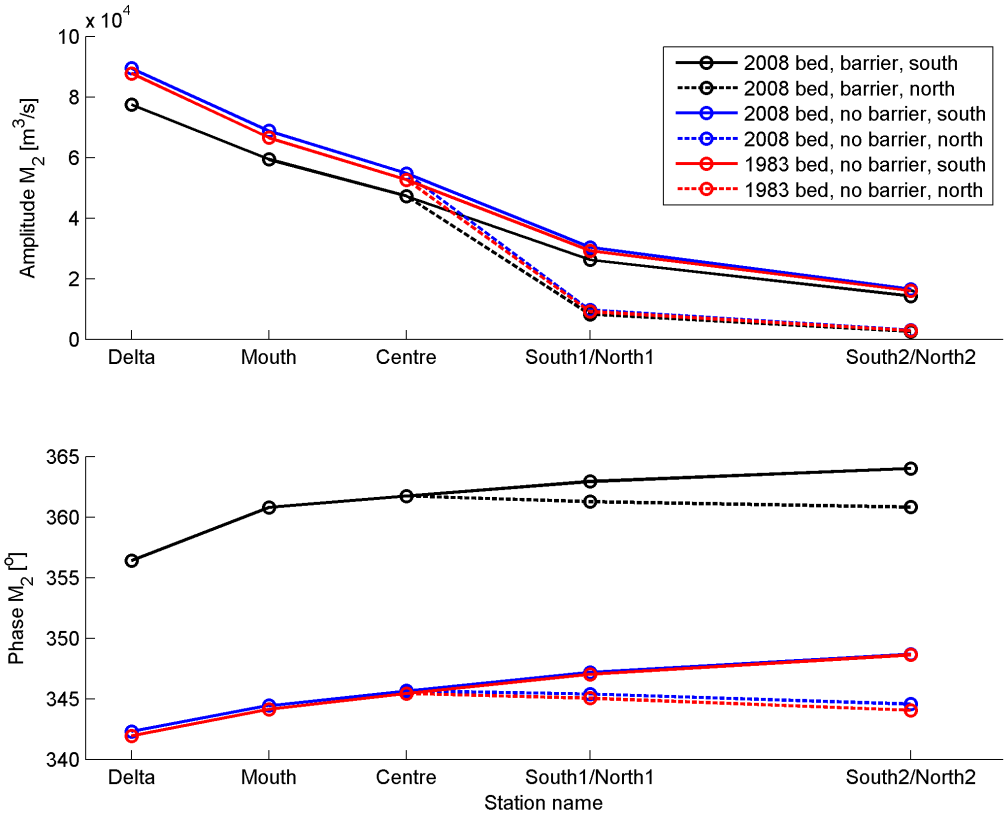

Figure 5.17: M_2 component: Discharge amplitude and phase of scenario 1,2 & 3

horizontal area behind the cross section where Q is defined. The area of the northern branch is approximately three times smaller than the southern branch, making this bifurcation asymmetric. The discharge flowing into the two branches together must be the same as in the cross section just before the bifurcation point because of mass conservation. When the discharges in both branches are expressed as complex numbers a simple vector addition can be carried out. In figure 5.20 the discharges are represented as vectors in the complex plane. The rotation angle of the vector is the phase of the signal, the length of the vector represents the amplitude. When the vectors of the northern (North1) and southern (South1) are added a vector in between those vectors is found, meaning that one of the two branches must have a phase lag with respect to the discharge at the other two cross sections. The total discharge before the bifurcation from the Delft3D calculation is also plotted in figure 5.20. This vector, with the label total, is longer than the vector obtained from the addition of the northern and southern discharges. The reason for this is that the cross section (Centre) before the bifurcation is not located directly before the bifurcation but a bit seaward, see figure 5.1. In between the three vectors an area remains that also has to be filled. The length difference therefore is the discharge that is necessary to fill this area.

So far the bifurcation of the northern and southern branch is analysed. However halfway the northern branch another bifurcation is present, see figure 5.1, this explains why the phase at the end of the northern branch is lower than at the first cross section North1. A calculation with extra cross sections shows that the phase is increasing behind both bifurcations. Implying that the asymmetric bifurcations are the only reason for the phase differences.

Figure 5.19 shows that the distortion of the wave gets stronger when the barrier is removed. The 2008 curve shows that the distortion gets less strong compared to the 1983 curve. According to the relative phase the system is ebb dominant for all scenarios. The present situation tends

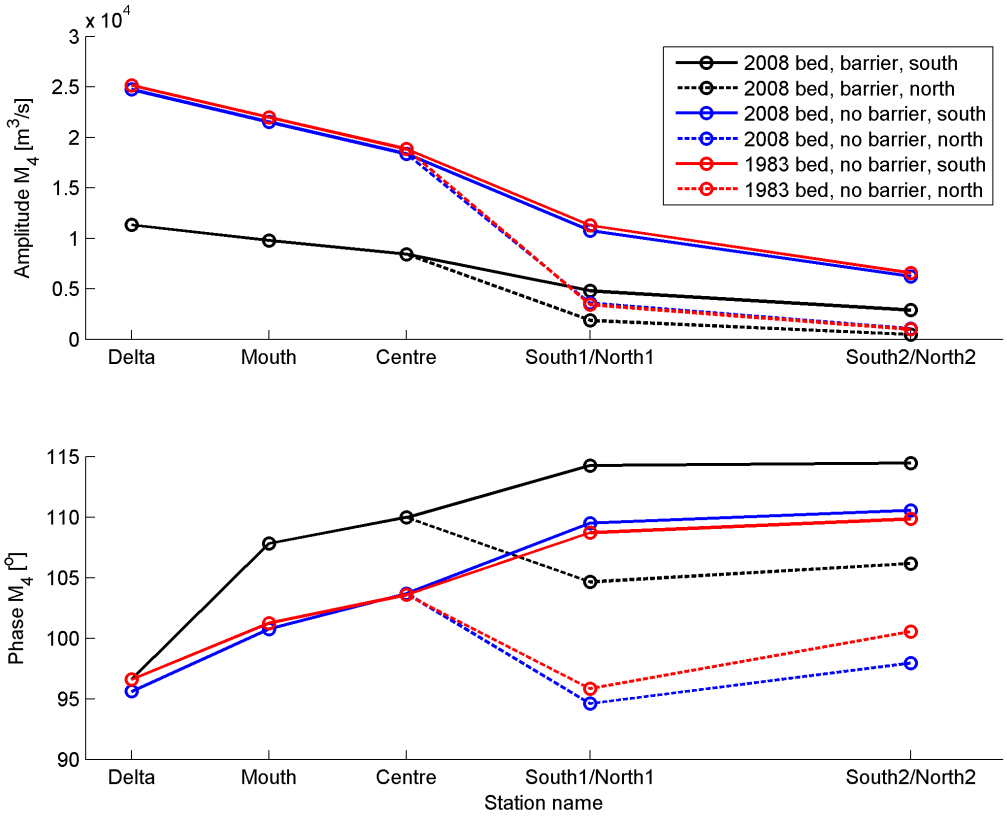

Figure 5.18: M_4 component: Discharge amplitude and phase of scenario 1,2 & 3

to a flood dominant system the most. Comparing the 1983 and 2008 scenarios does not give a clear view on development towards ebb or flood dominance of these simulations. The 2008 curve seems to develop to a less ebb dominant system with respect to 1983.

Figure 5.21 shows the timeseries of the discharge signal at the cross-section centre. This signal is more irregular than the water level signal because the amplitudes of the M_4, M_6 and other overtides get relatively larger due to the higher frequencies of the overtides, see equations 5.2, 5.3 and 5.4. Analysis of the tidal components shows that besides the M_2, M_4 and M_6 components also MS_4 and $2MS_6$ are important. The last mentioned components are generated by interaction with S_2, making the influence of MS_4 and $2MS_6$ vary over a spring-neap cycle.

$$\eta = a_{M2}cos(\omega t) + a_{M4}cos(2\omega t - \varphi) \tag{5.2}$$

$$Q(t) = A_{basin}(\eta)\frac{\partial \eta}{\partial t} \;\Rightarrow\; \frac{\partial \eta}{\partial t} = -\omega a_{M2}sin(\omega t) - 2\omega a_{M4}sin(2\omega t - \varphi) \tag{5.3}$$

$$\frac{a_{M4}}{a_{M2}} \propto \delta \;\Rightarrow\; \frac{Q_{M4}}{Q_{M2}} \propto 2\delta \tag{5.4}$$

The timeseries in figure 5.21 indicate that the flood discharge is higher than the ebb discharge. It must be noted that the shown series are generated by integrating the discharge in each cell over the cross section. This implies that the instantaneous discharge does not give information about the velocities, which in turn is the forcing of sediment transport. So a higher flood discharge does not directly mean higher flood velocities and thereby net transport in flood direction. This eliminates the possibility to check the method of [Friedrichs and Aubrey, 1988] by simply looking at the timeseries of the discharge, which was possible for the water level. In order to verify if analysis of only two components (M_2 and M_4) is a good indicator for the

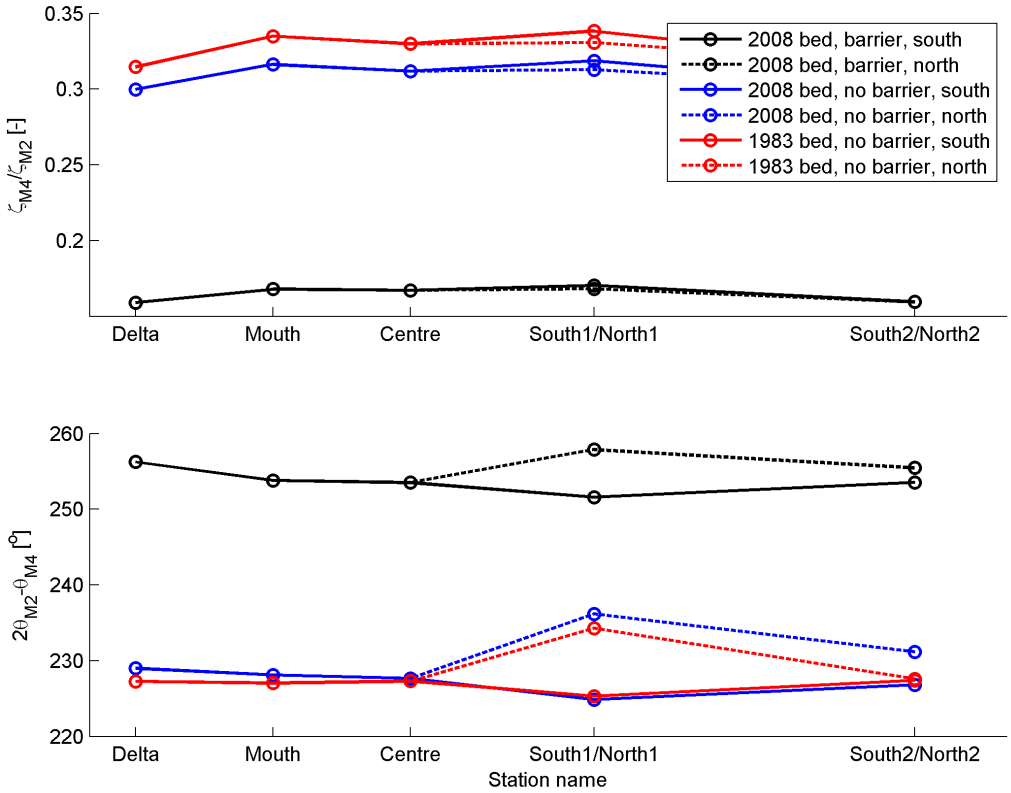

Figure 5.19: Parameters: Discharge amplitude and phase of scenario 1,2 & 3. Upper panel: amplitude ratio, Lower panel: relative phase

asymmetry of the discharge signal, the cumulative total transport is used. The cumulative total transport consists of the total bed load transport and the total suspended load transport. This parameter is obtained from Delft3D. It must be emphasized that the included numbers for the sediment transport are only indicative. The sediment transport is calculated with default values in Delft3D and not validated.

As mentioned above all three simulations are expected to be ebb dominant. Analysing scenario 1 (present situation), the total transport shows ebb directed transport for the cross-sections Delta, Centre and South 1. The remaining cross-sections show flood directed transport. However the volume transported through these cross-sections in the eastern part are small, see table 5.1. Scenario 2 and 3 show ebb directed transport.

Cross-section	2008 bed, barrier	2008 bed, no barrier	1983 bed, no barrier
Delta	-0.75	-29.15	-18.18
Mouth	0.51	-14.16	-15.20
Centre	-0.17	-35.41	-24.51
South 1	-0.26	-5.74	-4.86
South 2	0.05	-0.66	-0.84
North 1	0.00	-0.06	-0.01
North 2	0.00	0.00	0.00

Table 5.1: Total sediment transport scenario 1,2 & 3 in $10^4 m^3$ per month, negative transports are ebb-directed

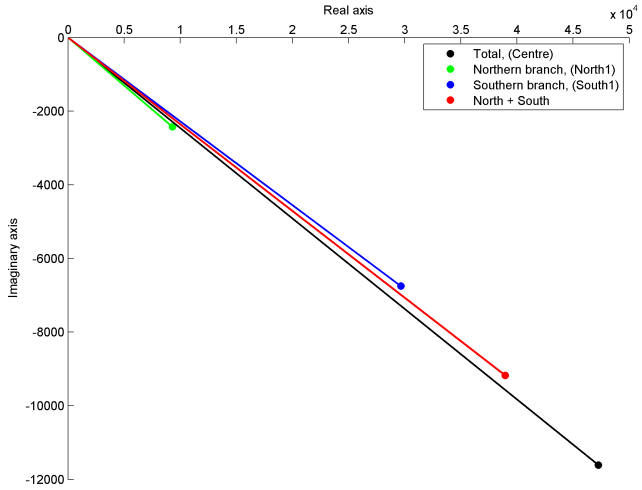

Figure 5.20: Representation of the discharge in the complex plane

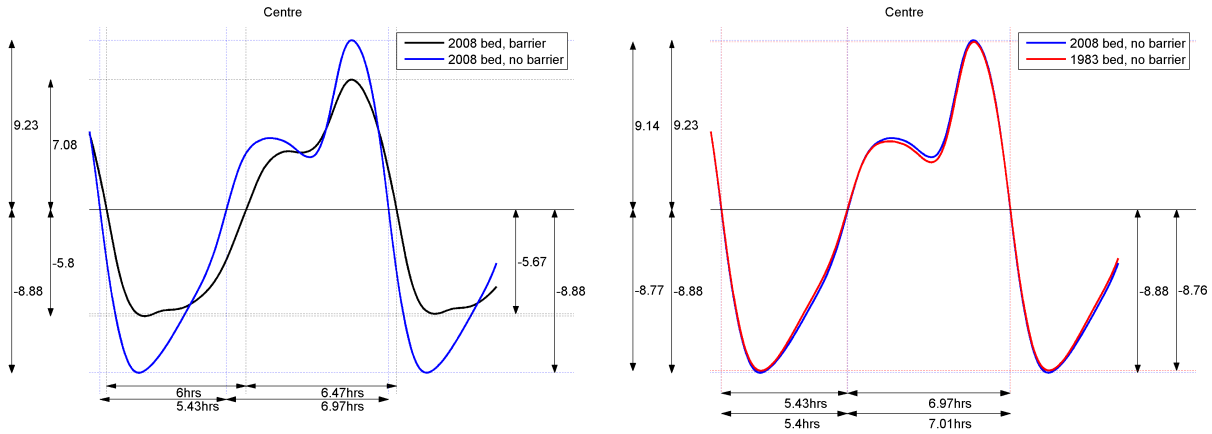

(a) Scenario 1 & 2 **(b)** Scenario 2 & 3

Figure 5.21: Timeseries of the instantaneous discharge in 10^4 m^3/s at cross section Centre

5.3.2 Scenario 4 & 5: Situation in 2100

The discharge signal obtained from the simulation of scenario 4 & 5 is analyzed in this paragraph. Figure 5.22 shows the amplitude and phase of the M_2 component. Because of the loss of sediment from the intertidal area the tidal prism grows further. This is visible in the amplitude of the M_2 component for both scenarios. Besides this the propagation speed of the wave gets lower, which is visible in the larger phase difference between the inlet and the end of the basin. The amplitude and phase of the M_4 component, shown in figure 5.23, shows that the amplitude of the M_4 component in 2008 is approximately equal to the amplitude 2100 in the scenarios with the barrier (1 & 4). When the barrier is removed from scenario 4, an increase of the M_4 amplitude is found, but the increase is not as large as in 2008. Figure 5.24 shows the amplitude ratio and relative phase. The amplitude ratio indicates that the tidal distortion in 2100 in both scenario's will be smaller than in 2008. The tidal distortion will get stronger when the barrier is removed in 2100, but not as much as in 2008. Considering the relative phase indicates that

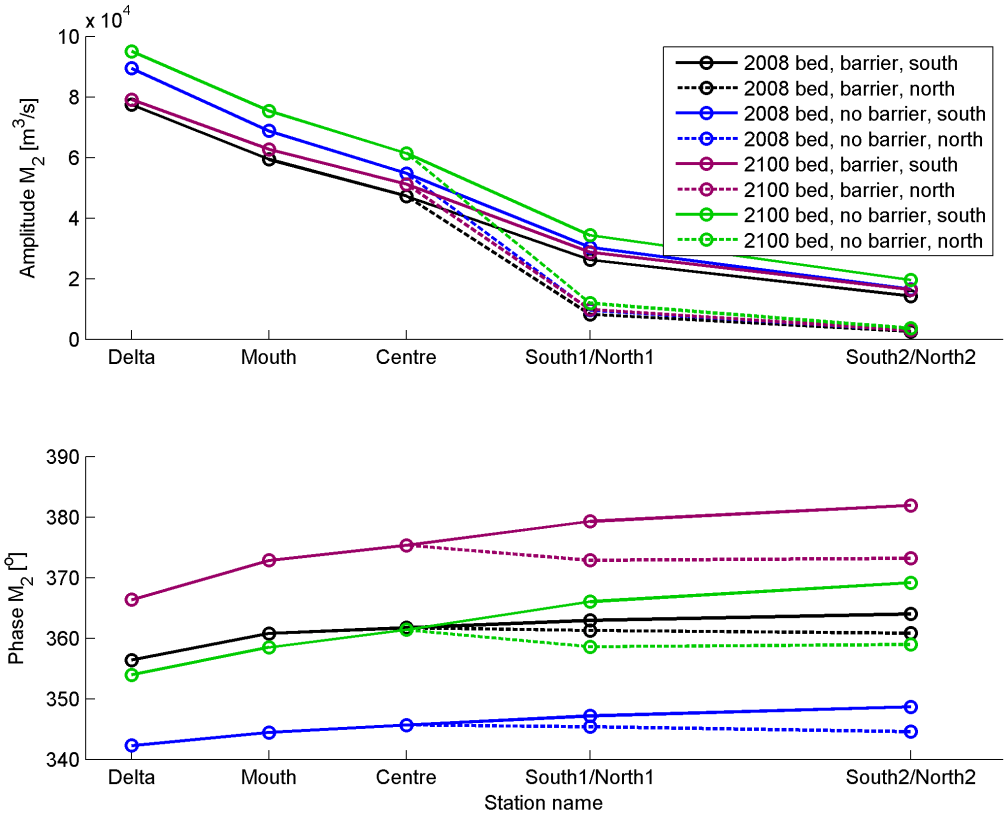

Figure 5.22: M_2 component: Discharge amplitude and phase of scenario 1,2,4 & 5

the basin will get flood dominant in 2100 looking at the scenario with the barrier. The scenario without barrier is on the border between an ebb and flood dominant system. The eastern parts are flood dominant while the western parts are ebb dominant.

The timeseries included in figure 5.25 show a more regular curve in 2100 compared to 2008. The bump visible before the flood peak is for the largest part generated by M_6, MS_4 and $2MS_6$. Due to the loss of sediment from the intertidal area the tidal wave gets more symmetric. This is also visible in the decreased influence of the M_6, MS_4 and $2MS_6$ components, the bump is smoothed out in figure 5.25. Another feature found in the timeseries is the lower propagation speed. The curves that represent the 2100 situation have a time delay with respect to the 2008 curves. As mentioned before the timeseries can not be used to check the M_2/M_4 approximation. Comparison of figure 5.24 with the transports in table 5.2 shows good agreement for the simulation with the 2100 bathymetry and barrier. The simulation without barrier shows ebb dominance except for the southern branch, see figure 5.24. Analysing the transports yields the same results. The only difference is found in the northern branch. The method of [Friedrichs and Aubrey, 1988] gives ebb dominance, while the calculated transports are in flood direction. Comparing this information with the water level results gives the same outcome for the situation with barrier. Removal of the barrier however shows different results. The water level indicates ebb-dominance in the entire system, while the discharge and the transports show flood dominance in parts of the system. It is noted again that a simplified bathymetry is used to represent the 2100 situation.

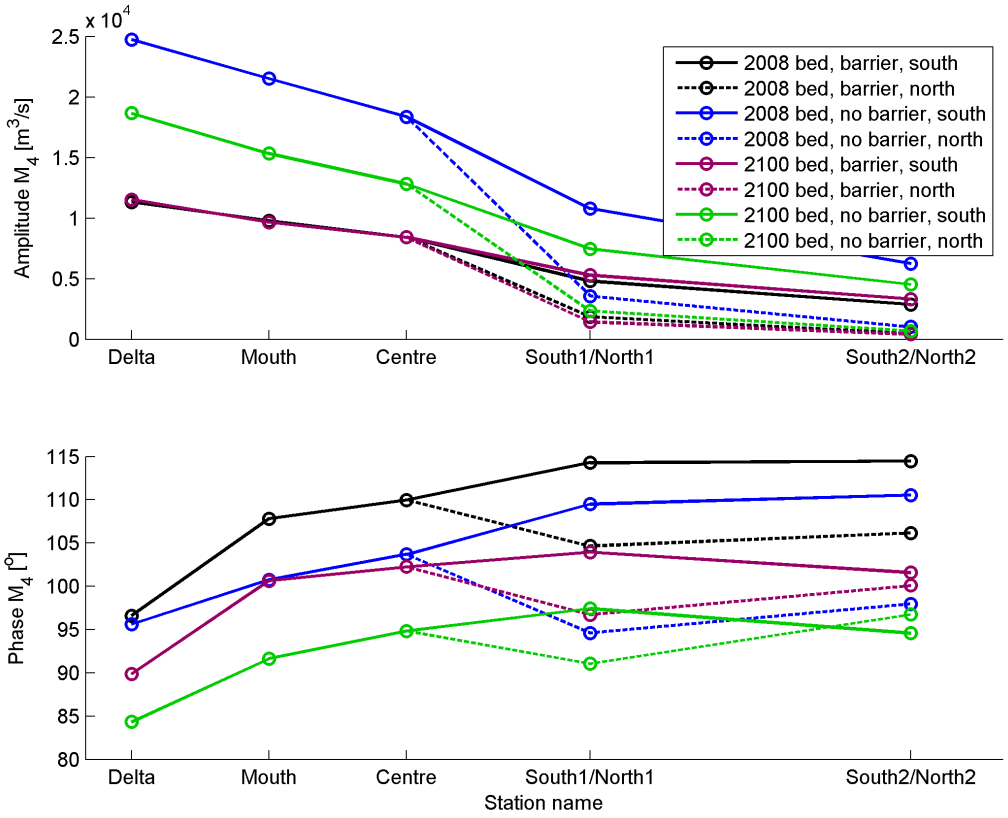

Figure 5.23: M_4 component: Discharge amplitude and phase of scenario 1,2,4 & 5

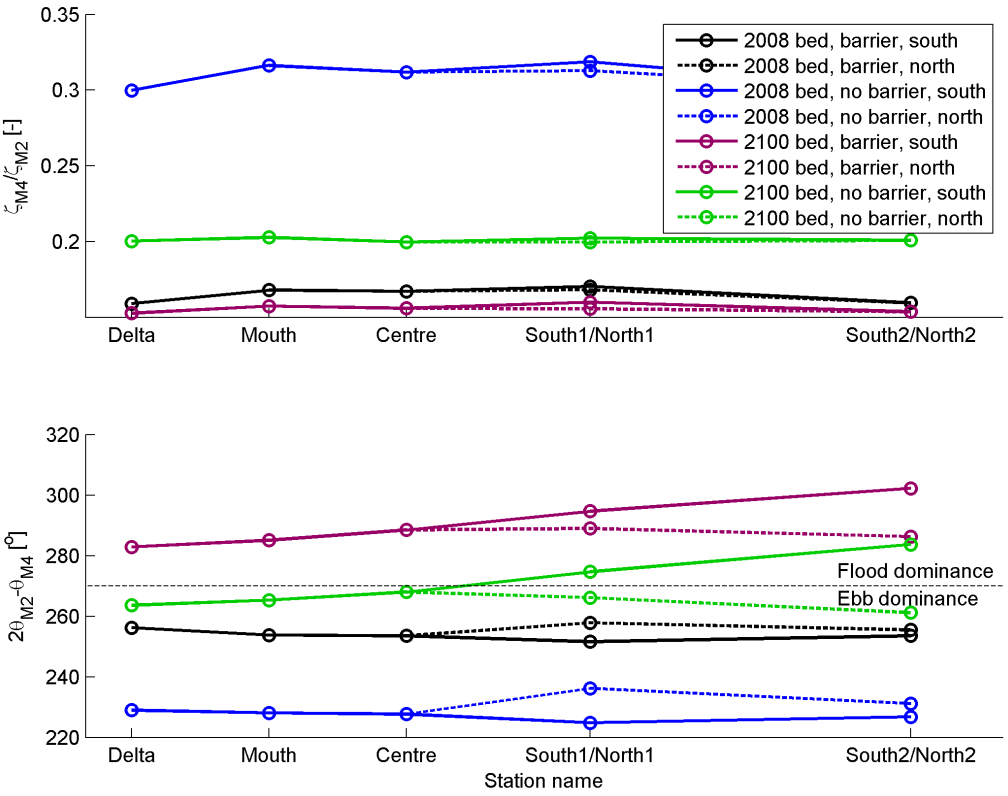

Figure 5.24: Parameters: Discharge amplitude and phase of scenario 1,2,4 & 5. Upper panel: amplitude ratio, Lower panel: relative phase

Cross-section	2008 bed, barrier	2008 bed, no barrier	2100 bed, barrier	2100 bed, no barrier
Delta	-0.75	-29.15	2.05	-8.91
Mouth	0.51	-14.16	11.77	-11.12
Centre	-0.17	-35.41	9.94	-24.64
South 1	-0.26	-5.74	13.95	21.62
South 2	0.05	-0.66	2.28	4.49
North 1	0.00	-0.06	0.69	1.18
North 2	0.00	0.00	0.01	0.08

Table 5.2: Total sediment transport scenario 1,2,4 & 5 in $10^4 m^3$ per month, negative transports are ebb-directed

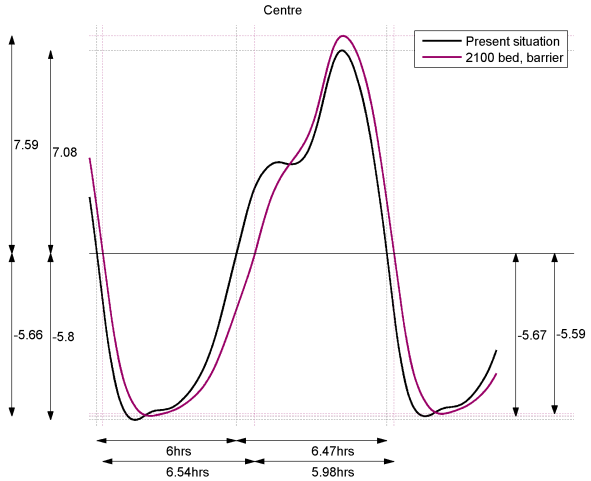

(a) Scenario 1 & 4

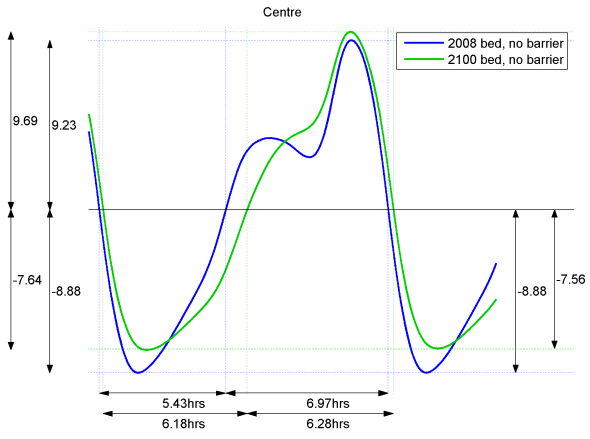

(b) Scenario 2 & 5

Figure 5.25: Timeseries of the instantaneous discharge in 10^4 m^3/s at cross section Centre

5.3.3 Scenario 6 & 7: Large scale realignment

In this paragraph the discharge of the realigned basin will be elaborated. The set back of part of the dikes, as described in paragraph 4.2.6, causes an increase of the discharge. Figure 5.26 shows the M_2 component of the discharge in which the increase is clearly visible. The phase of the M_2 component shows that the wave is propagating at approximately the same speed, the only exceptions are the central and northern part in both realigned scenarios. In the central part of the Oosterschelde a higher propagation speed is found when the basin is realigned and the barrier is removed. The northern branch shows slower propagation for the realigned basin. Besides this the propagation of the wave on the ebb tidal delta is slower in the situation without barrier, and faster in the simulation with barrier in the realigned scenarios. This was also found in the M_2 phase of the water level.

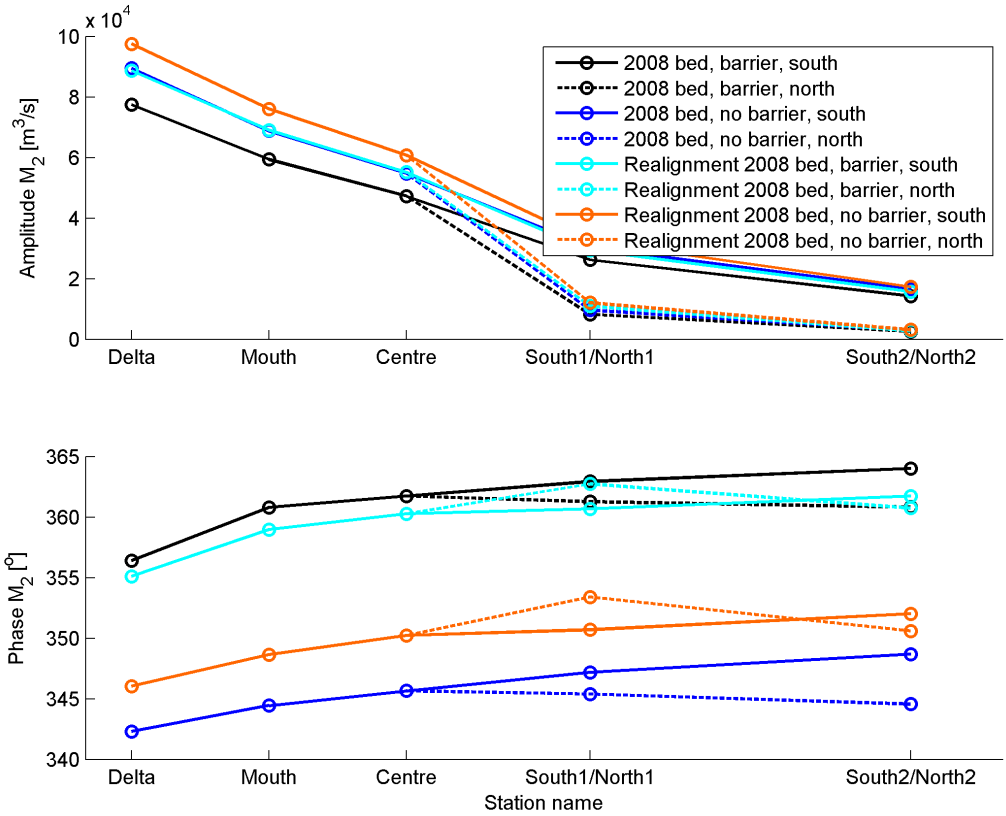

Figure 5.26: M_2 component: Discharge amplitude and phase of scenario 1,2,6 & 7

The amplitude of the M_4 component gets larger in the realigned basin, this holds for the situation with and without the barrier. The trend of the M_4 phase is roughly the same for all four simulations, see figure 5.27.

Looking at figure 5.28 learns that the distortion will get stronger when the dikes are set back. The relative phase shows that the system will be ebb dominant, and moreover that the ebb-dominance will be stronger when the basin is realigned. Comparison of the results with the total transport, see table 5.3, shows ebb transports for all cross-sections in both simulations with realignments except for one. The cross section Mouth in the simulation with barrier shows flood transports.

Figure 5.29 shows the timeseries of the instanteneous discharge. The increase of the discharge is also found in the timeseries. Furthermore hardly any time delay is observed, which was also indicated by the phase curves of the M_2 and M_4 components.

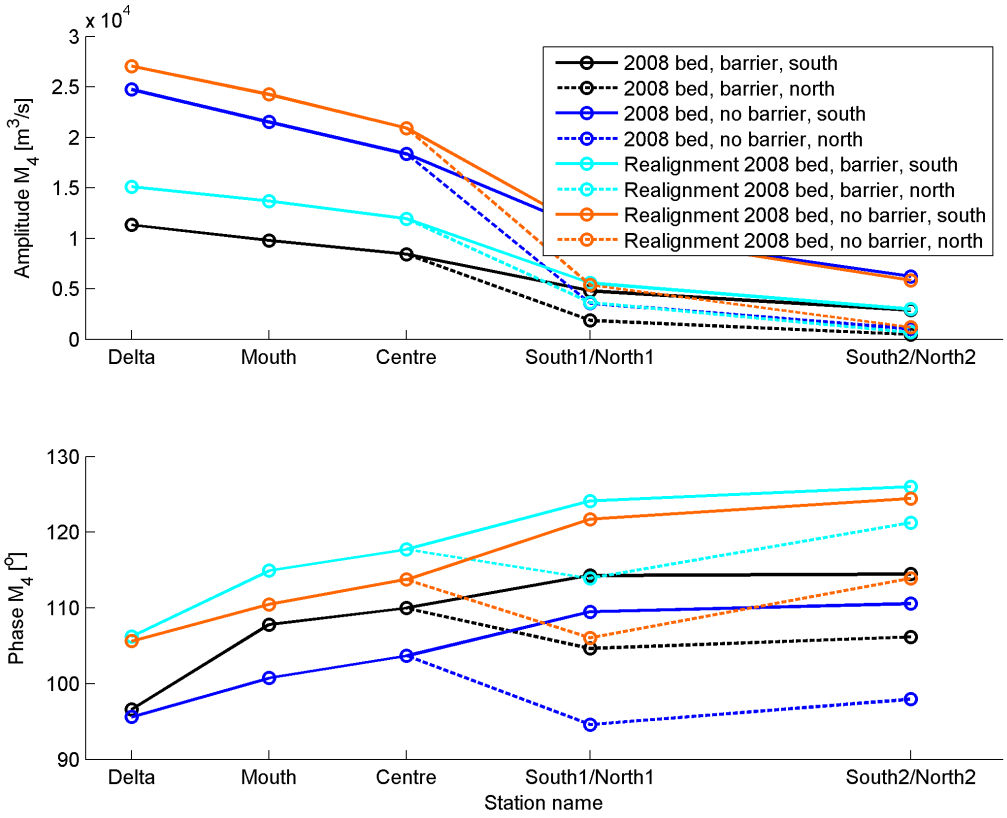

Figure 5.27: M_4 component: Discharge amplitude and phase of scenario 1,2,6 & 7

5.3.4 Implications

Analysis of the amplitude ratio, relative phase and timeseries of the discharge has resulted in predictions for the sediment transport. Those results are compared to sediment transports calculated with Delft3D. This paragraph gives a short description of the results. Removal of the barrier from the present situation results in a larger discharge/tidal prism and increased ebb dominance. Comparison of the 1983, 2008 and 2100 bathymetry shows an increase of the discharge due to the ongoing erosion of the tidal flats. The erosion of the tidal flats leads to decreased ebb dominance. The 2100 simulation with the barrier shows flood dominance for the entire system. Removal of the barrier from the 2100 simulation causes the western part and northern branch to become ebb-dominant. Realigning the Oosterschelde basin leads to increased ebb dominance.

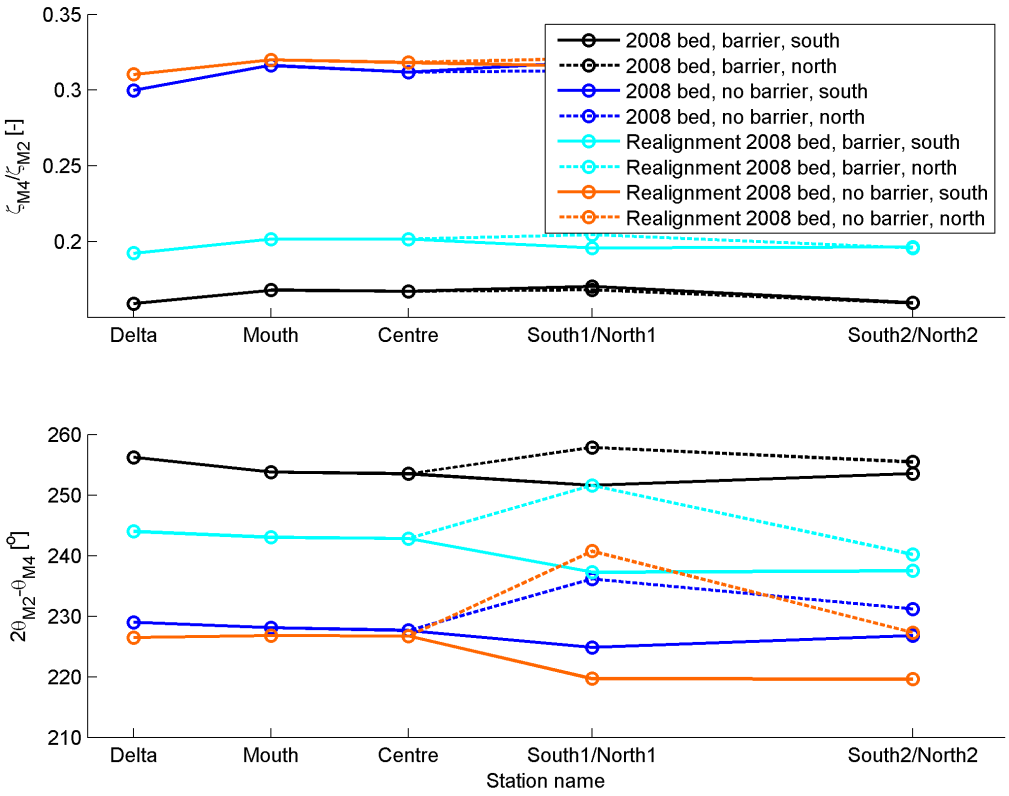

Figure 5.28: Parameters: Discharge amplitude and phase of scenario 1,2,6 & 7. Upper panel: amplitude ratio, Lower panel: relative phase

Cross-section	2008 bed, barrier	2008 bed, no barrier	Realignment, 2008 bed, no barrier	Realignment, 2008 bed, barrier
Delta	-0.75	-29.15	-54.22	-29.10
Mouth	0.51	-14.16	-28.69	20.45
Centre	-0.17	-35.41	-56.80	-9.39
South 1	-0.26	-5.74	-8.92	-1.77
South 2	0.05	-0.66	-1.28	-0.14
North 1	0.00	-0.06	-0.51	-0.09
North 2	0.00	0.00	-0.01	-0.01

Table 5.3: Total sediment transport scenario 1,2,6 & 7 in $10^4 m^3$ per month, negative transports are ebb-directed

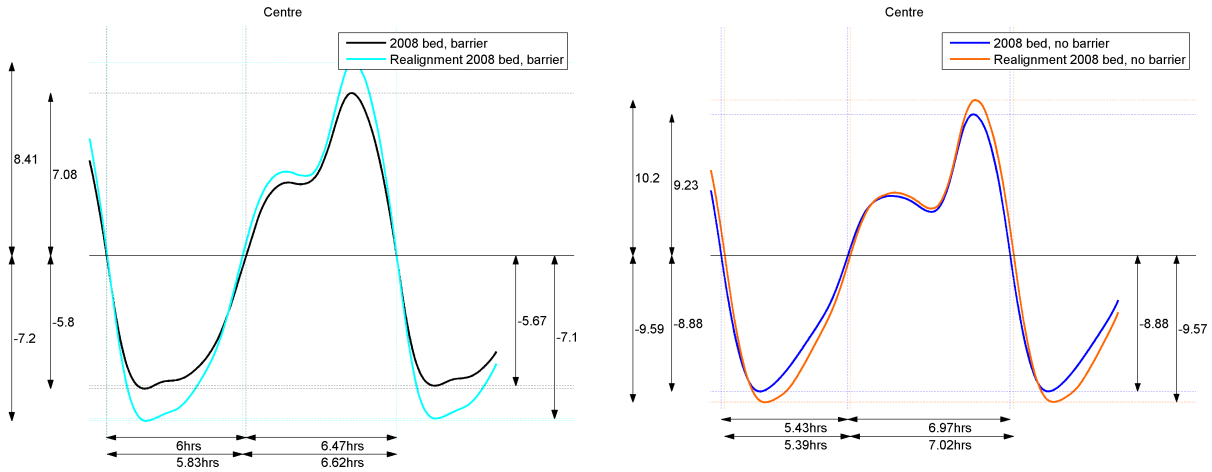

(a) Scenario 1 & 7

(b) Scenario 2 & 6

Figure 5.29: Timeseries of the instantaneous discharge in 10^4 m^3/s at cross section Centre

5.4 Velocity

In paragraph 2.2.1 it was already stated that it is not possible to apply the theory of [Friedrichs and Aubrey, 1988] to the velocity signal. The flow velocities however are the driving force for sediment transport. Therefore it is important to analyse the velocity signal. [Das, 2010] concluded that the tidal flow is the governing forcing for shoal build up. According to [Das, 2010] shoal build up will occur again when the barrier is removed. An increase of the flow velocities with 30 to 40% on the shoal is thought to enforce shoal building again. It must be noted that only one simulation with respect to increased flow velocities is performed by [Das, 2010], therefore it is possible that a smaller increase of the flow also causes shoal build up. The model used for this thesis is not detailed enough to investigate if smaller flow velocities will lead to shoal build up. Therefore the percentages given by [Das, 2010] are used to estimate if shoal build up will occur. [Das, 2010] evaluated maximum of the magnitude of the velocity signal on the Galgeplaat, this shoal is located in the southern branch of the Oosterschelde. Several observation points are defined on the Galgeplaat in Delft3D to check if shoal build up will occur again.

Figure 5.30: Observation points on the Galgeplaat

As explained in paragraph 2.2.3 [Das, 2010] assumed that a multiplication of the flow velocities by a factor 2 represents the situation without barrier, leading to 30 to 40 % increased flow velocities on the Galgeplaat. Table 5.4 shows the occuring flow velocities with two bathymetries 2008 and 1983, both without barrier. It appears that the flow velocities on the Galgeplaat are higher when the 2008 bathymetry is applied. In this scenario the flow velocities are 30 to 40% higher. Therefore shoal build up is expected when the barrier is removed. The increase of the flow velocities when the barrier is removed is clearly visible in figure 5.31.

Scenario 4 & 5 aim at a prediction of the situation in 2100. In these scenarios all sediment is lost from the intertidal area and evenly spread in the channels. It appears from table 5.5 that this causes a significant increase of the flow velocities on the Galgeplaat, both for the scenario

Observation point	Present situation [m/s]	2008 bed, no barrier [m/s]	[%]	1983 bed, no barrier [m/s]	[%]
Galgeplaat 1	0.36	0.52	43.8	0.56	53.7
Galgeplaat 2	0.53	0.75	40.5	0.7	31.5
Galgeplaat 3	0.41	0.56	35.3	0.53	27.9
Galgeplaat 4	0.37	0.51	37.1	0.46	23.6
Galgeplaat 5	0.48	0.63	30.9	0.55	14.9
Galgeplaat 6	0.41	0.55	35.7	0.5	24.3
Galgeplaat 7	0.42	0.59	41.3	0.54	29.5
Galgeplaat 8	0.39	0.54	37.5	0.48	21.8
Galgeplaat 9	0.59	0.63	8.1	0.59	0.4
Galgeplaat 10	0.62	0.79	26.4	0.78	26.3

Table 5.4: Velocities on the Galgeplaat in m/s for scenario 1,2 & 3, the percentages represent the increase with respect to the present situation

with barrier as for the simulation without barrier. Based on these values shoal build up is expected.

Realignment of the Oosterschelde will lead to increased flow velocities, see table 5.6. The additional intertidal area that is added to the Oosterschelde causes a small increase of the flow velocities on the Galgeplaat in the scenario with barrier. The increase however is not large enough to enforce shoal building. When the barrier is removed flow velocities that are sufficient to cause shoal build up are found. It must be noted that the flow velocities on the Galgeplaat are lower for the realigned basin without barrier compared to the present situation without the barrier.

Observation point	Present situation [m/s]	2100 bed, barrier [m/s]	[%]	2100 bed, no barrier [m/s]	[%]
Galgeplaat 1	0.36	0.57	58.1	0.75	107.5
Galgeplaat 2	0.53	0.67	25.8	0.9	69.4
Galgeplaat 3	0.41	0.52	25.3	0.69	65.2
Galgeplaat 4	0.37	0.63	70.5	0.82	121.5
Galgeplaat 5	0.48	0.71	48.3	0.9	87.6
Galgeplaat 6	0.41	0.56	37.8	0.72	78
Galgeplaat 7	0.42	0.68	61.9	0.91	118.4
Galgeplaat 8	0.39	0.55	39.7	0.69	75.8
Galgeplaat 9	0.59	0.66	12.9	0.83	41.4
Galgeplaat 10	0.62	0.89	43	1.09	75.4

Table 5.5: Velocities on the Galgeplaat in m/s for scenario 1,4 & 5, the percentages represent the increase with respect to the present situation

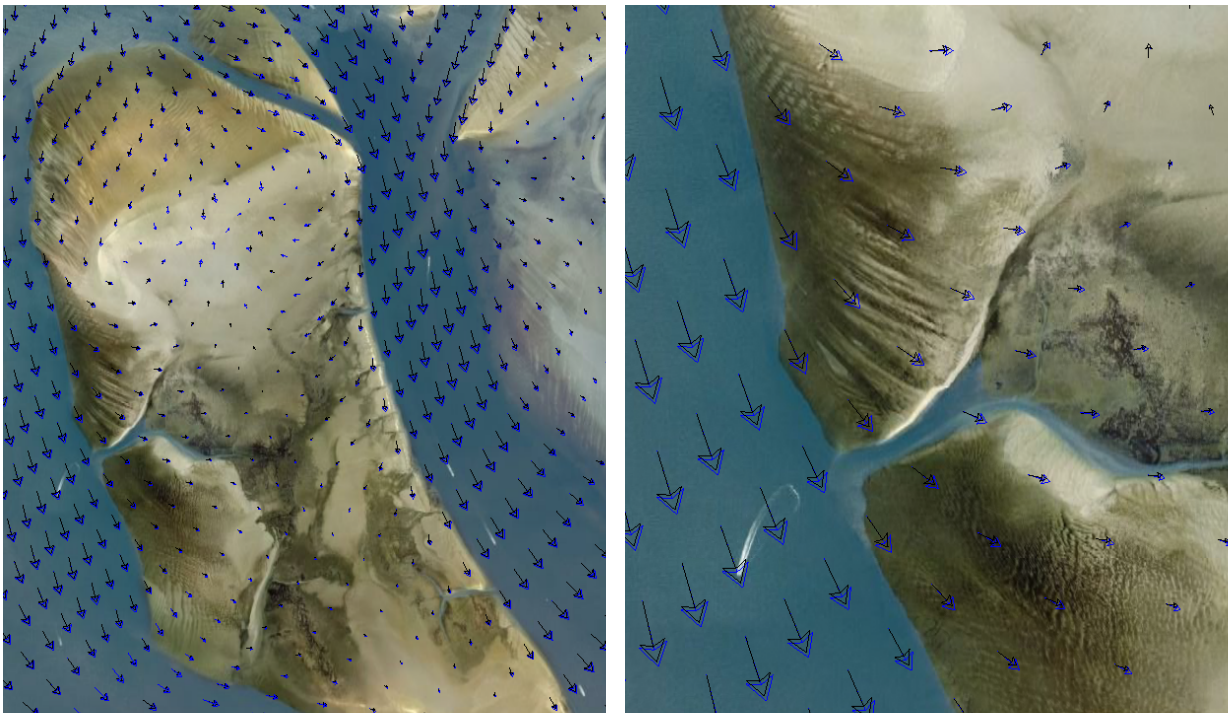

(a) Galgeplaat **(b)** Channel on the west side

Figure 5.31: Vector plot of the depth averaged velocity during flood. Black indicates 2008 bed, barrier. Blue indicates 2008 bed, no barrier

Observation point	Present situation	Realignment 2008 bed, barrier		Realignment 2008 bed, no barrier	
	[m/s]	[m/s]	[%]	[m/s]	[%]
Galgeplaat 1	0.36	0.38	5.2	0.49	35.5
Galgeplaat 2	0.53	0.58	7.9	0.71	33.8
Galgeplaat 3	0.41	0.44	5.3	0.54	31.3
Galgeplaat 4	0.37	0.41	9.6	0.5	35.4
Galgeplaat 5	0.48	0.51	6.1	0.63	31.8
Galgeplaat 6	0.41	0.44	9.5	0.55	35.7
Galgeplaat 7	0.42	0.46	9.6	0.58	38.9
Galgeplaat 8	0.39	0.42	7.6	0.53	35.4
Galgeplaat 9	0.59	0.62	6.4	0.64	8.4
Galgeplaat 10	0.62	0.72	16.6	0.83	33.8

Table 5.6: Velocities on the Galgeplaat in m/s for scenario 1,6 & 7, the percentages represent the increase with respect to the present situation

5.5 Empirical Relations

The output of the Delft3D model is used to evaluate the situation in the Oosterschelde and to make predictions for future development with the help of empirical relations. The tidal prism is obtained by using the cumulative discharge from Delft3D. The tidal prism is the difference between a peak and the consecutive trough and the other way around. This calculation is made for all peaks and troughs in the signal. The tidal prisms given in table 5.7 and 5.8 are the mean

of the results. [Geurts van Kessel, 2004] states that the average tidal prism is $880 \cdot 10^6 m^3$ after the closure. [de Bok, 2001] states that the mean tidal prism after the closure is about $930 \cdot 10^6 m^3$. Though in both reports the location of the inlet cross-section is not mentioned explicitly, it is likely that it is located somewhere near the barrier. Two cross-sections are used to determine the tidal prism at the barrier. The average of these two calculated tidal prisms is compared to literature. The average of the computed tidal prism is $1053 \cdot 10^6 m^3$ which is larger than the values from literature.

Cross-section	Present situation	2008 bed, no barrier	1983 bed, no barrier
Delta	1.191	1.399	1.388
Barrier sea side	1.067	1.246	1.227
Barrier Oosterschelde	1.038	1.222	1.191
Mouth	0.937	1.114	1.075
Centre	0.753	0.901	0.863
South1	0.424	0.511	0.493
South2	0.231	0.280	0.273
North1	0.130	0.155	0.148
North2	0.040	0.048	0.046

Table 5.7: Calculated mean tidal prism in $10^9 m^3$ for scenario 1,2 and 3

Looking at the calculated tidal prisms in table 5.7 it appears that the tidal prism will increase when the barrier is removed. It looks like it will be approximately as large as it was before the deltaworks, $1230 \cdot 10^6 m^3$ according to [Geurts van Kessel, 2004]. It must be stressed that the tidal prism is overestimated by Delft3D. It is likely that the tidal prism will be lower than it was before the delta works, because the tidal prism was reduced by the construction of the Philipsdam and Oesterdam. Comparison of the present situation without barrier with the two different bathymetries shows that the tidal prism increased because of the erosion of the tidal flats.

Applying the equilibrium relation for the stability of the inlet to the defined cross-sections (see figure 5.1) gives an instructive view on the expected development of the channels. The calculated equilibrium cross sectional areas in the western part of the Oosterschelde are approximately as large as the measured cross sections, the channels need to get slightly larger. In the eastern parts of the basin the channels have too large cross sectional areas compared to the equilibrium cross sectional area, indicating that sediment import is necessary. The cross sections in the northern branch are 2 to 3 times as large as the equilibrium cross section. This suggests, that sediment import is necessary to reach an equilibrium situation in the eastern parts of the basin.

When the equilibrium relation for the total channel volume is used, it appears that the channels are too small for the tidal prism that has to flow through it in case the barrier is removed. Considering the entire basin, based on the channel volume relation, export of sediment is expected when the barrier is removed.

Table 5.8 shows that the tidal prism increases towards 2100. Considering the relation for the stability of the cross-sections, it is found that the cross-sections in the western part need to erode to attain equilibrium dimensions. Similar to the 2008 scenarios, the channels in the eastern parts have to develop smaller channels to attain an equilibrium as well in the northern branch as in the southern branch.

Using the equilibrium relation for the total channel volume indicates that the channels need to get deeper when the barrier is removed in 2100. Relative to the 2008 scenario the channel volume is higher in 2100, due to the larger tidal prism. This does not directly mean that the

Cross-section	2008 bed, barrier	2100 bed, barrier	2100 bed, no barrier
Delta	1.191	1.199	1.445
Barrier sea side	1.067	1.092	1.318
Barrier Oosterschelde	1.038	1.066	1.286
Mouth	0.937	0.966	1.166
Centre	0.753	0.795	0.96
South1	0.424	0.457	0.552
South2	0.231	0.262	0.316
North1	0.13	0.148	0.183
North2	0.04	0.046	0.058

Table 5.8: Calculated mean tidal prism in $10^9 m^3$ for scenario 1,4 and 5

Oosterschelde will tend to an equilibrium with deeper channels when the barrier is removed in 2100 compared to 2008. In paragraph 5.4 it was found that shoal build up will occur again when the barrier is removed in 2008. When the barrier is removed in 2100 higher velocities are expected, because of the higher tidal prism, leading to stronger shoal build up. The consequence of shoal build up is that the tidal prism decreases and thereby the flow velocity and the related shoal build up.

Cross-section	2008 bed, barrier	Realignment 2008 bed, barrier	Realignment 2008 bed, no barrier
Delta	1.191	1.365	1.533
Barrier sea side	1.067	1.235	1.36
Barrier Oosterschelde	1.038	1.203	1.355
Mouth	0.937	1.091	1.24
Centre	0.753	0.88	0.997
South1	0.424	0.473	0.539
South2	0.231	0.252	0.287
North1	0.13	0.176	0.2
North2	0.04	0.045	0.051

Table 5.9: Calculated mean tidal prism in $10^9 m^3$ for scenario 1,6 and 7

The tidal prisms that are calculated for the realigned basin are included in table 5.9. The tidal prism in the realigned basin is larger than in the present situation and moreover larger than the tidal prism in 2100. When the calculated tidal prisms are substituted in the empirical relations a result similar to the previous findings is obtained. The relation for the equilibrium cross sections shows erosion in the western part and sedimentation in the eastern parts. The relation for the total channel volume shows erosion througout the basin.

So far only the volume of the channels is elaborated. To evaluate the development of the intertidal area some relations are stated in paragraph 2.2.2. Those relations however do not relate the horizontal area of the flats to the tidal prism. The relation suggested by [Renger and Partenscky, 1974], is extended to the Oosterschelde by [Eysink, 1991]. The curve that fits the Oosterschelde does not show large variations when the total basin area changes, see figure 2.4. When the Oosterschelde is realigned on a large scale a decrease of the relative flat area is expected based on figure 2.4. The absolute area of the intertidal flat area however may increase due to the realignment. The effect of a large increase of the tidal prism, by removing the barrier, cannot be evaluated by using this relation.

5.6 Sedimentation/erosion

In the preceding paragraphs of this chapter, several parameters and relations are used to make predictions about the sediment transport. Besides that the cumulative transport through the defined cross-sections is evaluated. Those paragraphs give a good view on the overall effect of the investigated interferences, but not on local effects. In order to get insight in the spatial distribution of the sedimentation and erosion several sedimentation and erosion plots are included. It must be emphasized that the grid of the Kustzuid model is coarse, meaning that the figures only give a simplified view on the developments. Next to that it is stressed the calculations with sediment transport are executed with the default settings of Delft3D. The stated results can therefore only be used to get an indication of the transport. The figures 5.32 and 5.33 show the transport in the present situation with and without barrier. The impact of the increased flow velocities is clearly visible in the sedimention erosion patterns. In particular the channels show increased activity. On the shoals hardly any difference is visible.

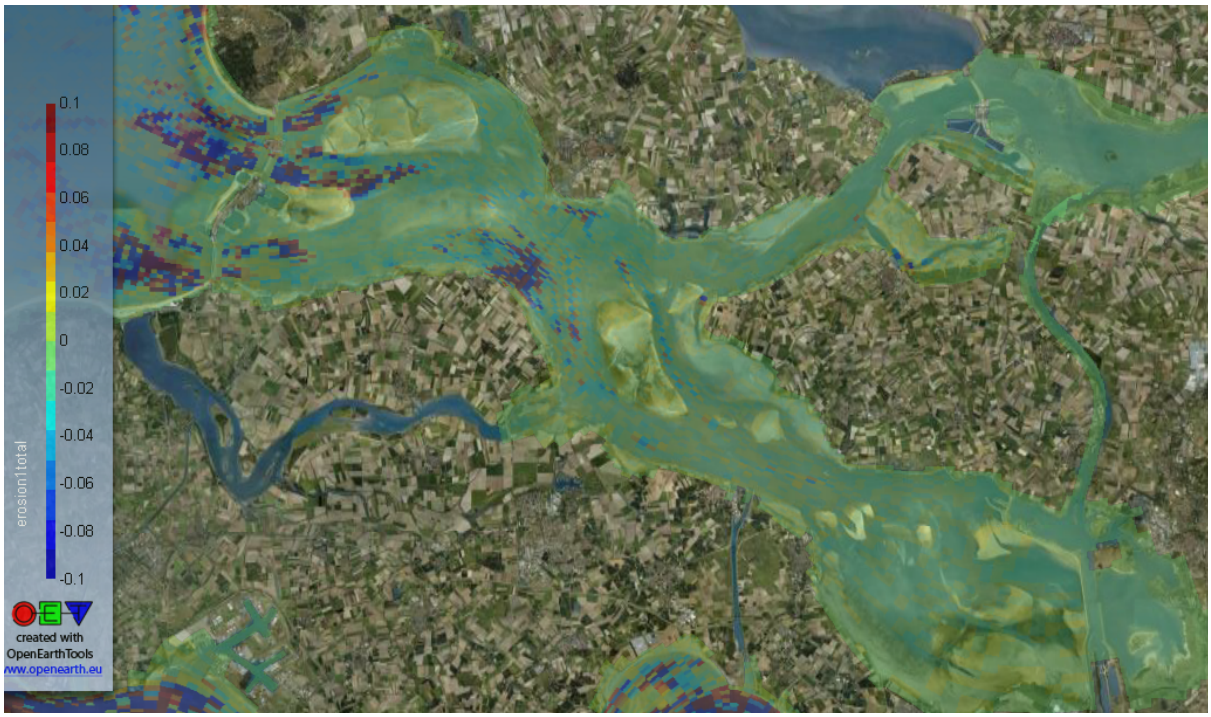

Figure 5.32: Sedimentation/erosion pattern of the present situation, red is sedimentation and blue is erosion in metres

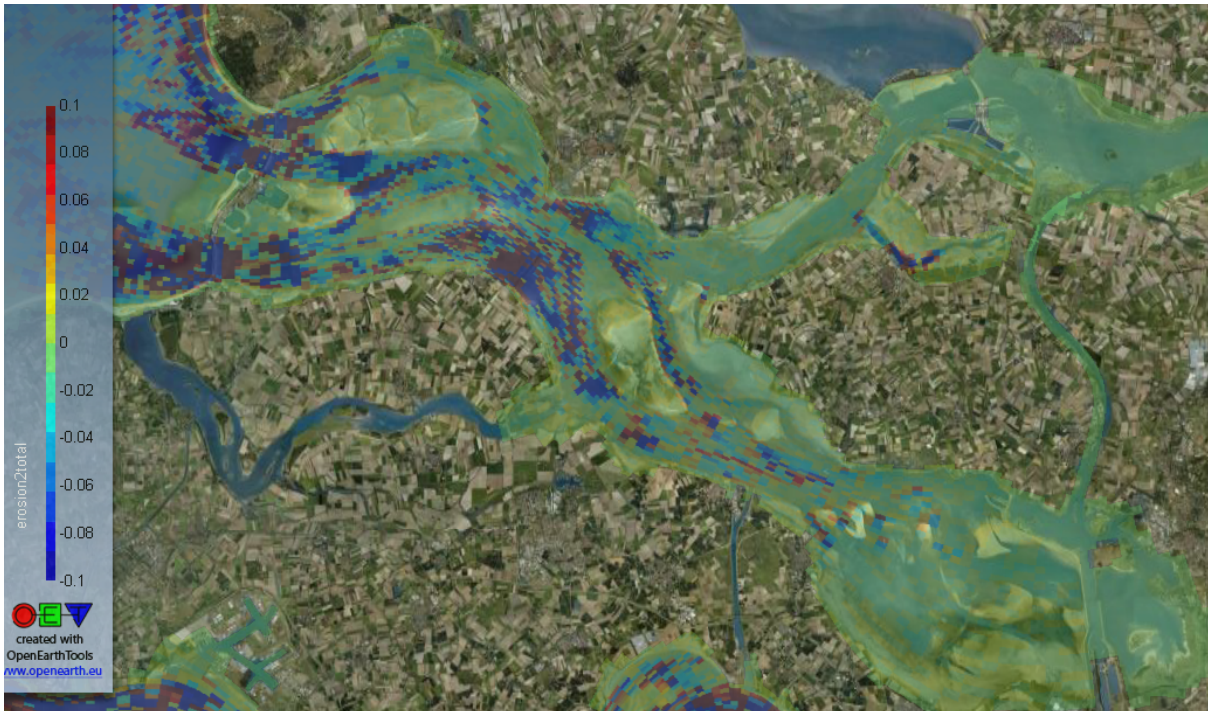

Figure 5.33: Sedimentation/erosion pattern of the present situation without barrier, red is sedimentation and blue is erosion in metres

Chapter 6

Conclusions and recommendations

The goal of this study is to investigate the effect of removal of the Oosterschelde storm surge barrier on the hydrodynamics and morphodynamics. In this chapter first a discussion of the research approach will be given. Subsequently the study goals are attained by answering the research questions stated in paragraph 1.2. These questions are stated again below. Finally a list of recommendations is presented.

- What is the effect of the Philipsdam and Oesterdam on the hydrodynamics in the Oosterschelde basin?
- What is the development of the hydrodynamic response under changing bathymetry in the period 1983 to 2008?
- Will removal of the barrier stop shoal erosion?
- Will the Oosterschelde start exporting sediment like before the closure when the barrier is removed? And what will the equilibrium situation look like?
- What is to be expected for the hydrodynamic and morphological situation in 2100?
- Are there other measures possible to enhance growth of the intertidal area, besides removal of the barrier?

6.1 Discussion

In this paragraph the research approach is discussed. The timeseries that are obtained from the Delft3D simulations are analysed with t_tide. This yields a set of components that represent the original signal. The M_2 and M_4 components are used to evaluate the tidal asymmetry. This means a simplification of reality, therefore the question is stated whether the method to asses tidal asymmetry as proposed by [Friedrichs and Aubrey, 1988] is a reliable indicator of the distortion of the tidal wave. Based on the results the theory of [Friedrichs and Aubrey, 1988] appears to be a reliable indicator of the distortion of the tidal wave. Analysis of the timeseries of the water level show that the theory gives good predictions. Next to that the predictions of the ebb and flood dominance match with the cumulative sediment transport in most cases. This holds both for the water level signal as for the instantaneous discharge signal. In the literature study a remark was made that the theory could only be applied to short basins with a standing wave. [Wang et al., 2002] states that the theory is also applicable for long basins with a 'partly' progressive wave like the Westerschelde. This thesis shows that the theory holds qualitatively for the instantaneous discharge in the Oosterschelde with a partially standing wave.

6.2 Conclusions

In this paragraph the research questions, as stated at the begin of this chapter, will be answered.

What is the effect of the Philipsdam and Oesterdam on the hydrodynamics in the Oosterschelde basin?

The Philipsdam and Oesterdam are built after the finalization of the Oosterschelde storm surge barrier to maintain the tidal range in the basin. Application of the simplified analytical model indicates that the basin is further away from the resonance length when the barrier is removed because of shortening of the basin by the Oesterdam. However the amplification of the tidal wave will be larger when the barrier is removed, because the effect of friction gets lower due to the decreased tidal prism/discharge. Calculations with the analytical model and the Delft3D model both show an increase of the tidal range of 10 to 20%. The model results also indicate that the tidal prism will increase when the barrier is removed but it will not be as large as it was before the Delta project.

What is the development of the hydrodynamic response under changing bathymetry in the period 1983 to 2008?

In general it can be concluded that the changed bathymetry has a negligible effect on the amplitude of the water level. The ebb-dominance of the water level is slightly reduced compared to the 1983 situation. The discharge signal shows that the loss of intertidal area causes an increased discharge/tidal prism. It seems, from the discharge signal, that the system is developing to a less ebb dominant system. The changes however are not strong enough to state this as a conclusion. Taking both the water level and discharge signal into account it is justified to conclude that the system is developing to a less ebb dominant system.

Will removal of the barrier stop shoal erosion?

Flow velocities at 10 observation points on the Galgeplaat are evaluated to check if shoal build up will occur when the barrier is removed. Removal of the barrier causes an increase of the flow velocities of 30 to 40%. Based on those values it can be concluded that shoal build up will start again when the barrier is removed.

Will the Oosterschelde start exporting sediment like before the closure when the barrier is removed? And what will the equilibrium situation look like?

The conclusion can be drawn that export of sediment will occur when the barrier is removed. Evaluation of the asymmetry of the water level and discharge signal indicates ebb-dominance. Furthermore analysis of the cumulative transport shows export of sediment. Application of empirical relations also shows that export is necessary to attain an equilibrium in the Oosterschelde. With respect to the equilibrium situation only global remarks can be made. In the equilibrium situation the channels will be deeper than in the present situation. The equilibrium area of the intertidal flats will be in the range of 40 to 50% of the total basin area which is more or less the same as in the present situation.

What is to be expected for the hydrodynamic and morphological situation in 2100?

The situation in 2100 is represented by removing all sediment above a level of -2m NAP and spreading the removed sediment in the channels. Analysis of the water level signal with the barrier shows that the tidal distortion will get stronger in 2100 (compared to 2008) and that the system is slightly flood dominant. The discharge signal shows the same for the direction, namely slight flood dominance, the distortion however is weaker than in 2008.

The scenario without the barrier shows that the system is ebb dominant, the discharge signal shows slight flood dominance in the eastern parts of the basin. The strength of the distortion is weaker for both the discharge and water level signal. The cumulative transport supports the stated conclusions regarding the situation in 2100.

Are there other measures possible to enhance growth of the intertidal area, besides removal of the barrier?

Simulations with large scale realignment of the Oosterschelde are performed to evaluate if this will increase the intertidal area. Realignment increases the tidal prism in the Oosterschelde and thereby enhances sediment export. In the situation with barrier slightly higher flow velocities on the Galgeplaat are found, however the increased velocities are not strong enough to restore the shoal building capacity.

Removal of the barrier leads to increased flow velocities that will enforce shoal build up. The velocities are of the same order of magnitude as the 2008 situation with barrier.

Furthermore based on empirical relations it is expected that large scale realignment will not have a large effect on the relative flat area.

6.3 Recommendations

During this study it appeared that there are several subjects that need extra attention. Therefore a list of recommendations is presented, divided in two categories.

Model schematization
The Kustzuid model contains some uncertainties and inaccuracies. It is recommended to improve the model to be able to make better predictions in the future.

- The geometry of the basin is of importance for the distortion of the tidal wave. Moreover the tidal prism depends on the volume of the intertidal area. Improvement of the bathymetry will lead to more accurate model results and reduce the uncertainty in the calculation of the tidal prism. A thorough investigation of the bathymetry data is recommended to find an explanation for the inconsistencies in the bathymetry. The investigation should consider the date and measurement method of the files from which the bathymetry file is composed. Besides that the interpolation from the measurement grid to the Kustzuid grid should be checked.

- It is recommended to asses and improve the schematization of the barrier because the M_4 component is not represented well in the vicinity of the barrier. This holds for both the original Kustzuid model and the new schematization that is described in this report. An improved schematization of the barrier reduces the uncertainty in the predictions of the relative phase in the simulations with barrier. The M_4 phase jump causes a shift of the relative phase which has effect on the relative phase in the entire basin.

- When predictions are made for 2100, sea level rise comes into play. The effect of sea level rise is not included in this thesis. Sea level rise will cause a rise of the sediment demand and has an effect on the tidal asymmetry. It is therefore advised to study the effect of sea level rise on the Oosterschelde on the long term.

- In this thesis a simplified representation of the bed in 2100 is applied. It is recommended to predict the bathymetry in 2100 with a more advanced model including wind and waves. The volume of sediment that is removed from the intertidal area and spread in the channels is probably too large. The result of this is uncertainty in the prediction of the tidal asymmetry.

Follow-up study

- Long term morphodynamic calculations for the Oosterschelde with a more detailed model are advised to gain insight in the development of the intertidal area over a longer period. The results of the 2100 simulations indicate that parts of the basin get flood dominant. Long term morphodynamic calculations can be used to investigate if this will lead to infilling of the basin in the eastern parts.

- It is recommended to look into the processes that cause shoal build up. In this thesis it is assumed that 30 to 40% higher flow velocities will cause shoal build up, smaller flow velocities however may also cause shoal build up. More knowledge on the processes that induce shoal build up will make it possible to evaluate the effect of interferences better.

- The theory of [Friedrichs and Aubrey, 1988] only takes the M_2 and M_4 into account. The M_6 however also influences the asymmetry of the wave. It is recommended to analyse the effect of the M_6 on the sediment transport. Including the effect of the M_6 component will lead to more accurate predictions of the tidal asymmetry.

Bibliography

Battjes. CT3310 Stroming in waterlopen, 2002.

C. de Bok. Long term morphology of the Eastern Scheldt. Technical report, Rijkswaterstaat, 2001.

J. Bosboom and M.J.F. Stive. *Lecture notes Coastal dynamics I.* VSSD, 2011.

I. Das. Morphodynamic modelling of the Galgeplaat. Master's thesis, Delft University of Technology, 2010.

Deltacommittee. Bevindingen van de Deltacommissie, 2008.

Deltares. Delft3D FLOW User Manual 3.15 edition September, 2011.

M. Eelkema. Personal communication, 2012.

M Eelkema, Z.B. Wang, and M.J.F. Stive. Impact of back-barrier dams to the development of the ebb-tidal delta of the Eastern Scheldt. 2011.

W.D. Eysink. Impact of sea level rise on the morphology of the Wadden Sea in the scope of its ecological function. Technical report, Delft hydraulics, 1991.

C.T. Friedrichs and D.G. Aubrey. Non-linear Tidal Distortion in Shallow Well-mixed Estuaries: a Synthesis. *Estuarine, coastal and Shelf Science*, 27:521–545, 1988.

A.J.M. Geurts van Kessel. Verlopend tij. Technical report, RIKZ/Rijkswaterstaat, 2004.

Royal Haskoning. Toekomstprognose ontwikkeling intergetijdengebied Oosterschelde, Doorvertaling naar effecten op veiligheid en natuurwaarden. Technical report, Royal Haskoning, 2008.

B.J.A. Huisman and A.P. Luijendijk. Sand demand of the Eastern Scheldt. Technical report, Deltares, 2009.

J. van de Kreeke and J. Haring. Equilibrium flow areas in the Rhine-Meuse delta. *Coastal engineering*, 3:97–111, 1979.

J. van de Kreeke and K. Robaczewska. Tide-induced residual transport of coarse sediment; Application to the Ems estuary. *Netherlands Journal of Sea Research*, 31(3):209–220, 1993.

T. Louters, J.H. van den Berg, and J.P.M. Mulder. Geomorphological Changes of the Oosterschelde Tidal system during and after the implementation of the Delta project. *Journal of Coastal Research, Royal Palm Beach Florida*, 14(3):1134–1151, 1998.

J. Mulder and S. van Heteren. Gulzige geulen en slinkende slikken in de Zuidwestelijke delta. Technical report, Deltares, 2009.

Rich Pawlowicz, Bob Beardsley, and Steve Lentz. Classical tidal harmonic analysis including error estimates in MATLAB using T_TIDE. *Computers & Geosciences*, 28:929–937, 2002.

B.N. Quyen. Morphology of the Eastern Scheldt ebb-tidal delta. Master's thesis, Delft University of Technology, 2010.

E. Renger and H.W. Partenscky. Stability criteria for tidal basins. *ICCE Proc 14th Conference on Coastal Engineering, Copenhagen, Denmark*, 2:1605–1618, 1974.

Rijkswaterstaat. Ontwerpnota stormvloedkering Oosterscheldekering boek 2. Technical report, Ministerie van verkeer en waterstaat, 1991b.

RWS Waterdienst and Deltares. Beschrijving Modelschematisatie simona-kustzuid-2004-v4, versie 2009-01, 2009.

P. Speer, D.G. Aubrey, and C.T. Friedrichs. Non-linear hydrodynamics of shallow tidal inlet/bay systems. *Parker, B.B. Tidal hydrodynamics, J.Wiley & Sons, New York*, :, 1991.

T.L. Walton and W.D. Adams. Capacity of inlet outer bars to store sand. In *Proceedings of the 15th Coastal Engineering Conference, Honolulu, HI:ASCE, pp. 1919-37*, 1976.

Z.B. Wang. Tidal asymmetry and residual sediment transport in estuaries. Technical report, WL|Delft hydraulics, 1999.

Z.B. Wang, M.C.J.L. Jeuken, H. Gerritsen, H.J. de Vriend, and B.A. Kornman. Morphology and asymmetry of the vertical tide in the Westerschelde estuary. *Continental Shelf Research*, 22:2599–2609, 2002.

Actuele waterdata. by rijkswaterstaat, http://live.getij.nl, 2012.

E. van Zanten and L.A. Adriaanse. Verminderd getij, verkenning naar mogelijkheden om het verlies van platen, slikken en schorren in de Oosterschelde te beperken. Technical report, Rijkswaterstaat, 2008.

Historische waterdata. by rijkswaterstaat, http://live.waterbase.nl/, 2012.

Appendix A

Theory: Analytical model

The harmonic method is based on the propagation of a sine shaped wave that is travelling through prismatic channels. Five parameters are used to describe the branches, those parameters are stated in table A.1. The input parameters are used to calculate the branch constants,

Parameter	**Symbol**	**Unit**
Length of the branch	L	[m]
Storage channel width	B	[m]
Flow carrying channel width	B_s	[m]
Flow carrying depth	D	[m]
Friction factor	c_f	[-]

Table A.1: Input parameters

see table A.2. The solution of the system of equations is written in a complex form. By doing

Parameter	**Symbol**	**Unit**	**Formula**
Flow carrying area	A_s	$[m^2]$	$A_s = DB_s$
Hydraulic radius	R	$[m]$	$R = A_s/(B_s + 2D)$
Loss factor	χ	$[m^{-3}]$	$\chi = \frac{8}{3\pi}\frac{c_f}{A_s R}$
Frictionless wave number	k_0	$[rad/m]$	$k_0 = \frac{\omega}{\sqrt{gA_s/B}}$

Table A.2: Branch constants

this the variables place and time are separated. The general equations for the wave motion in a branch are given below. ζ represents the water level amplitude and Q the discharge amplitude.

$$\tilde{\zeta}(x) = C_+ e^{-px} + C_- e^{px} \tag{A.1}$$

$$\tilde{Q}(x) = \frac{i\omega B}{p}\left[C_+ e^{-px} - C_- e^{px}\right] \tag{A.2}$$

The factor p is a complex number that holds information about the variation of the amplitude and phase of the wave. The definition of p is given in eq A.3, σ represents the friction eq A.4.

$$p = ik_0\sqrt{1 - i\sigma} \tag{A.3}$$

$$\sigma = \frac{\chi Q_{rep}}{\omega} \tag{A.4}$$

By rewriting the general equations, a system of equations is obtained which gives the relations between the four water levels and discharges at both sides of a branch. The system $A\zeta$ is solved for the boundary conditions that are imposed. This yields a vector with values for the water level amplitude ζ. The obtained water level amplitudes are used to calculate the discharge amplitude vector Q.

$$A = \frac{i\omega B}{p} \begin{bmatrix} coth(pL) & -sinh^{-1}(pL) \\ -sinh^{-1}(pL) & coth(pL) \end{bmatrix} \tag{A.5}$$

$$A\zeta = \zeta_{BC} \text{ solving yields } \begin{bmatrix} \zeta_{\text{node1}} \\ \zeta_{\text{node2}} \end{bmatrix} \tag{A.6}$$

$$\begin{bmatrix} Q_{\text{to node1}} \\ Q_{\text{to node2}} \end{bmatrix} = \frac{i\omega B}{p} \begin{bmatrix} coth(pL) & -sinh^{-1}(pL) \\ -sinh^{-1}(pL) & coth(pL) \end{bmatrix} \begin{bmatrix} \zeta_{\text{node1}} \\ \zeta_{\text{node2}} \end{bmatrix} \tag{A.7}$$

The value of Q_{rep} is used to calculate σ, because this value is not known on beforehand iteration is necessary. The first calculation is performed with Q_{rep} values of zero. In the subsequent iteration the obtained values of Q are used for a new estimation of Q_{rep}. For each branch the value of the representative discharge must model the total energy loss well. In relatively short branches it is justified to approximate the representative discharge with eq A.8, under the assumption that Q varies linear with x.

$$\hat{Q_{rep}} = \sqrt[1/3]{(\hat{Q_1}\hat{Q_2})(\hat{Q_1}^2\hat{Q_2}^2)/4} \tag{A.8}$$

The representative discharge is bigger than the average discharge in the branch, because the energy loss does not vary proportional with the discharge but to the third power. Due to this the higher discharges contribute more than the lower ones. The calculation can be expanded for a system of several branches. In that case the matrices A for each branch are added to a big matrix. Solving this matrix yields the amplitudes of h and subsequently Q. [Battjes, 2002]

Appendix B

Input Analytical model

B.1 Situation in 1971

Branch nr	Node nr left	Node nr right	L	B	B_s	D	c_f
1	1	8	4500	4500	1500	20	0.006
2	2	9	2300	2300	2300	13	0.006
3	3	10	3600	3800	1900	16	0.006
4	4	11	3600	2300	750	13	0.006
5	5	11	7100	3000	2300	13	0.006
6	6	14	7500	3800	3800	6	0.006
7	7	18	4800	1800	750	13	0.006
8	8	12	4650	2300	900	32	0.006
9	9	13	6600	3000	1900	13	0.006
10	10	11	4500	2300	750	20	0.006
11	11	13	5850	2300	1500	17	0.006
12	11	14	5250	1500	1500	20	0.006
13	13	16	4050	1500	1500	20	0.006
14	13	15	1650	3000	750	30	0.006
15	15	16	2100	3000	750	40	0.006
16	14	18	1950	1500	750	20	0.006
17	14	17	3300	2300	750	17	0.006
18	18	21	2100	1500	1500	30	0.002
19	16	19	550	1600	1600	40	0.002
20	19	22	1500	3000	3000	35	0.002
21	17	20	900	1500	1500	20	0.002
22	20	23	550	1100	1000	20	0.002
23	23	24	850	2300	2300	20	0.002
24	21	25	750	1100	1100	25	0.002
25	22	26	7800	1500	1250	35	0.005
26	22	27	7800	2300	750	15	0.005
27	24	27	5250	2300	750	25	0.005
28	25	28	4800	1600	500	30	0.005
29	26	29	3150	1600	750	15	0.005
30	27	30	2400	1500	1250	25	0.005
31	28	31	3900	2100	500	35	0.005

32	31	30	2700	3000	750	20	0.005
33	30	32	3150	1200	950	40	0.005
34	30	29	3900	750	750	15	0.005
35	29	33	5000	3000	750	35	0.003
36	32	34	2700	2300	1250	25	0.003
37	33	35	3150	2300	750	40	0.003
38	34	36	6750	3150	500	20	0.003
39	34	37	3600	1600	750	30	0.003
40	35	38	4950	1200	750	30	0.003
41	36	39	3300	2900	1900	15	0.003
42	38	39	1200	1500	1500	20	0.003
43	38	46	11250	3150	3150	6	0.001
44	39	42	4500	1500	750	40	0.001
45	42	43	3600	1800	1250	20	0.001
46	43	45	5100	3000	3000	20	0.001
47	42	44	4050	1900	1800	10	0.001
48	37	40	4950	2300	750	30	0.001
49	40	41	5100	1600	1600	8	0.001
50	40	47	4950	1450	1300	28	0.001
51	47	48	2700	2100	600	20	0.001
52	48	49	4800	4500	1250	15	0.001
53	49	50	6900	2700	2700	10	0.001
54	50	51	4650	2300	2300	8	0.001
55	45	52	3750	5700	5700	20	0.001

B.2 Situation in 2008

Branch nr	**Node nr left**	**Node nr right**	L	B	B_s	D	c_f
1	1	8	4500	4500	1500	20	0.006
2	2	9	2300	2300	2300	13	0.006
3	3	10	3600	3800	1900	16	0.006
4	4	11	3600	2300	750	13	0.006
5	5	11	7100	3000	2300	13	0.006
6	6	14	7500	3800	3800	6	0.006
7	7	18	4800	1800	750	13	0.006
8	8	12	4650	2300	900	32	0.006
9	9	13	6600	3000	1900	13	0.006
10	10	11	4500	2300	750	20	0.006
11	11	13	5850	2300	1500	17	0.006
12	11	14	5250	1500	1500	20	0.006
13	13	16	4050	1500	1500	20	0.006
14	13	15	1650	3000	750	25	0.006
15	15	16	2100	3000	750	40	0.006
16	14	18	1950	1500	750	20	0.006
17	14	17	3300	2300	750	20	0.006
18	18	21	2100	1500	1500	32	0.006

19	16	19	550	1600	1300	7	0.006
20	19	22	1500	3000	3000	45	0.006
21	17	20	900	1500	1500	25	0.006
22	20	23	550	1100	670	7	0.006
23	23	24	850	2300	2300	30	0.006
24	21	25	750	1100	630	7	0.006
25	22	26	7800	1500	1250	32	0.005
26	22	27	7800	2300	750	20	0.005
27	24	27	5250	2300	750	25	0.005
28	25	28	4800	1600	500	32	0.005
29	26	29	3150	1600	750	20	0.005
30	27	30	2400	1500	1250	25	0.005
31	28	31	3900	2100	500	32	0.005
32	31	30	2700	3000	750	25	0.005
33	30	32	3150	1200	950	38	0.005
34	30	29	3900	750	750	13	0.005
35	29	33	5000	3000	750	30	0.003
36	32	34	2700	2300	1250	25	0.003
37	33	35	3150	2300	750	40	0.003
38	34	36	6750	3150	500	20	0.003
39	34	37	3600	1600	750	25	0.003
40	35	38	4950	1200	750	25	0.003
41	36	39	3300	2900	1900	20	0.003
42	38	39	1200	1500	1500	20	0.003
43	38	46	11250	3150	3150	6	0.001
44	39	42	4500	1500	750	38	0.001
45	42	43	3600	1800	1250	20	0.001
46	43	45	5100	3000	3000	13	0.001
47	42	44	4050	1900	1800	13	0.001
48	37	40	4950	2300	750	28	0.001
49	40	41	5100	1600	1600	8	0.001
50	40	47	4950	1450	1300	28	0.001

B.3 Removal of the Oosterschelde barrier

Branch nr	**Node nr left**	**Node nr right**	L	B	B_s	D	c_f
1	1	8	4500	4500	1500	20	0.006
2	2	9	2300	2300	2300	13	0.006
3	3	10	3600	3800	1900	16	0.006
4	4	11	3600	2300	750	13	0.006
5	5	11	7100	3000	2300	13	0.006
6	6	14	7500	3800	3800	6	0.006
7	7	18	4800	1800	750	13	0.006
8	8	12	4650	2300	900	32	0.006
9	9	13	6600	3000	1900	13	0.006
10	10	11	4500	2300	750	20	0.006

11	11	13	5850	2300	1500	17	0.006
12	11	14	5250	1500	1500	20	0.006
13	13	16	4050	1500	1500	20	0.006
14	13	15	1650	3000	750	25	0.006
15	15	16	2100	3000	750	40	0.006
16	14	18	1950	1500	750	20	0.006
17	14	17	3300	2300	750	20	0.006
18	18	21	2100	1500	1500	32	0.002
19	16	19	550	1600	1600	25	0.002
20	19	22	1500	3000	3000	45	0.002
21	17	20	900	1500	1500	25	0.002
22	20	23	550	1100	1100	25	0.002
23	23	24	850	2300	2300	30	0.002
24	21	25	750	1100	1100	25	0.002
25	22	26	7800	1500	1250	32	0.005
26	22	27	7800	2300	750	20	0.005
27	24	27	5250	2300	750	25	0.005
28	25	28	4800	1600	500	32	0.005
29	26	29	3150	1600	750	20	0.005
30	27	30	2400	1500	1250	25	0.005
31	28	31	3900	2100	500	32	0.005
32	31	30	2700	3000	750	25	0.005
33	30	32	3150	1200	950	38	0.005
34	30	29	3900	750	750	13	0.005
35	29	33	5000	3000	750	30	0.003
36	32	34	2700	2300	1250	25	0.003
37	33	35	3150	2300	750	40	0.003
38	34	36	6750	3150	500	20	0.003
39	34	37	3600	1600	750	25	0.003
40	35	38	4950	1200	750	25	0.003
41	36	39	3300	2900	1900	20	0.003
42	38	39	1200	1500	1500	20	0.003
43	38	46	11250	3150	3150	6	0.001
44	39	42	4500	1500	750	38	0.001
45	42	43	3600	1800	1250	20	0.001
46	43	45	5100	3000	3000	13	0.001
47	42	44	4050	1900	1800	13	0.001
48	37	40	4950	2300	750	28	0.001
49	40	41	5100	1600	1600	8	0.001
50	40	47	4950	1450	1300	28	0.001

Appendix C

Timeseries of the water level

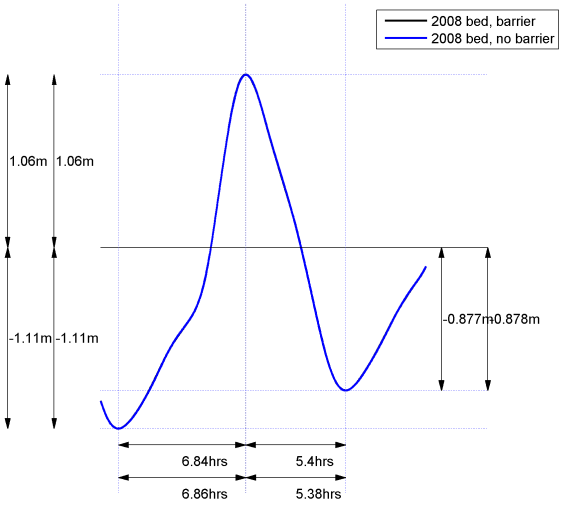

(a) Europlatform

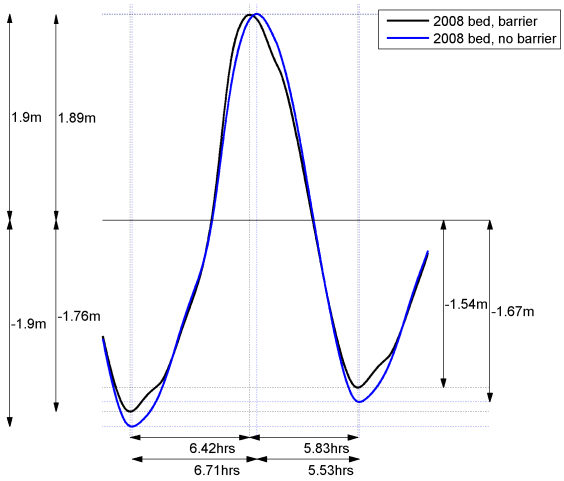

(b) Roompot buiten

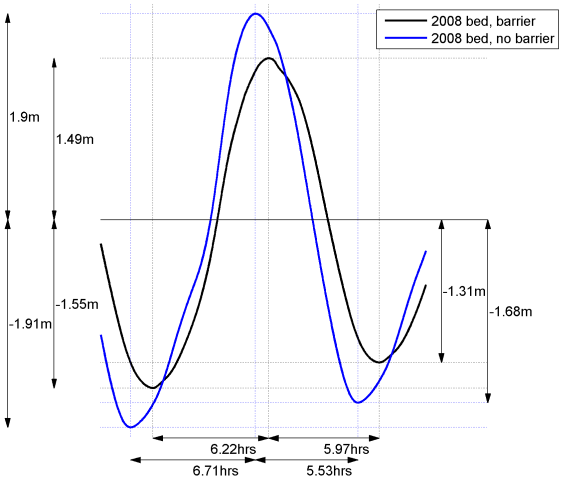

(c) Roompot binnen

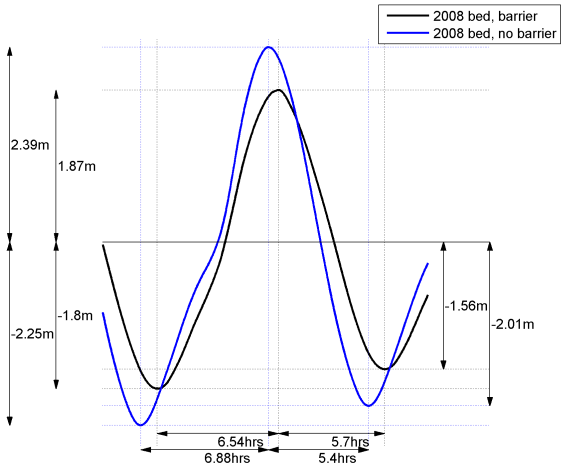

(d) Stavenisse

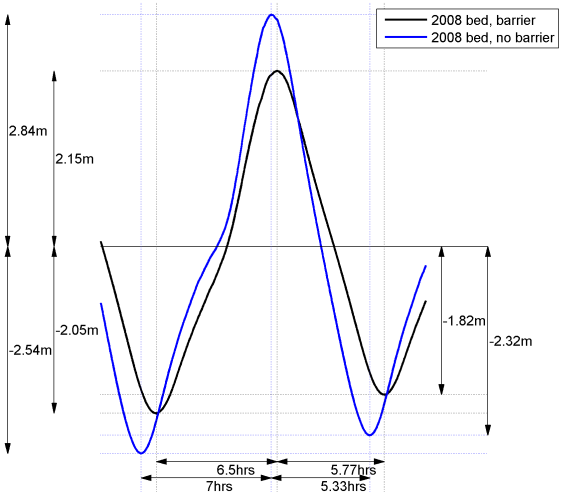

(e) Bergse diepsluis west

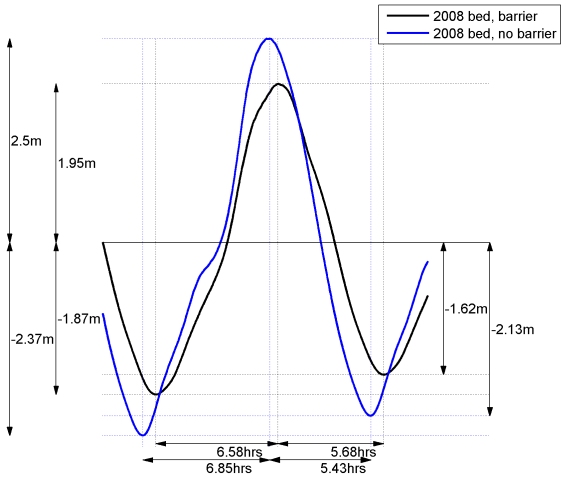

(f) Krammersluizen

Figure C.1: Timeseries of the water level, scenario 1 and 2

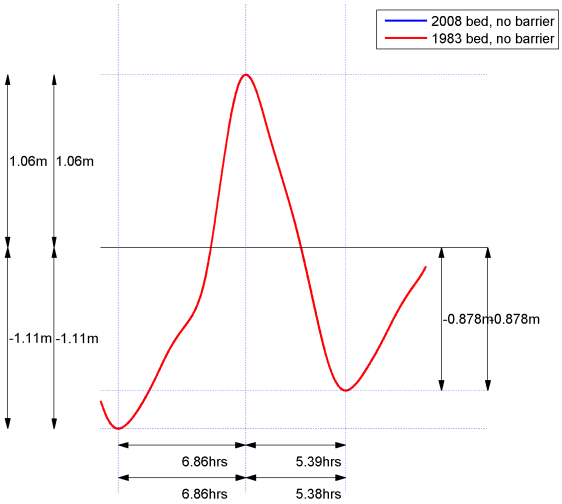

(a) Europlatform

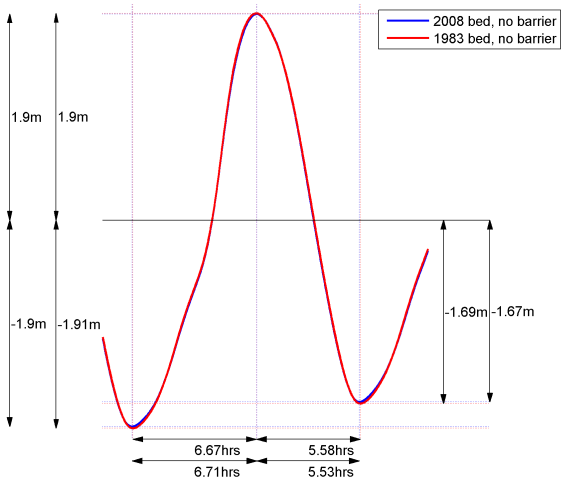

(b) Roompot buiten

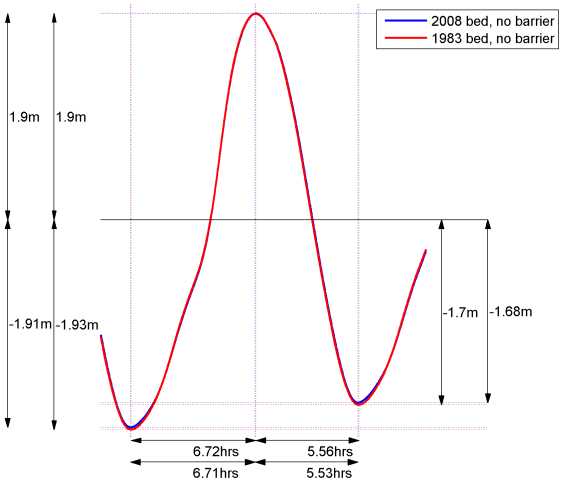

(c) Roompot binnen

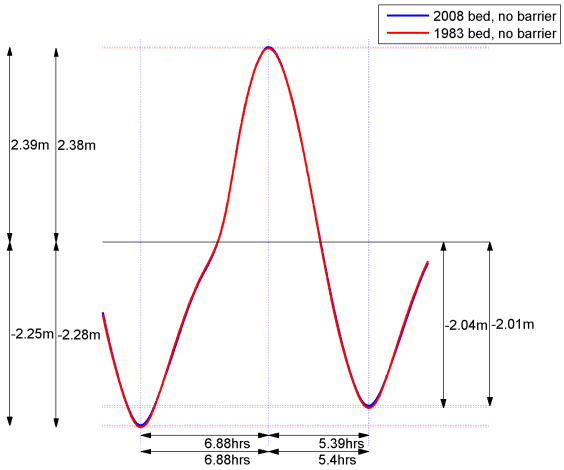

(d) Stavenisse

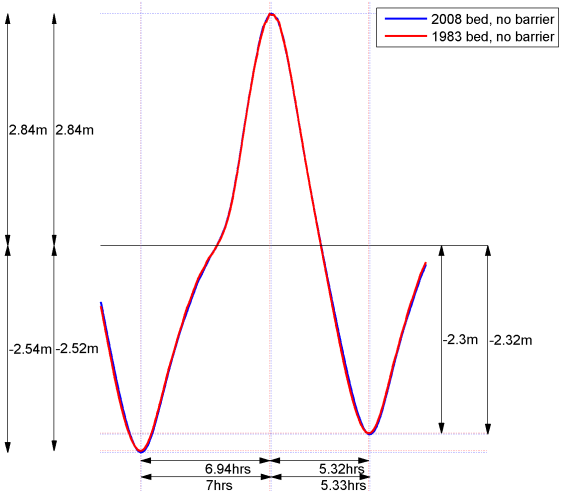

(e) Bergse diepsluis west

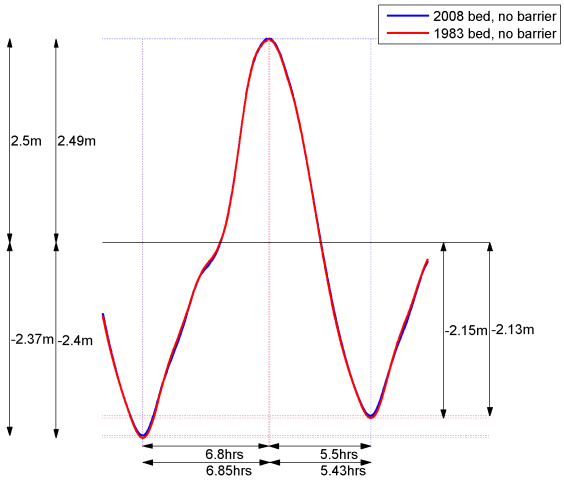

(f) Krammersluizen

Figure C.2: Timeseries of the water level, scenario 2 and 3

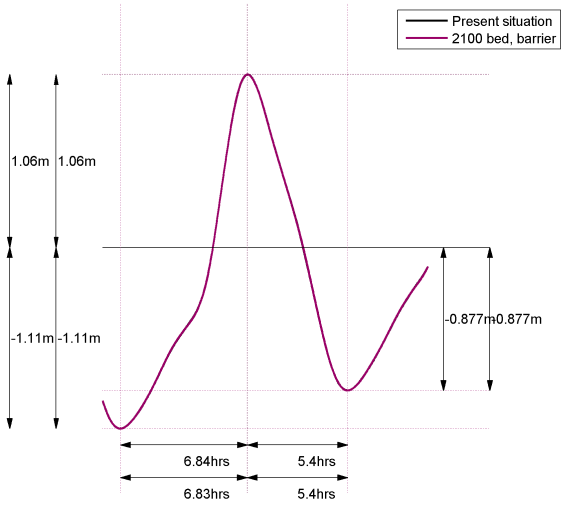

(a) Europlatform

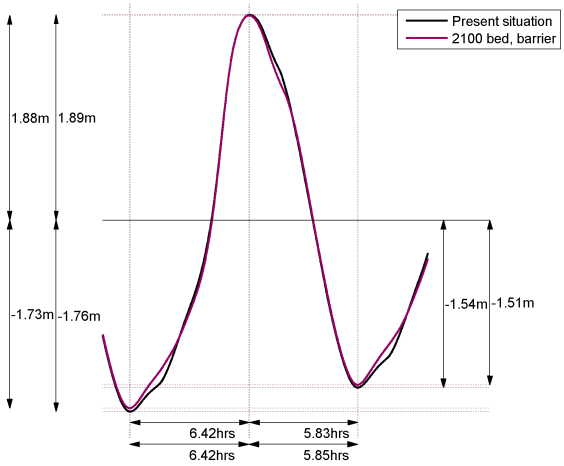

(b) Roompot buiten

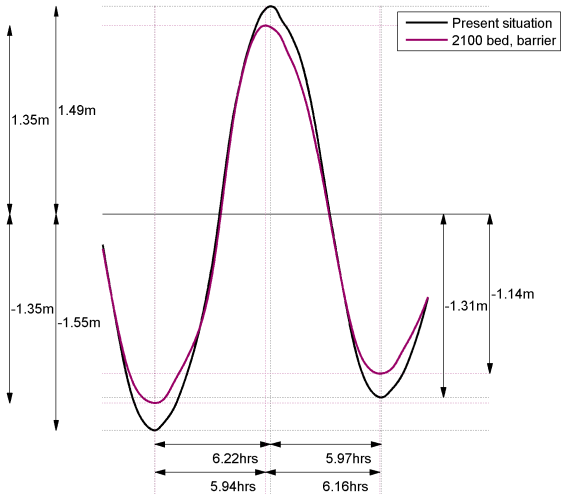

(c) Roompot binnen

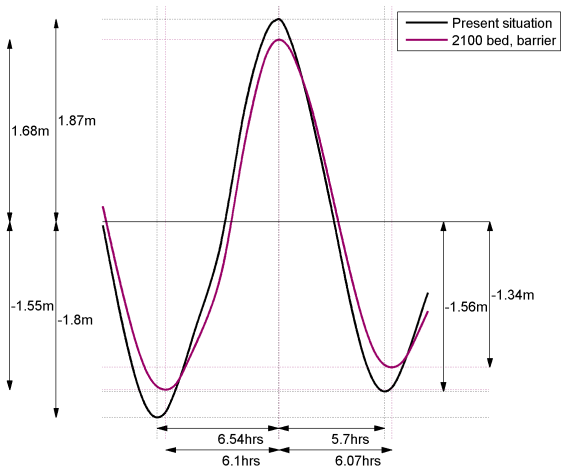

(d) Stavenisse

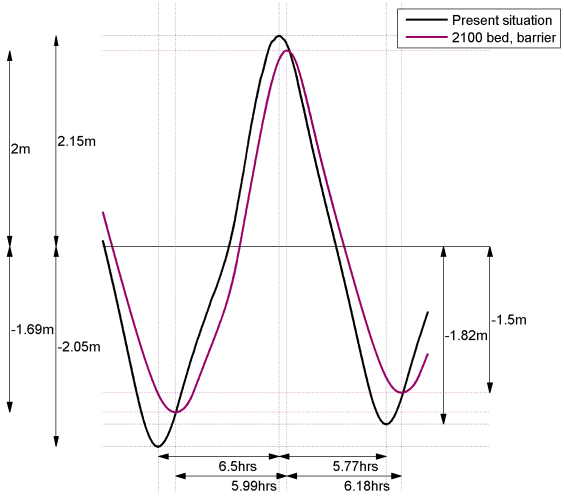

(e) Bergse diepsluis west

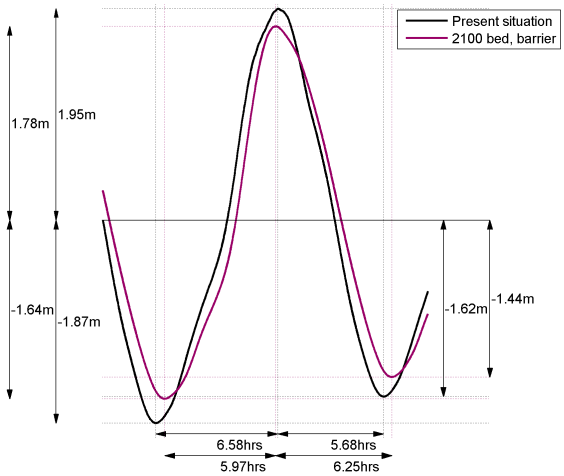

(f) Krammersluizen

Figure C.3: Timeseries of the water level, scenario 1 and 4

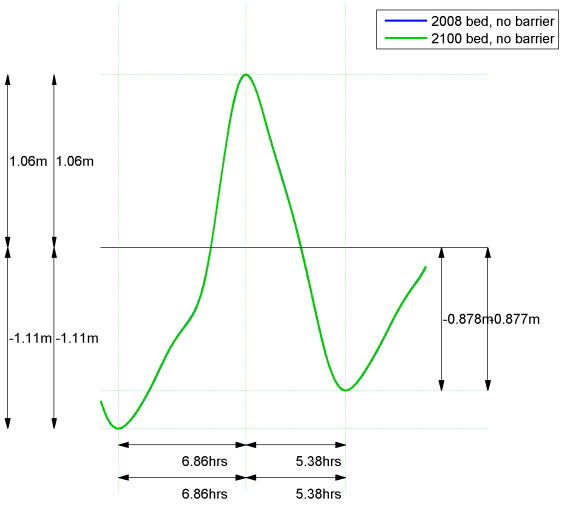

(a) Europlatform

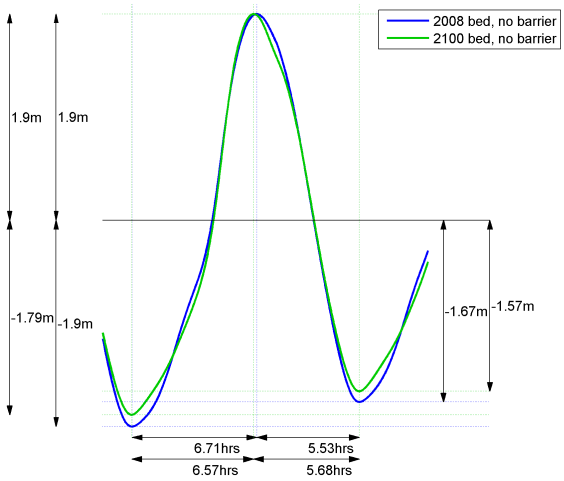

(b) Roompot buiten

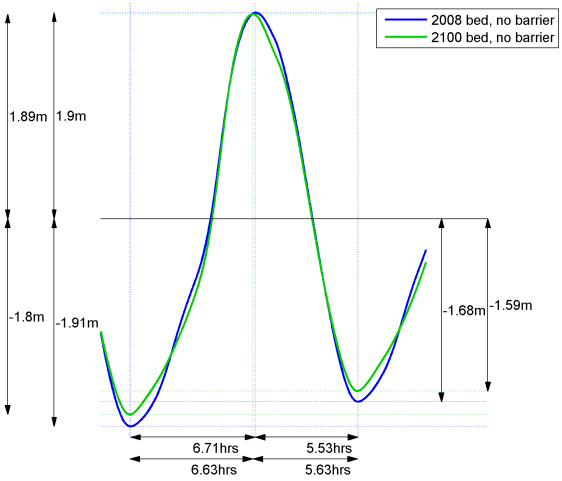

(c) Roompot binnen

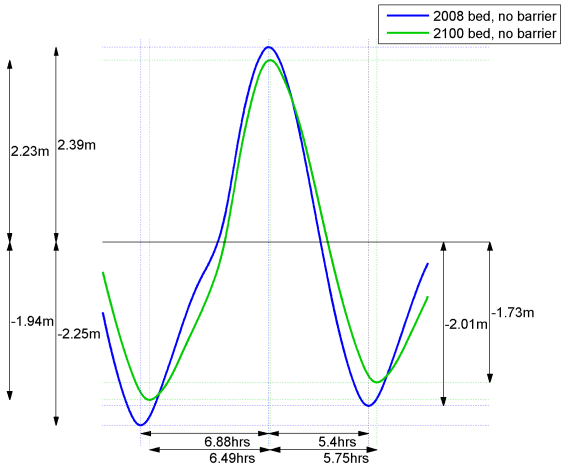

(d) Stavenisse

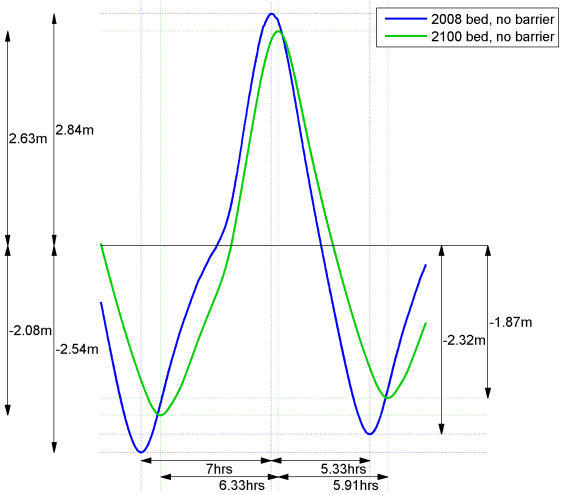

(e) Bergse diepsluis west

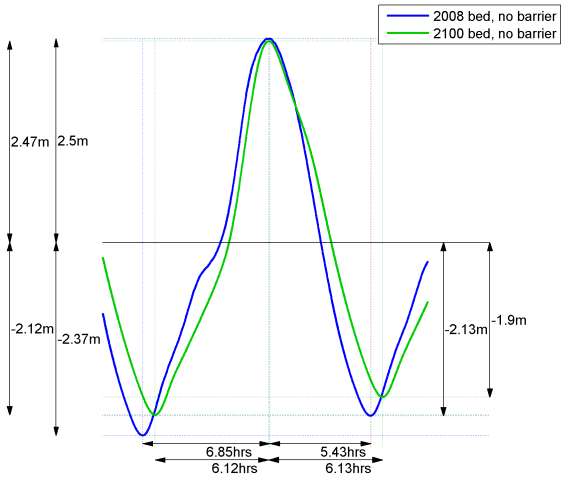

(f) Krammersluizen

Figure C.4: Timeseries of the water level, scenario 2 and 5

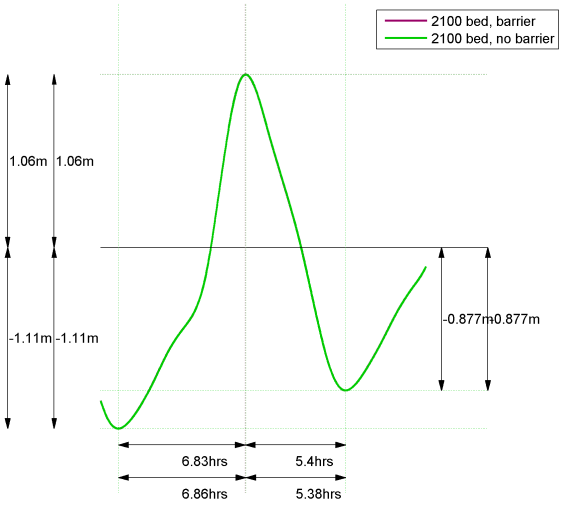

(a) Europlatform

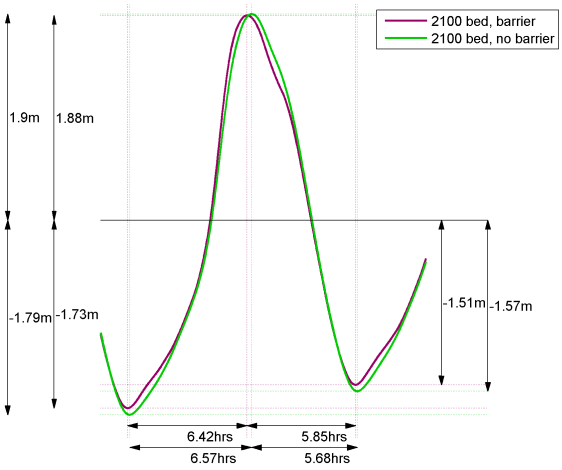

(b) Roompot buiten

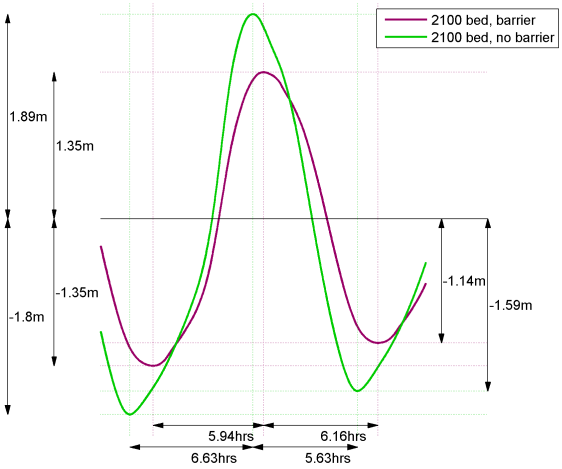

(c) Roompot binnen

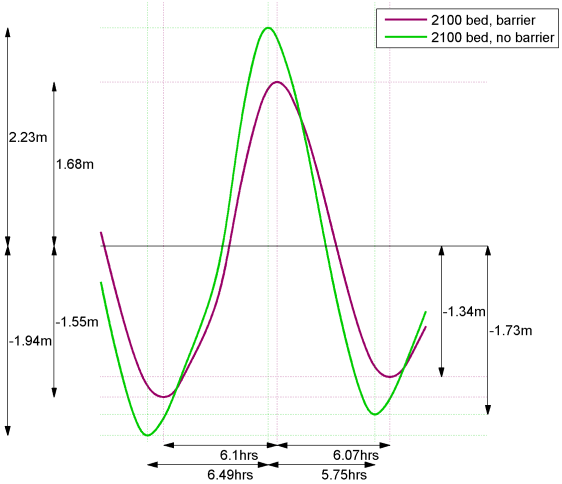

(d) Stavenisse

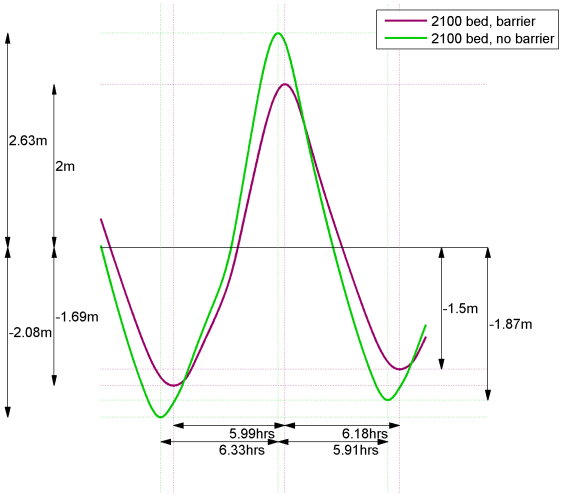

(e) Bergse diepsluis west

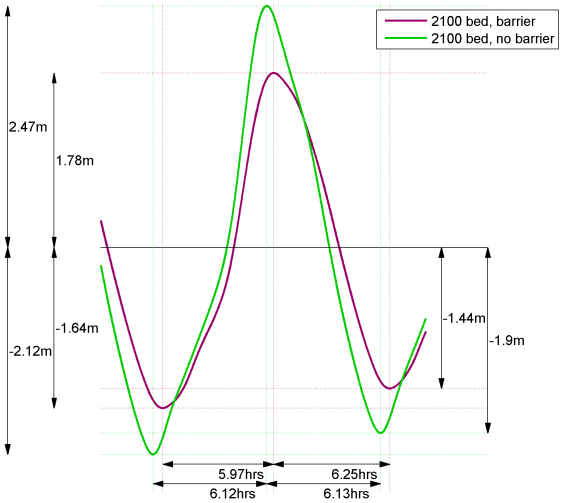

(f) Krammersluizen

Figure C.5: Timeseries of the water level, scenario 4 and 5

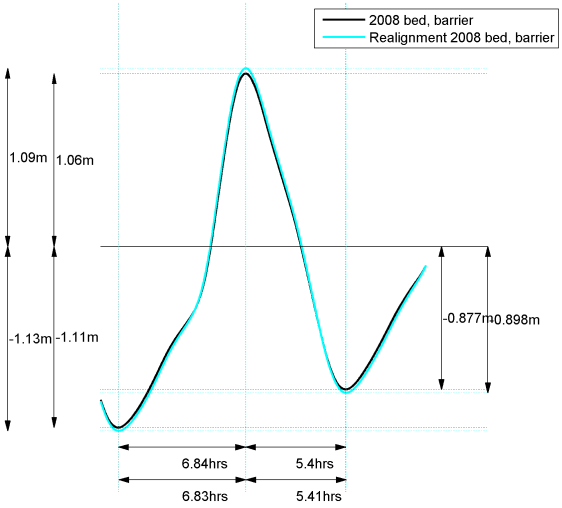

(a) Europlatform

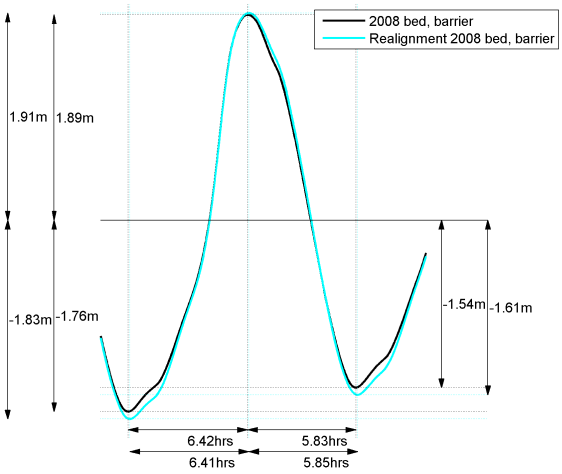

(b) Roompot buiten

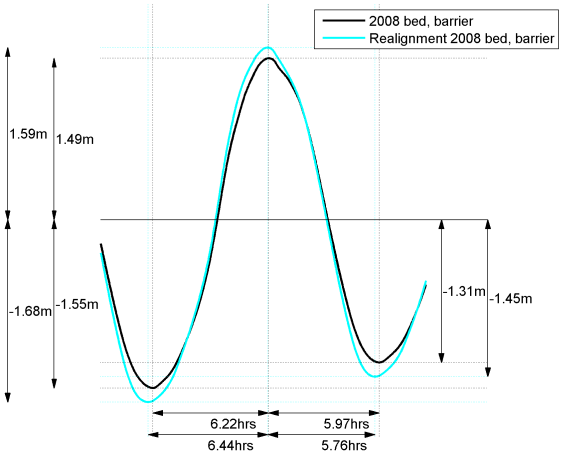

(c) Roompot binnen

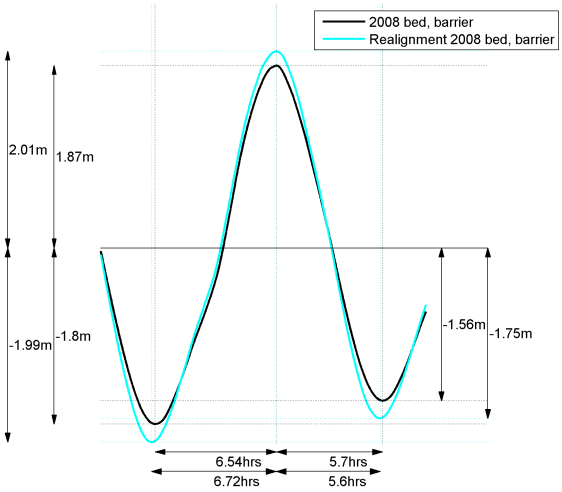

(d) Stavenisse

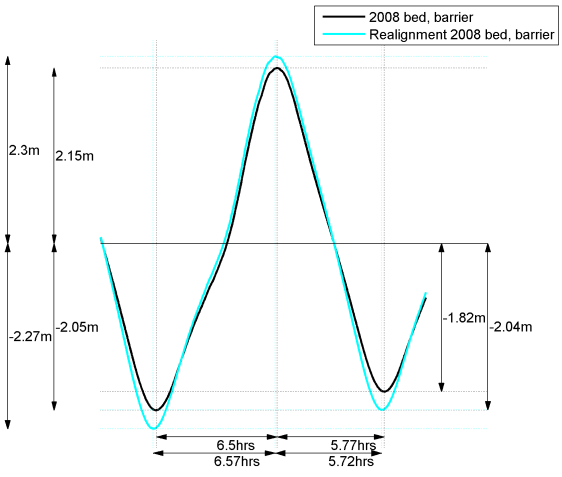

(e) Bergse diepsluis west

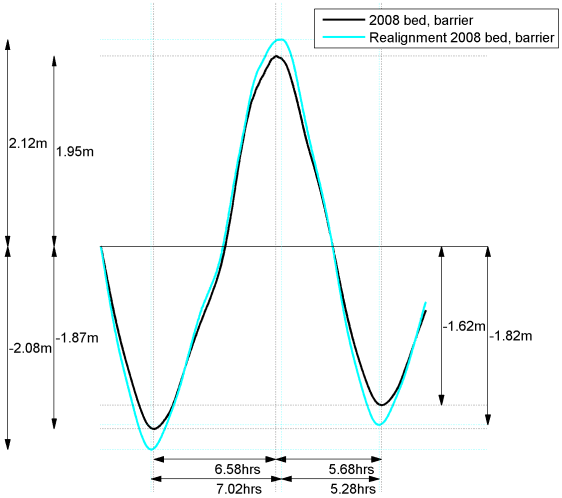

(f) Krammersluizen

Figure C.6: Timeseries of the water level, scenario 1 and 7

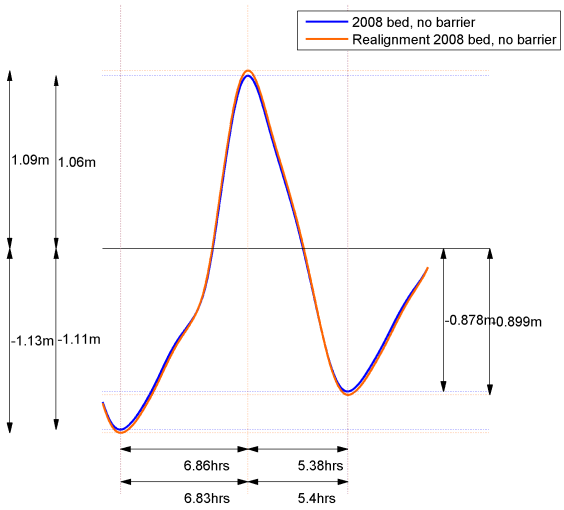

(a) Europlatform

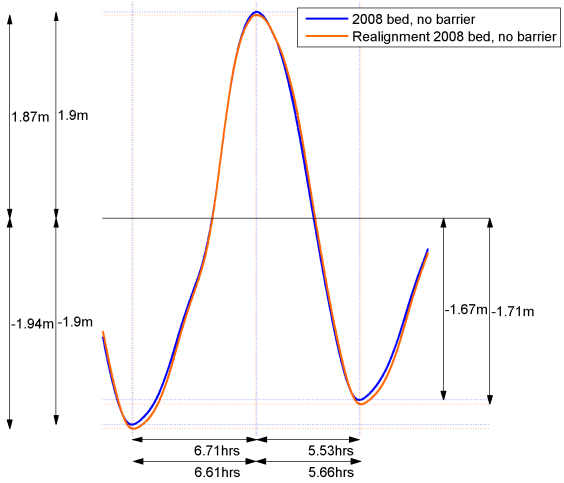

(b) Roompot buiten

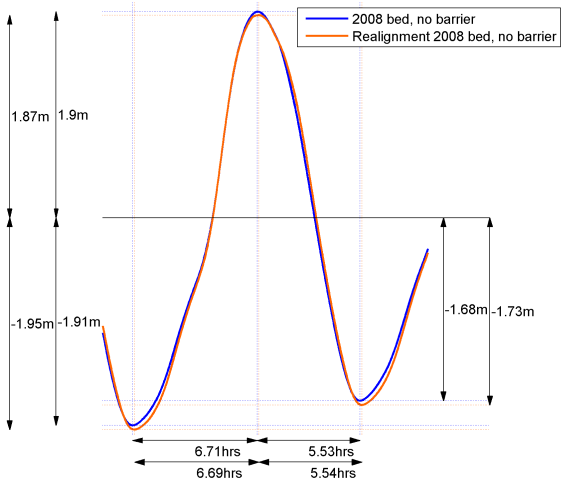

(c) Roompot binnen

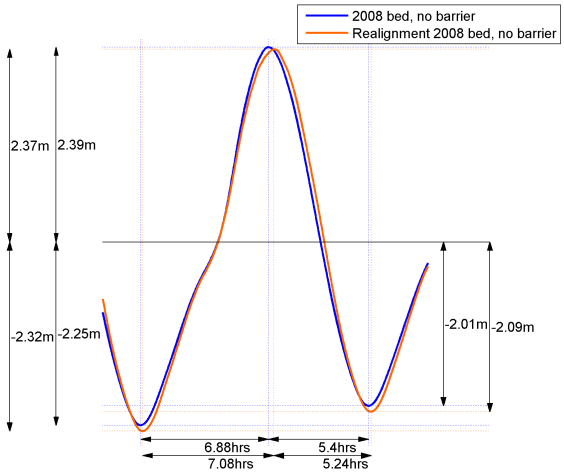

(d) Stavenisse

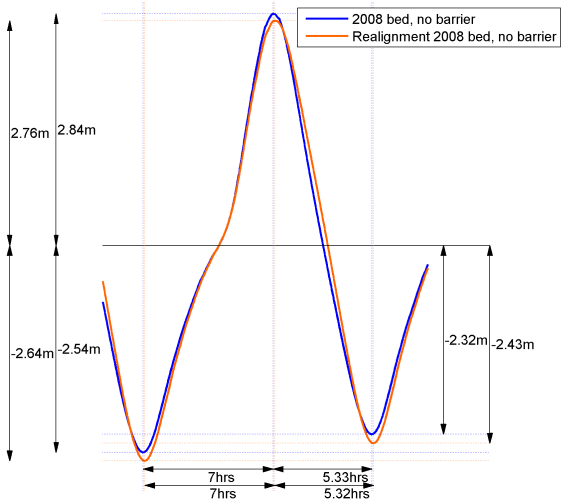

(e) Bergse diepsluis west

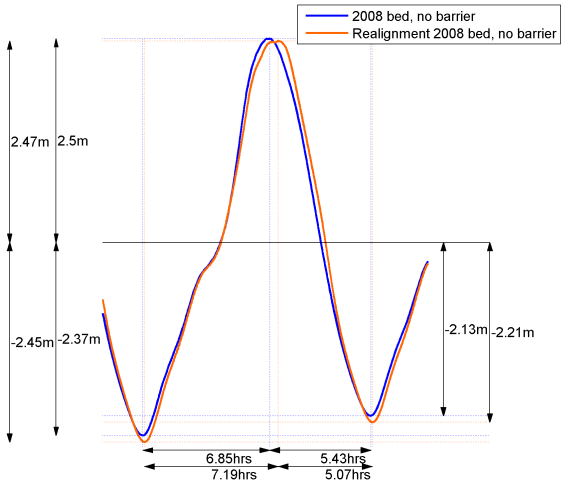

(f) Krammersluizen

Figure C.7: Timeseries of the water level, scenario 2 and 6

Appendix D

Timeseries of the instantaneous discharge

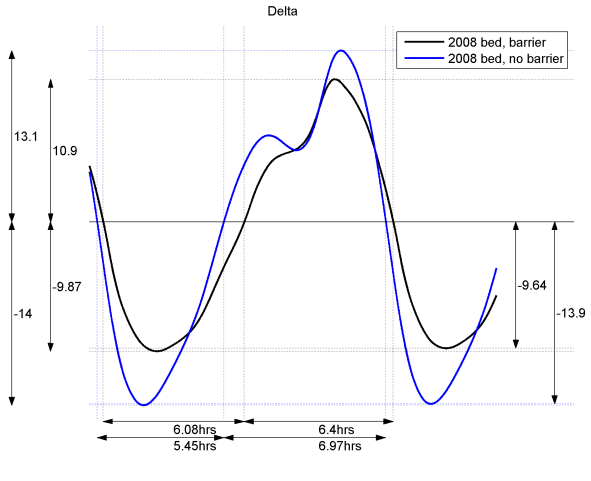

(a) Delta

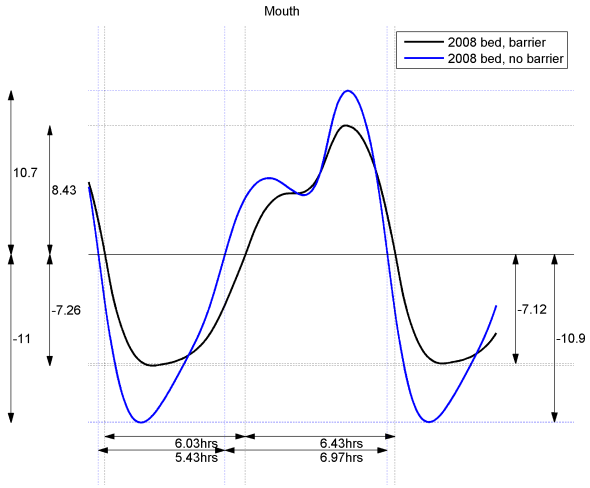

(b) Mouth

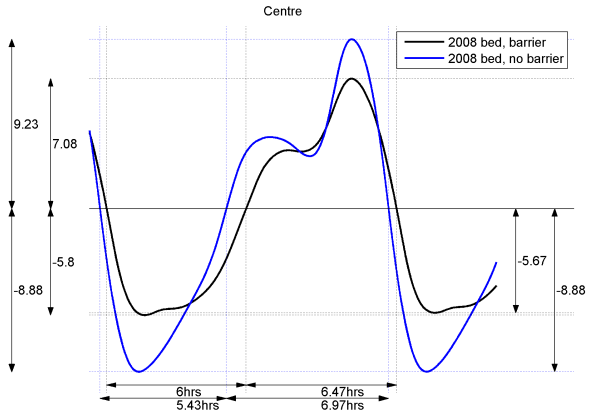

(c) Centre

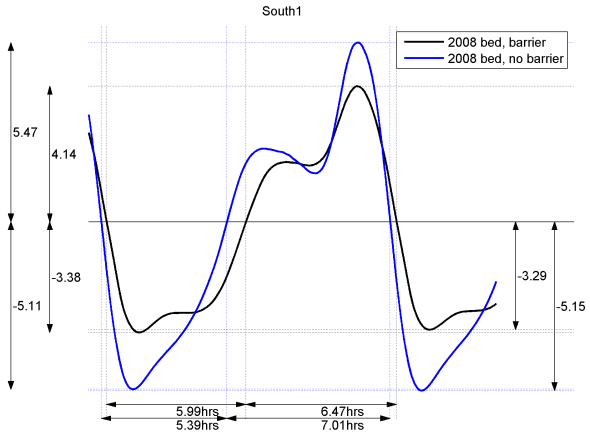

(d) South1

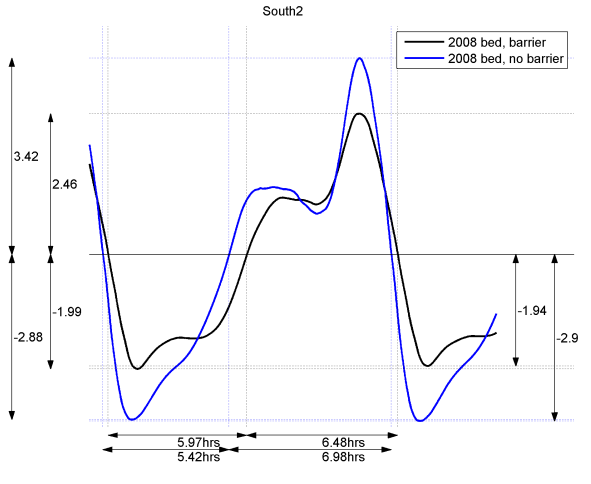

(e) South2

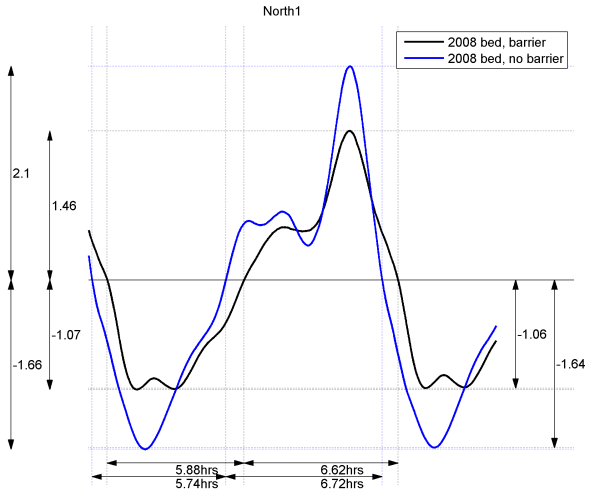

(f) North1

Figure D.1: Timeseries of the instantaneous discharge in 10^4 m^3/s, scenario 1 and 2

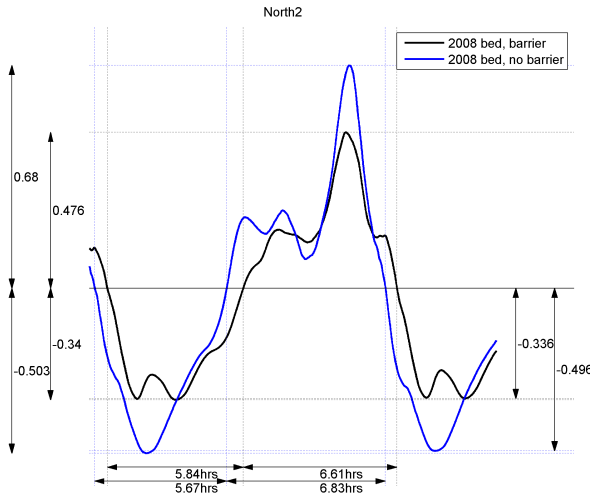

(g) North2

Figure D.1: Timeseries of the instantaneous discharge in 10^4 m^3/s, scenario 1 and 2

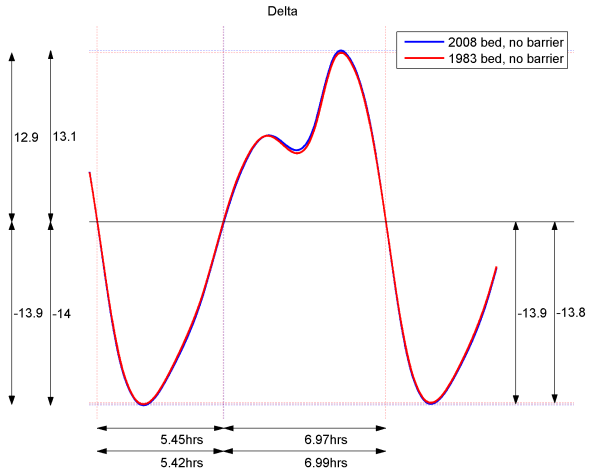

(a) Delta

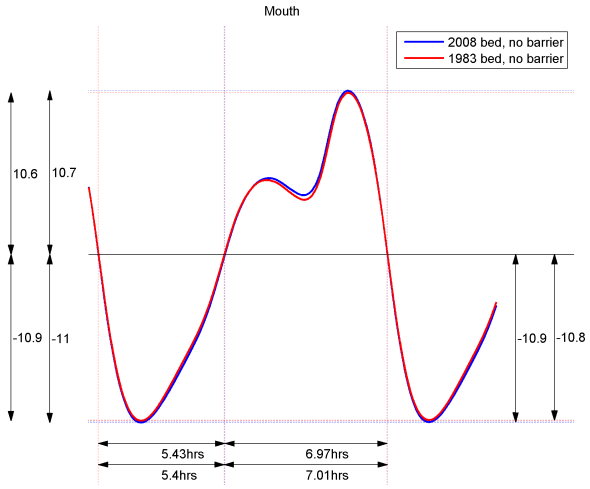

(b) Mouth

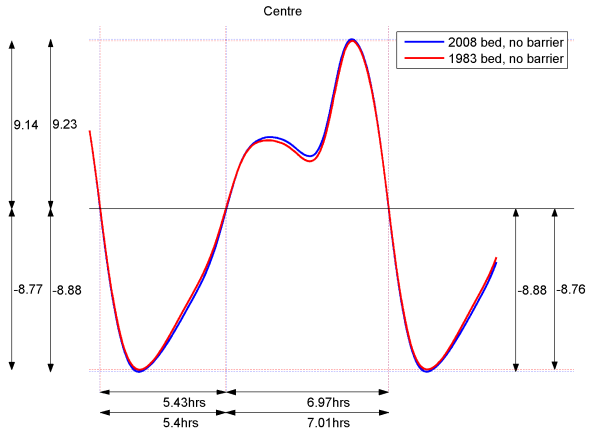

(c) Centre

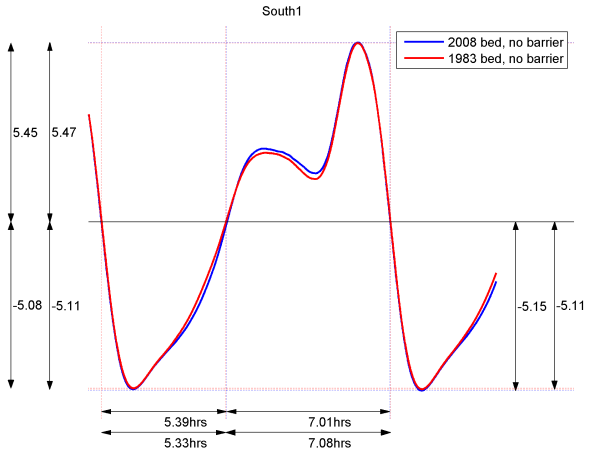

(d) South1

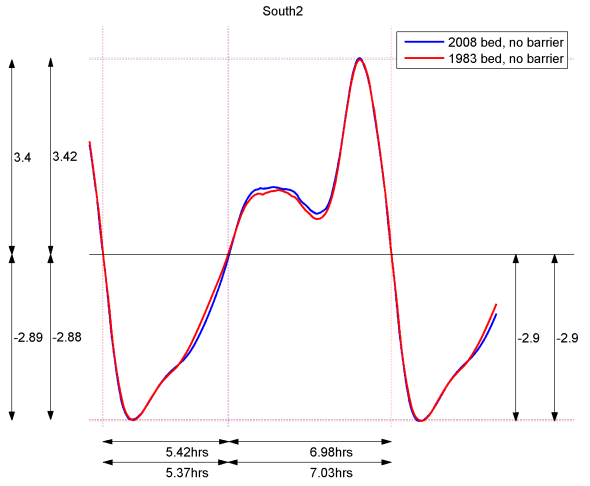

(e) South2

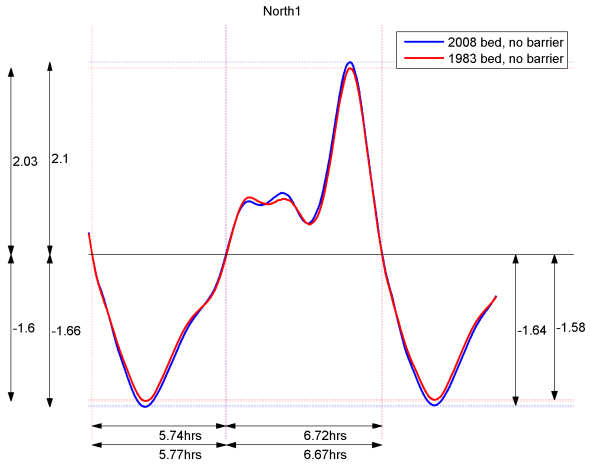

(f) North1

Figure D.2: Timeseries of the instantaneous discharge in 10^4 m^3/s, scenario 2 and 3

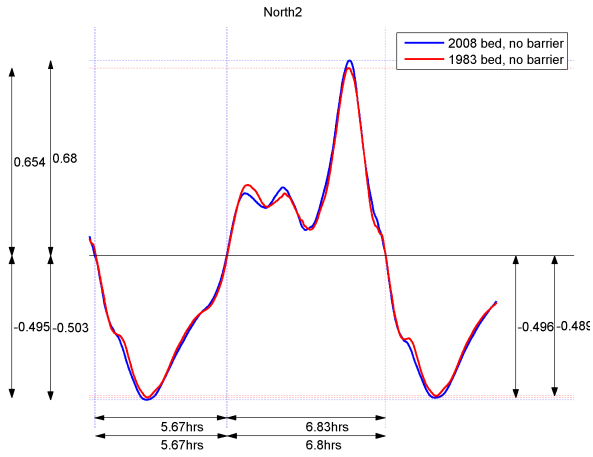

(g) North2

Figure D.2: Timeseries of the instantaneous discharge in 10^4 m^3/s, scenario 2 and 3

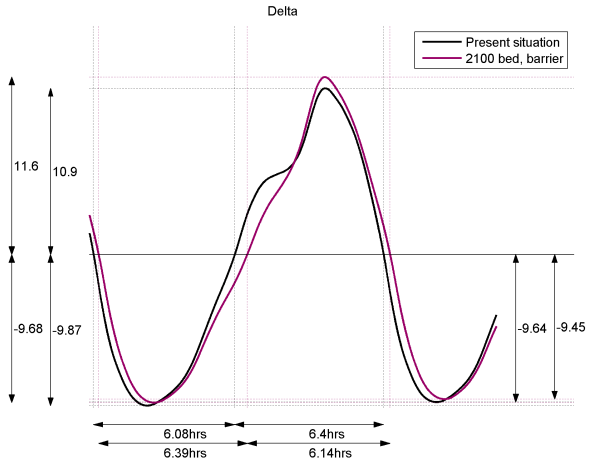

(a) Delta

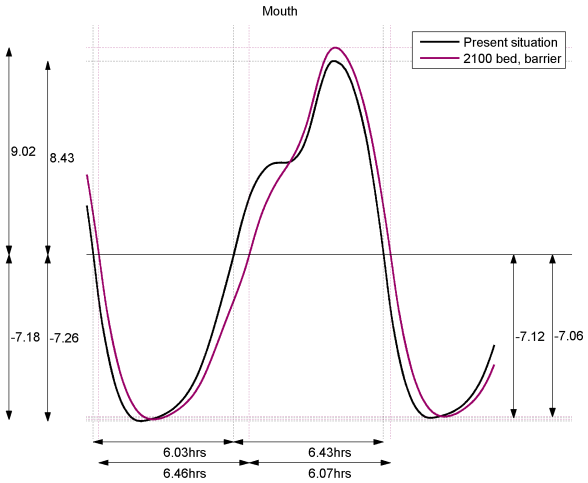

(b) Mouth

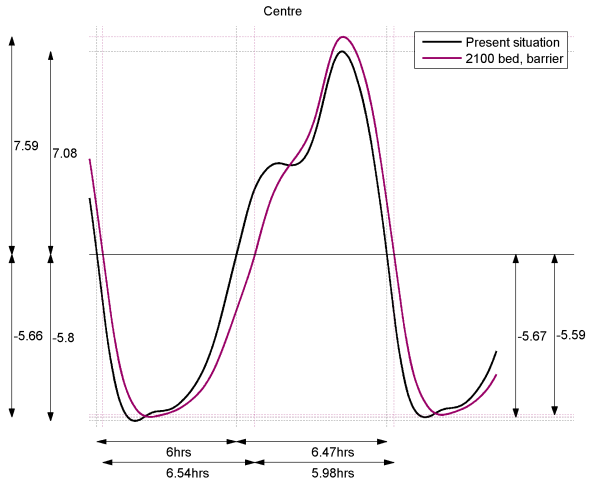

(c) Centre

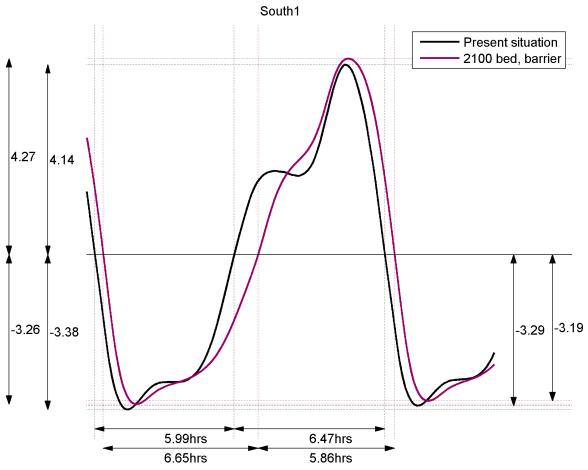

(d) South1

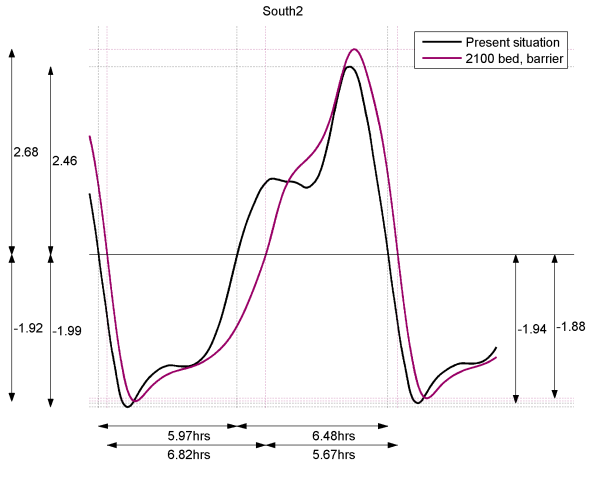

(e) South2

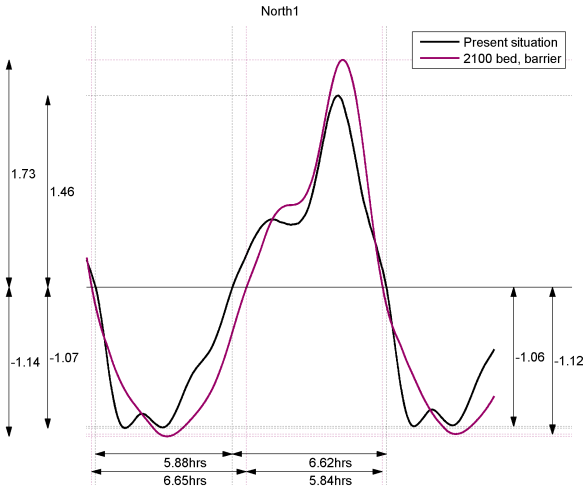

(f) North1

Figure D.3: Timeseries of the instantaneous discharge in 10^4 m^3/s, scenario 1 and 4

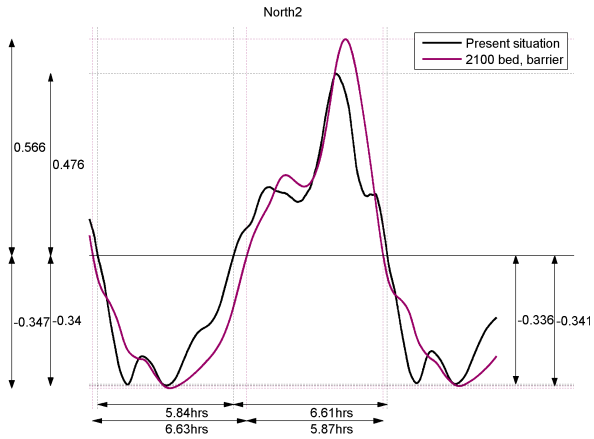

(g) North2

Figure D.3: Timeseries of the instantaneous discharge in 10^4 m^3/s, scenario 1 and 4

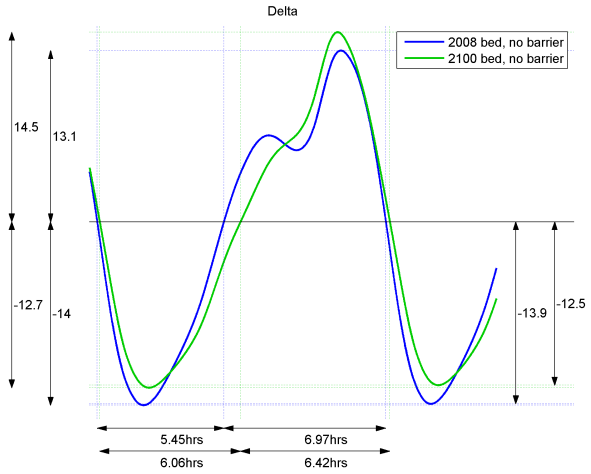

(a) Delta

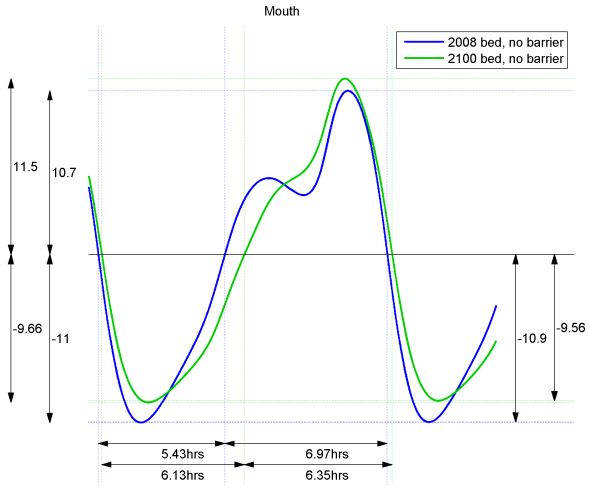

(b) Mouth

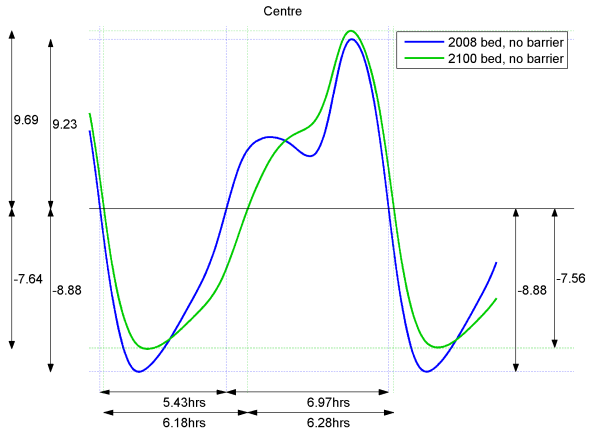

(c) Centre

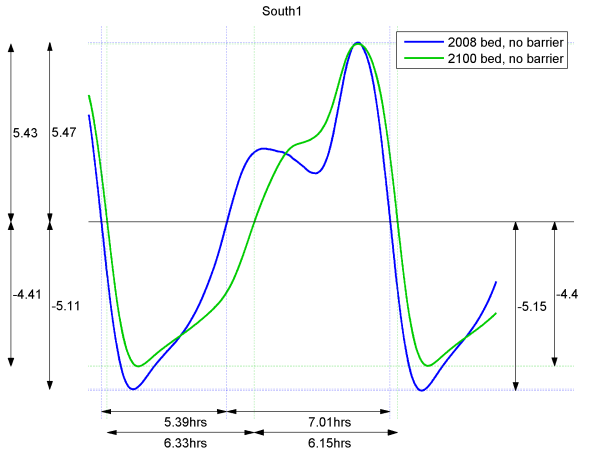

(d) South1

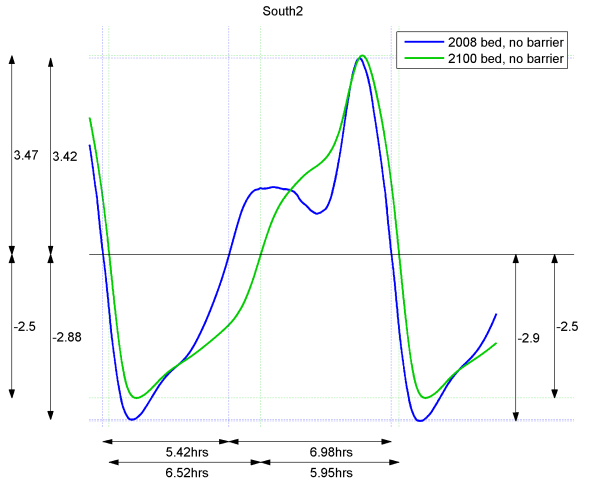

(e) South2

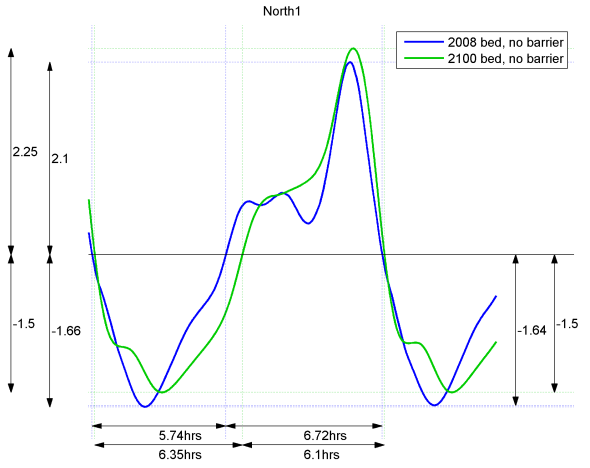

(f) North1

Figure D.4: Timeseries of the instantaneous discharge in 10^4 m^3/s, scenario 2 and 5

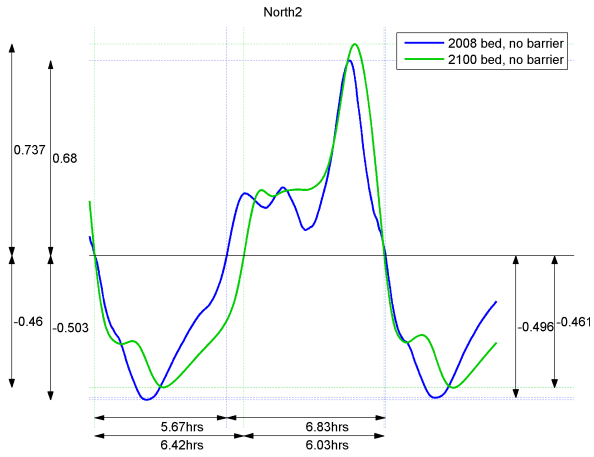

(g) North2

Figure D.4: Timeseries of the instantaneous discharge in 10^4 m^3/s, scenario 2 and 5

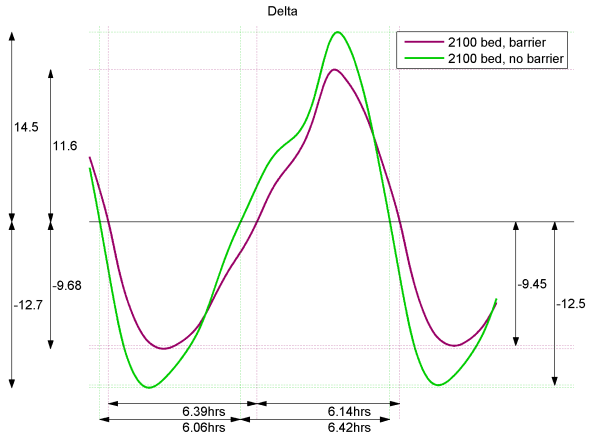

(a) Delta

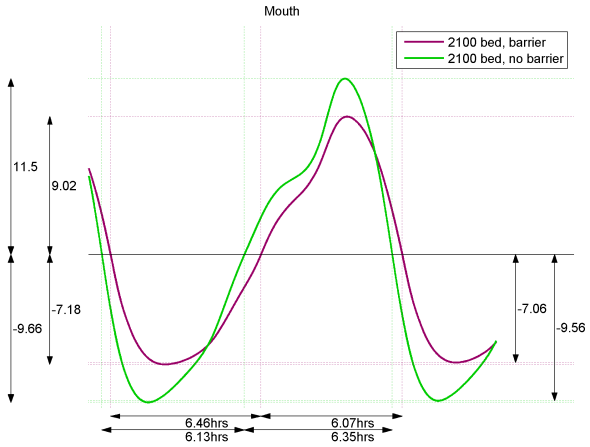

(b) Mouth

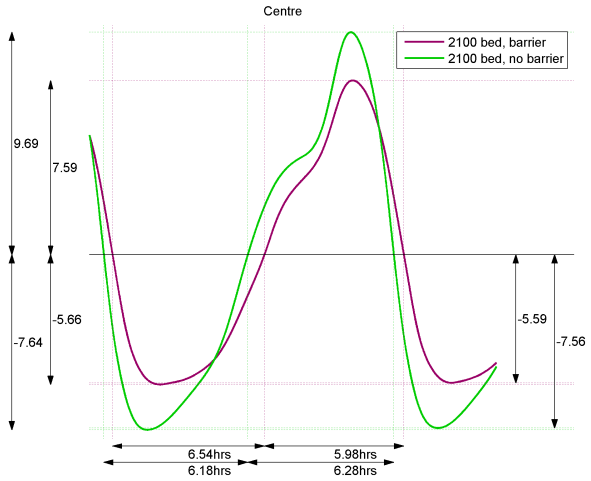

(c) Centre

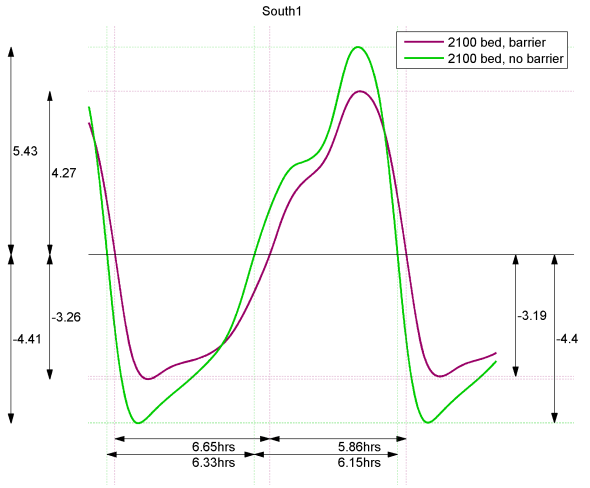

(d) South1

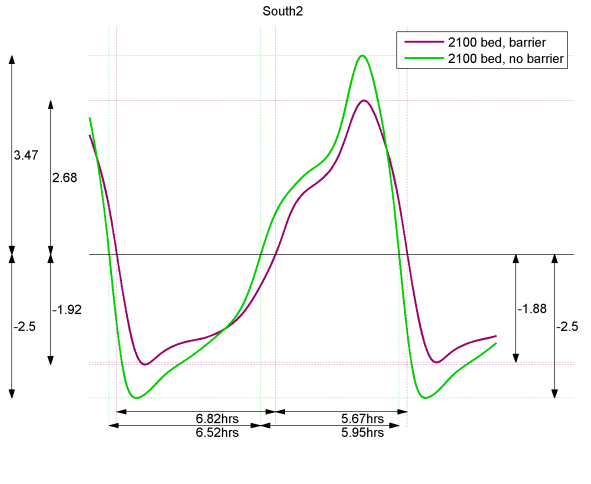

(e) South2

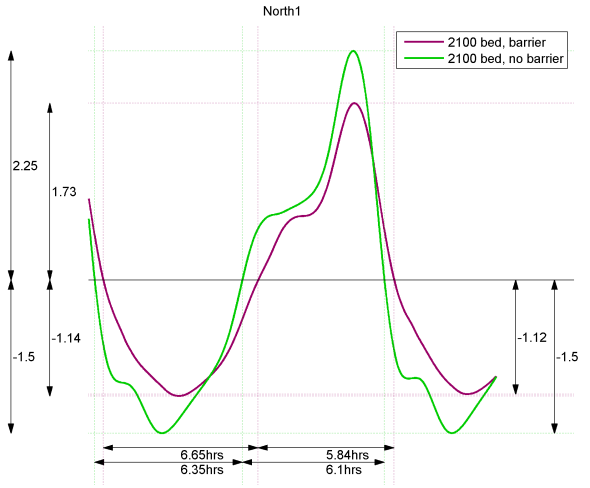

(f) North1

Figure D.5: Timeseries of the instantaneous discharge in 10^4 m^3/s, scenario 4 and 5

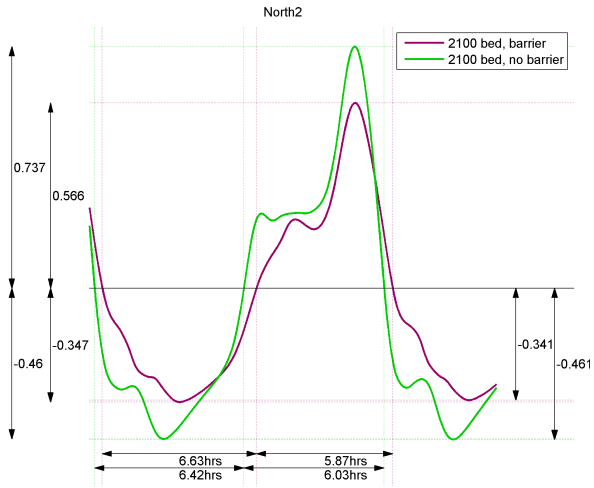

(g) North2

Figure D.5: Timeseries of the instantaneous discharge in 10^4 m^3/s, scenario 4 and 5

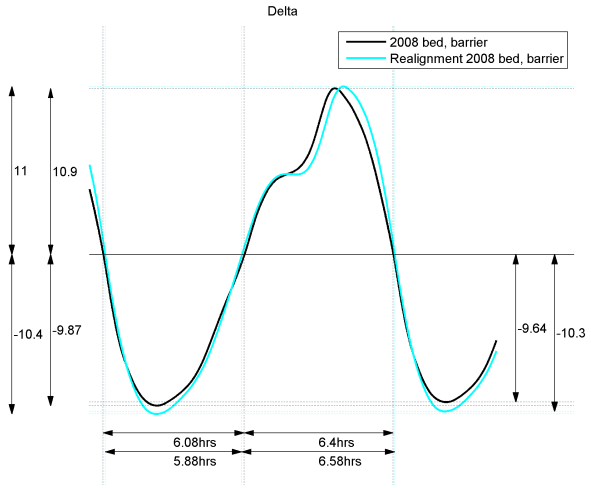

(a) Delta

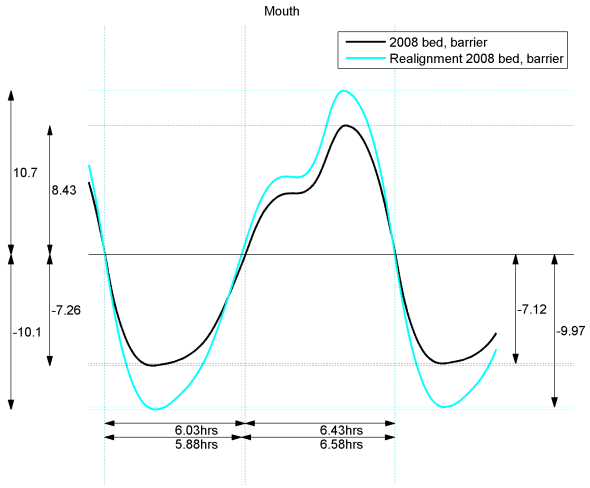

(b) Mouth

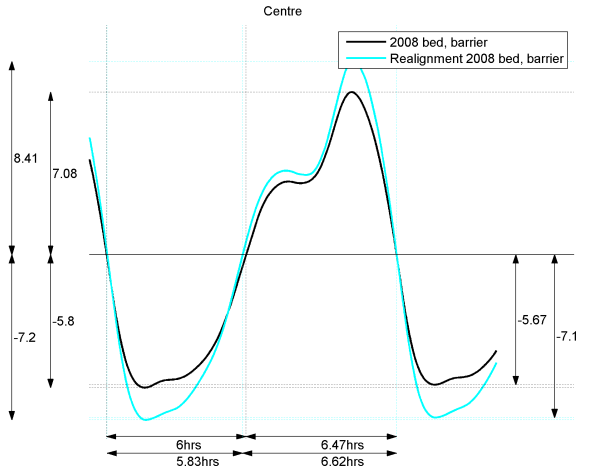

(c) Centre

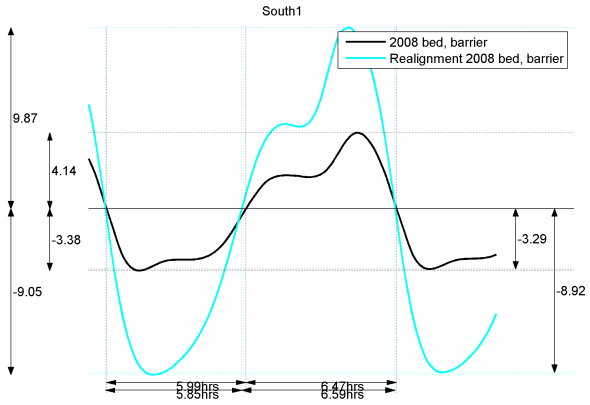

(d) South1

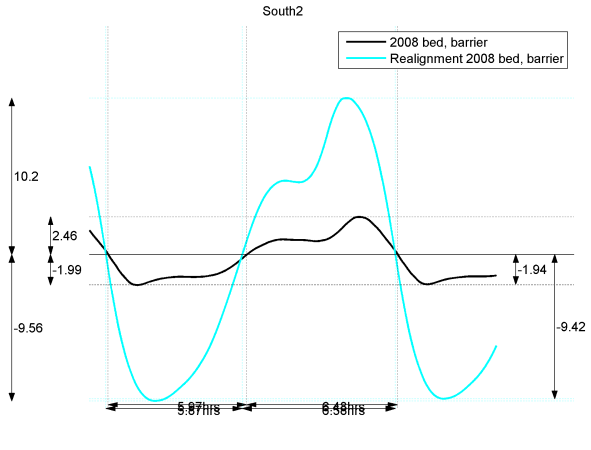

(e) South2

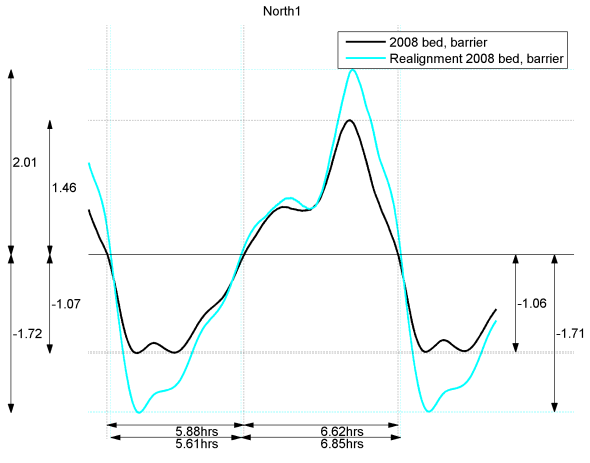

(f) North1

Figure D.6: Timeseries of the instantaneous discharge in 10^4 m^3/s, scenario 1 and 7

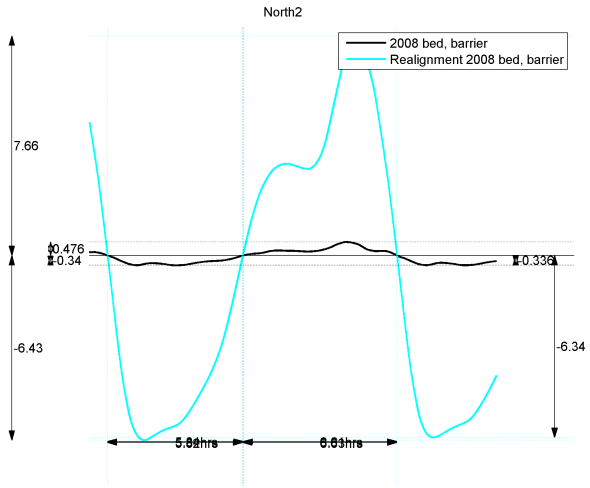

(g) North2

Figure D.6: Timeseries of the instantaneous discharge in 10^4 m^3/s, scenario 1 and 7

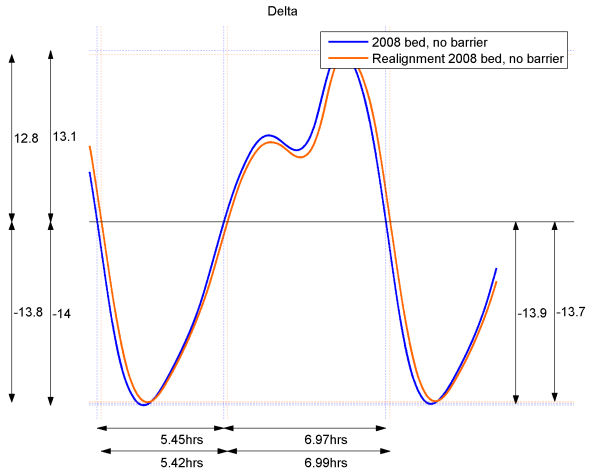

(a) Delta

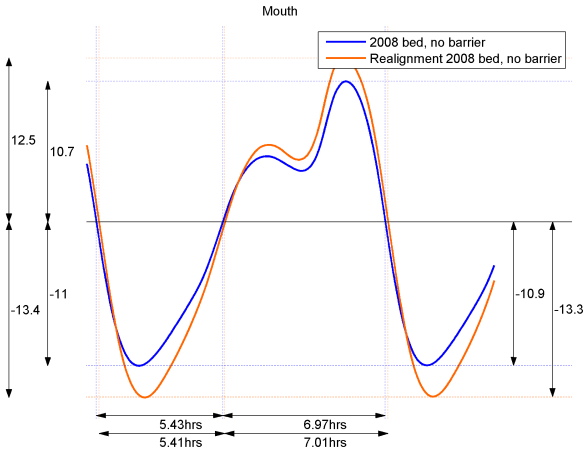

(b) Mouth

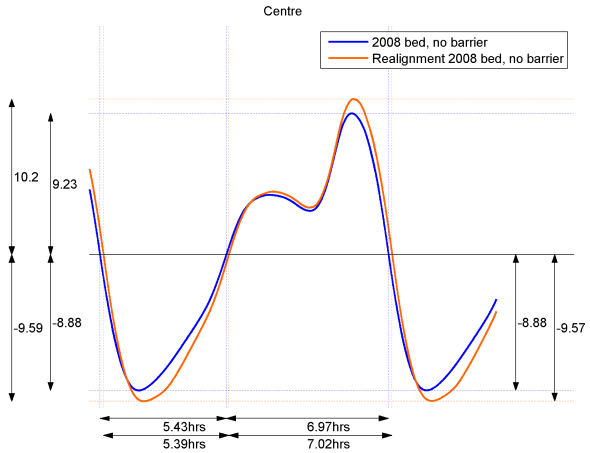

(c) Centre

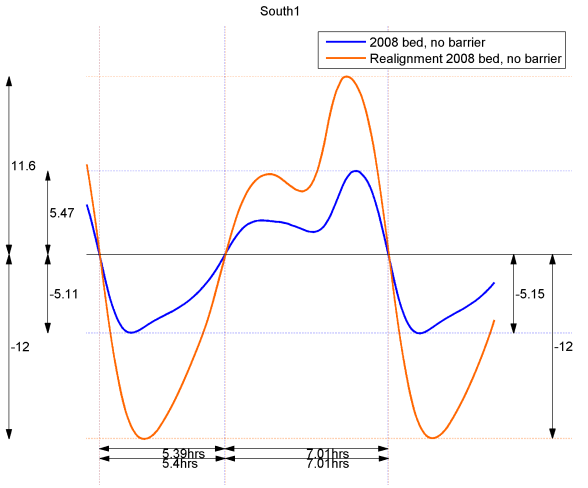

(d) South1

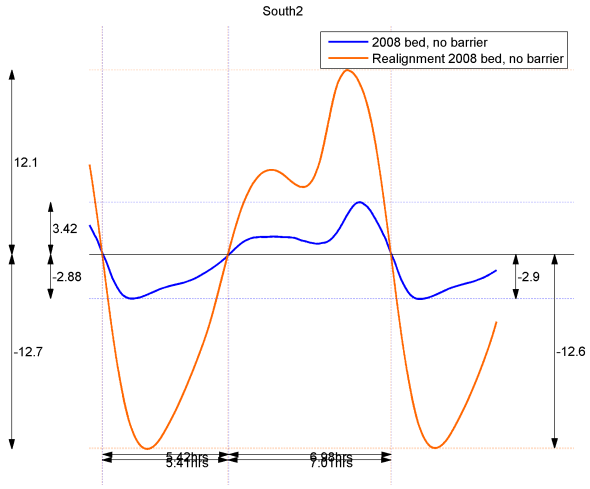

(e) South2

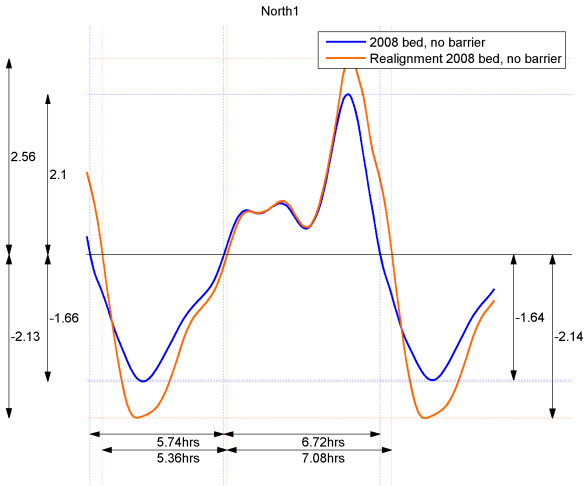

(f) North1

Figure D.7: Timeseries of the instantaneous discharge in 10^4 m^3/s, scenario 2 and 6

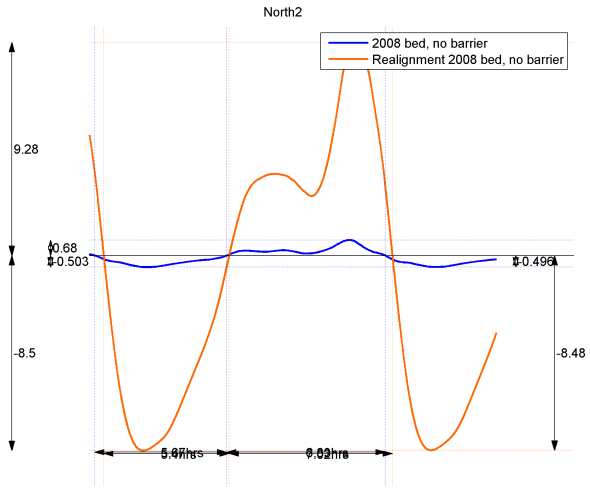

(g) North2

Figure D.7: Timeseries of the instantaneous discharge in 10^4 m^3/s, scenario 2 and 6